Study of Behaviour of Fermions in Some Holographic Theories using Gauge/Gravity Duality

A Thesis Submitted

To

Sikkim University

In partial fulfilment of the Requirement for the
Degree of Doctor of Philosophy

By

Nishal Rai

Department of Physics,
School of Physical Sciences

June 2019

DECLARATION

I declare that the thesis entitled **"Study of Behaviour of Fermions in Some Holographic Theories using Gauge/Gravity Duality"** submitted by me for the award of **Doctor of Philosophy** in Physics of **Sikkim University** is my original work. The content of this thesis is based on the work which I have performed myself. This thesis has not been submitted for any degree to any other University. The content of this Ph.D thesis has been subjected to the anti-plagiarism software (URKUND) and was found satisfactory.

Date:

(**Nishal Rai**)

Roll No.: 14PDPY01

Reg. No.: 14/PhD/PHY/01

Recommended that the thesis be placed before the Examiners for evaluation.

(**Dr. Subir Mukhopadhyay**)
Head of Department
Department of Physics
School of Physical Sciences

(**Dr. Subir Mukhopadhyay**)
Ph.D Supervisor
Department of Physics
School of Physical Sciences

CERTIFICATE

This is to certify that the thesis entitled **"Study of Behaviour of Fermions in Some Holographic Theories using Gauge/Gravity Duality"** submitted to Sikkim University in partial fulfilment of the requirement for the degree of **Doctor of Philosophy** in Physics embodies the result of *bona fide* research work carried out by **Mr. Nishal Rai** under my guidance and supervision. No part of the thesis has been submitted for any other degree, diploma, associate-ship, fellowship.

All the assistance and help received during the course of the investigation have been duly acknowledged by him.

Place: Gangtok, Sikkim

Date:

(**Dr. Subir Mukhopadhyay**)

Ph.D Supervisor

Department of Physics

School of Physical Sciences

PLAGIARISM CHECK CERTIFICATE

This is to certify that plagiarism check has been carried out for the following Ph.D thesis with the help of URKUND software and the result is within the permissible limit decided by the University.

"Study of Behaviour of Fermions in Some Holographic Theories using Gauge/Gravity Duality"

Submitted by **Mr. Nishal Rai** under the supervision of **Dr. Subir Mukhopadhyay** of Department of Physics, School of Physical Sciences, Sikkim University, Gangtok, 737102, India.

Signature of the candidate

Signature by the Supervisor

Vetted by Librarian

Dedicated to my parents

papa - GAGAN RAI,

aama - GAYATRI RAI

&

dada - TUSHAL RAI

Acknowledgement

It is my pleasure to thank those people who've assisted me in innumerable ways in the course of writing the thesis.

I am particularly grateful to my supervisor **Dr. Subir Mukhopadhyay**, Department of Physics, Sikkim University for his keen supervision, guidance and insight throughout my research process. His inestimable knowledge, valuable suggestion and sage advice have greatly improved and enriched my work. I shall remain eternally beholden for his supervision.

My sincere gratitude towards the entire faculty members from the department for giving me this platform to undertake this research study and to preserve and complete it satisfactorily. I am indebted to all the non-teaching staffs who also have laid an assistance in every possible way, throughout my stay in Sikkim University. Heartfelt thanks to my friends, brothers, sisters and colleagues from the Department of Physics who have been immense support without whom the list of thanksgiving would have been incomplete.

I thank my entire family for their constant faith, encouragement and loving support over a great distance. My father Gagan Rai and mother Gayatri Rai have always been an inspiration and driving force. It is their belief and faith towards me that has brought me this far. I am extremely thankful to my brother Tushal Rai and Rachana for their love and understanding that they gave me during my journey.

The share of acknowledgement also goes to the funding agency, University Grant Commission (UGC), Government of India for providing financial assistance to complete my thesis in the form of UGC-NET-JRF/SRF.

It's been an honour to work in the Department of Physics, Sikkim University (2012-2019).

Abstract

Gauge/Gravity duality relates a strongly coupled d-dimensional field theory to a weakly coupled $d+1$-dimensional gravity theory and vice versa. This holographic duality provides extremely powerful machinery to unravel and explore strongly coupled regimes giving rise to wide applications in diverse areas, such as gauge theory, hydrodynamics, condensed matter theories etc.

This thesis is based on the application of Gauge/Gravity duality in some aspects of strongly coupled condensed matter systems. Though these kinds of systems are not amenable to perturbative techniques of quantum field theory, there are formalisms, within the framework of condensed matter theory, such as Fermi liquid theory, which can capture its dynamics in most of the cases. However, vaious materials have been discovered in the eighties, which exhibit behaviour different from predictions of Fermi liquid theory and dubbed as non-Fermi liquid. Examples of such materials are high (T_c) cuprates superconductors and heavy fermions near a quantum phase transition. In the present work, we aim at understanding the behaviour of such systems using the Gauge/Gravity duality. We have adopted a top-down approach, where one considers a well established theory following from String theory on the gravity side with an exactly known dual field theory.

We begin with maximally gauged supergravity theory in seven dimension. The dual of this theory is conjectured to be (2,0) conformal field theory in six dimension. This theory admits asymptotically AdS blackhole solution characterised by two chemical potentials. The extremal limit of this blackhole corresponds to a one parameter family of solutions. We consider analysis of the fermionic modes in this

background that reveals existence of the Fermi surface. Depending on the fermionic mode we have obtained a pair of Fermi surfaces or a single Fermi surface. Study of fermionic excitations shows that they mostly belong to the non-Fermi regime. We have obtained excitations belonging to Fermi regime as well. By varying the charge parameter one observes that the modes approach marginal Fermi liquid regime at one of the extremes. We observe modes with larger fermionic charge are more prone to admit Fermi surface. From the dual field theory, it turns out that gauginos are playing a dominant role in determining the Fermi surface.

We have extended this analysis to finite temperature. Analysis of the spectral function of these fermionic modes leads to an agreement with the zero temperature result. We find that at a finite temperature one can also consider a limiting case of this blackhole background with a single charge where only certain modes admit a Fermi surface. In case of a single charge blackhole, scalars in the dual field theory also play a prominent role in determining the existence of Fermi surface. We found that the dual operators admit Fermi surface where scalar in the dual fermionic operator acquires a non-zero expectation value.

Next, we turn to the systems characterised with spontaneously broken symmetry. We have considered such variants of the gravity solutions namely domain wall solutions. They can be considered as a zero temperature limit of holographic superconductor. We have obtained a domain wall solution in maximally gauged seven dimension supergravity theory which approaches AdS at both IR and UV. We have studied optical conductivity as a function of frequency, where we find the real part of conductivity obeys a cubic law in the limit of high frequency while in case of small frequency it goes with the power of certain exponent. We have considered fermions that follow from supergravity theory and studied the spectral function. We find that the system admits a gapped spectrum. From the analysis of dual field theory it turns out that the fermionic operators involving bosons with non zero expectation value give rise to the gapped spectrum.

The other work along similar line involves a supergravity theory obtained through

compactification on a Sasaki-Einstein manifold. This theory is five dimensional, has less supersymmetry and its dual field theory turns out to be a superconformal quiver gauge theory living in four dimension. We consider a domain wall solution in this theory which approaches AdS geometry both in the IR and UV limit. In this supergravity theory, fermions get partitioned in different decoupled sectors. We have considered fermions of one particular sector in the background of this domain wall and studied the dispersion relation of these fermionic modes. For a smaller charge of the fermion, the dispersion relation shows a hyperbolic nature in the positive ω region, giving rise to a gapped spectrum. As we increase the charge, the entire profile of the dispersion curve comes down and for a critical value of the charge, it touches $\omega = 0$ axis resulting in a gapless spectrum. We have also studied the effect of Pauli coupling in this model and find that there are local maxima for the gap. However, for the charge that follows from supergravity theory, we could not find a normal mode, or peak of the spectral function, as the value of the charge is quite small. A higher value of charge leads to a gapless spectrum.

To summarise, we have studied the behaviour of the fermions and roles played by different kinds of degrees of freedom in some strongly correlated dual field theories using Gauge/Gravity duality. Our work has shed light on understanding of some systems occuring in non-Fermi regime.

List of publications

- S. Mukhopadhyay and N. Rai, "Holographic Fermi surfaces in the six-dimensional (2, 0) theory," Phys. Rev. D 96, no. 2, 026005 (2017). doi:10.1103/PhysRevD.96.026005
- S. Mukhopadhyay and N. Rai, "Holographic Fermi surface at finite temperature in six-dimensional (2, 0) theory," Phys. Rev. D 96, no. 6, 066001 (2017). doi:10.1103/PhysRevD.96.066001
- S. Mukhopadhyay and N. Rai, "Gapped fermionic spectrum from a domain wall in seven dimension," Phys. Lett. B 780, 608 (2018). doi:10.1016/j.physletb.2018.03.037
- S. Mukhopadhyay and N. Rai, "Fermionic spectrum from a domain wall in five di- mensions," Phys. Rev. D 98, no. 2, 026007 (2018) doi:10.1103/PhysRevD.98.026007 [arXiv:1904.06147 [hep-th]].

Contents

List of Figures

List of Tables

Chapter 1

Introduction

In the last century, an interesting duality has been conjectured relating the gauge theory and gravity. It has been proposed that gauge theories are in a certain sense equivalent to gravity theory on an anti-de Sitter space (AdS). There were several hints that such a relation exists [1] but the first concrete realisation was given in [2–4]. This is slightly unusual to have a relation between two such theories which are so distinctly different, but this emerges as a consistent picture because of the facts that these two theories are valid in two different regimes of coupling constants. To be more precise, the gauge theory in its strongly coupled regime has been found to be dual to the gravity theory in its weakly coupled regime and vice versa, hence called gauge/gravity duality. Soon after its advent, it was generalised to other geometries. In general, the gravity theory lives in the bulk of AdS spacetime in $(d+1)$-dimension, while the dual field theory lives on the d-dimensional boundary of the AdS space and so it is often referred to as holographic duality as well. The various fields in the bulk of AdS correspond to operators in the field theory living on the boundary. This holographic duality provides extremely powerful machinery to unravel and explore strongly coupled regimes giving rise to wide applications in diverse areas [5–11], such as gauge theory, hydrodynamics, condensed matter theories etc.

We will be considering the application of this duality in the case of strongly correlated systems that occur in condensed matter theories. The field theoretic frame-

work for dealing with strongly correlated systems often experience the disadvantage, that the essential physics is strongly coupled and the standard perturbative techniques can play only a limited role. Perhaps the most successful approach for dealing with such non-perturbative systems is Fermi liquid theory, proposed by Landau. It describes such systems by replacing the electrons with weakly interacting quasi-particles. These can be thought of as electrons "dressed" with photons. Since the interaction among the quasi-particles is weak, it can analyse the system within the perturbative formulation. Fermi liquid theory turns out to be quite successful till the 1980s in explaining behaviours of metals and semiconductors.

Afterwards, new materials were discovered which cannot be described using Fermi liquid theory. Cuprate superconductors and heavy fermions turn out to have Fermi surface but the quasi-particle excitations around them are short-lived and unstable. Indeed Angular Resolved Photoemission Spectroscopy (ARPES) experiment shows the existence of Fermi surface along with the instability of quasi-particles. These materials are classified as a non-Fermi liquid. Considering their transport properties, the materials in strange metal phase shows the linear temperature dependence of resistivity, which is different from the T^2 behaviour predicted by Fermi liquid theory. It becomes clear that such strongly correlated systems are not amenable to the Fermi liquid theory and calls for new non-perturbative techniques. This poses new challenges and provides an arena for the application of gauge/gravity duality.

In order to address the issues in such finite density systems with finite temperature within a holographic formulation, it turns out the charged black holes provide the necessary gravity duals. Fermionic fields can easily be incorporated in those gravity duals and one can study the fermionic excitations in the dual system. Study of Fermi surfaces using holography first appeared in [12–14]. Sharp quasi-particle-like fermionic excitations at low energies with scaling behaviour different from Fermi liquid were found. A more elaborate analysis of the behaviour of such fermionic excitations was done in [15]. They have studied the scaling exponents of the spectral function and the dimensions of the dual operators in the dual field

theory. They also found that the Fermi surface exists over a range of momentum beyond which it ceases to exist and the peak of the spectral function shows log periodic behaviour. By turning on the coupling of fermions in the gravity theory with electromagnetic field via dipole coupling it was shown that one can generate a gapped spectrum of the density of states [16–18], which is similar to Mott insulators. Initially, in the proposal, the gravity theories are asymptotically AdS. Soon it was generalised to other asymptotic geometries. Analyses for Lifshitz geometry at finite temperature appeared in [19,20] showing gapped spectrum. A similar study of Fermi surfaces and excitations were considered in [21,22] for hyperscaling violating Lifshitz geometry.

In these works, the gravity models were chosen so as to have necessary symmetries expected in the dual field theories. These are commonly called bottom-up approach. They are convenient, flexible and simpler to capture different mechanisms in the dual field theory. However, there is one limitation that the exact dual field theories are often not known. That leads to the complementary top-down approach, where the gravity theory is obtained from String theory and the corresponding dual field theories are also known exactly. Variations of the parameters within the theory also help to make identification of states in the dual theory. The prototype example is IIB supergravity on $\text{AdS}_5 \times S^5$ whose dual is $\mathcal{N} = 4$ super Yang-mills theory (SYM). The dual operators living on the boundary field theory corresponding to the fields in the gravity theory in the bulk are also known in this approach. On the flip side, these involve a large number of fields and Lagrangians representing the system are also quite involved. Also, it does not have the flexibility of bottom-up approach.

In top-down approach, Fermi surfaces were first studied in a probe approximation [23, 24]. Subsequently, minimal $\mathcal{N} = 2$ supergravity theories was considered [25–28]. These supergravity theories include fermionic fields, such as gravitinos. The behaviour of the dual fermionic operators was analysed but it did not lead to Fermi surface.

Holographic Fermi surface in top-down approach was first obtained in five di-

mensional maximally gauged supergravity whose dual field theory is $N = 4$ Super-Yang-Mills (SYM) in four dimension [29, 30]. The considered spin-1/2 fermions in this supergravity theory in the background of a black hole solution and restricted themselves only to those which do not couple to gravitini. They find the dual fermionic operators are in the non-Fermi regime, though it approaches marginal Fermi liquid at the limiting value of the chemical potential of the black hole. They also studied the excitation width of quasi-particles. Later these analyses were extended to other maximal gauged supergravity, as well. In particular, it was applied to the supergravity theory in 4 dimensions, which is dual to Aharony-Bergman-Jafferis-Maldacena (ABJM) theory in three dimension [29–31]. These were zero temperature analyses and similar analyses at finite temperature appeared in [32], which also studied the role of scalar and spinor operators in the dual field theory. Discussions of Fermi surfaces in similar context appeared in [33–35].

In the above works, the gravity duals are black holes. However, most of the solutions considered there are characterized with zero-point entropy [1]. In other words, the entropy does not vanish for $T \to 0$. On the other hand, there exists an interesting class of backgrounds on the gravity side, which are free from this problem. In the dual theory, they correspond to condensation of charged scalar and gives rise to spontaneous breaking of $U(1)$ gauge symmetry. These are the features that characterise holographic superconductors and these solutions, known as domain walls, are considered as zero temperature limit of them [37, 38]. Study of fermions for such a condensed phase of holographic superconductor at zero temperature appeared in [39] and it shows a spectrum similar to that obtained in APRES experiment. Several works appeared towards an understanding of the mechanism responsible for such gapped spectrum. [40] In particular, self coupled Majorana fermions interacting with scalar also gives rise to similar gapped spectrum.

On the score of top-down approach, studies of fermionic excitations for holographic superconductors obtained from string theory and M theory appeared in [41],

[1] One exception is [36] where a model with vanishing zero-point entropy was analysed leading to stable fermionic fluctuation with a gap around Fermi surface.

where they considered generic fermions with a domain wall solution as the background, in a four dimensional supergravity that follows from compactification of M theory. They obtained bands of normalisable modes in the region $\omega^2 < k^2$. Further studies of domain wall solutions with a symmetry breaking source in four dimensional gauged supergravity (dual to Aharony-Bergman-Jafferis-Maldacena (ABJM) theory) [42] shows both gapped and gapless bands of stable excitations. Similar solutions dual to states in ABJM theory with broken $U(1)$ symmetry [43] also reported gapped spectrum. Gaps in the spectra have been attributed to low fermionic charge and particle-hole interaction.

In the present thesis, we have extended these studies of fermionic excitations for different classes of systems in the holographic framework. We begin with maximally gauged supergravity in seven dimensions. This is one of the three maximally symmetric theories, of which the other two have already been studied as mentioned above and is interesting on its own right. Because of large symmetry, the dual field theory operators are simpler. Moreover, we have used top-down approach, where we can precisely identify the operators in the dual field theory, which enable one to address the mechanisms in the field theory set up. Another characteristic of this dual theory is it involves tensor multiplet, which is different from the field theories considered elsewhere.

In the next chapter, we begin with the survey of relevant literature, which will set up the context and motivation for our work. In chapter 3, we have studied the nature of the Fermi surface in maximally gauged supergravity theory in seven dimension, where we have consider the extremal limit of the black hole $T = 0$ [44]. We have studied the dependence of Fermi surface with respect to the $U(1)$ charge of the system as our parameter. We find for a higher net charge of the fermion leads toward two branches of the Fermi surface, which are in Fermi regime and non-Fermi regime. On the other hand lower net charge of the fermion, gives a single branch lying in the non-Fermi regime. In both cases, the system moved toward marginal Fermi liquid regime at the end of the parameter space.

In chapter 4, we have extended our analysis of this model at finite temperature case [45]. We have studied the cases with two charge and one charge background. In case of two charge, we find the existence of Fermi surface for all the fermionic modes, while for the one charge case Fermi surface persists only for certain modes. Single charge case has been considered only at finite temperature regime due to the fact that we could not find an extemal limit for single charge case.

In chapter 5, we have obtained a domain wall solution for the model in maximally gauged supergravity theory in seven dimension. Using this domain wall solution as the background, we have studied the optical conductivity and also the fermionic response [46]. We find with this domain wall solution as a background give rise to gapped fermionic spectrum.

In chapter 6, domain wall in five dimensional gravity theory is considered which correspond to some four dimensional field theory. In this background, we have considered fermions which do not couple to other fermions or gravitino to study the dispersion relation and nature of the spectrum of these fermions [47]. We find for a lower charge we get a gapped spectrum and as we increase the charge, the system admits a gapless spectrum. In chapter 7, we end with a conclusion.

Chapter 2

Literature survey

2.1 AdS/CFT correspondence

The first concrete realization between the dynamics of gauge theory and a gravity theory was put forward by Maldacena [2] in the form of AdS/CFT correspondence [1]. He conjectured that gravity theory with AdS space in the background and a super Yang-Mills (SYM) theory in the boundary are two different descriptions of the same theory. The fact that the descriptions are so different may be traced back to the fact that these two appearances correspond to different regimes of the coupling constants of the theory. In other words, the strongly correlated field theory living in the boundary corresponds to the gravity theory in one extra dimension, which is weakly coupled. As one of its consequences, it has opened up new avenues to analyse and explore systems at strong coupling living at the boundary using a simpler form of weakly coupled gravity theories and vice versa. Our main focus will be the application of these techniques to study and unravel strongly correlated systems. Before embarking to such endeavour, in this chapter we will briefly review the basics of this correspondence as well as some of the works that have been done in this vein. This will help us to set up the essentials, that we will use in the following chapters.

[1] It is also referred as a holographic duality or gauge/gravity duality.

2.1.1 Anti-de Sitter Space

Since on the gravity side we will be dealing with anti de-sitter space (AdS) or asymptotically AdS space let us begin with its description. AdS is the maximally symmetric solution of Einstein's equation with negative cosmological constant. In Euclidean signature, the AdS spacetime is the hyperboloid embedded in $R^{(d-1,1)}$ whose metric is given as

$$-(X^0)^2 + (X^1)^2 + (X^2)^2 + ... + (X^{d-1})^2 = -R^2, \tag{2.1.1}$$

where $X^0 > 0$. As one can observe, this metric is invariant under $SO(d+1,1)$ transformation, which is the conformal group of the boundary. To see AdS as a solution of Einstein's field equation, consider the most general metric in $(d+1)$ dimension which has Poincare symmetry in d-dimension as given by,

$$ds^2 = f(r)(-dt^2 + d\vec{x^2} + dz^2), \tag{2.1.2}$$

where, d is the spacetime dimension with $\vec{x} = (x^1, ..., x^{d-1})$ and z is the radial dimension. If z is the length scale and the theory is length invariant, then ds^2 must also be invariant under the scaling transformation, i.e $(t, \vec{x}) \to \lambda(t, \vec{x})$ and $r \to \lambda r$. Imposing this condition on ds^2 we get

$$ds^2 = \frac{L^2}{z^2}(-dt^2 + d\vec{x^2} + dz^2), \tag{2.1.3}$$

which represent the line element or metric of AdS space in $(d+1)$ dimension denoted by AdS$_{d+1}$. L is called the radius of anti-de Sitter space. The metric is a solution to gravity action given by [48]

$$S = \frac{1}{16\pi G_N}\int d^{d+1}x\sqrt{-g}(-2\Lambda + R + c_2R^2 + c_3R^3 + ...), \tag{2.1.4}$$

where, G_N is the Newton constant, c_i are constants, g =det$(g_{\mu\nu})$, $R = g^{\mu\nu}R_{\mu\nu}$ is the scalar curvature and Λ is a cosmological constant. If we set $c_i = 0$ the action becomes the Einstein-Hilbert (EH) action of general theory of relativity with a cosmological constant, which we will discuss in more details in upcoming section 2.2. Here the equation of motion turns out to be the Einstein equation

$$R_{\mu\nu} - \frac{1}{2}g_{\mu\nu}R = -\Lambda g_{\mu\nu} \tag{2.1.5}$$

taking the trace of (2.1.5) gives,

$$R = 2\frac{\Lambda(d+1)}{d-1} \tag{2.1.6}$$

inserting the Ricci scalar R in (2.1.5) we get,

$$R_{\mu\nu} = \frac{2}{d-1}\Lambda g_{\mu\nu} \tag{2.1.7}$$

From the metric one can find the Ricci tensor directly, which is

$$R_{\mu\nu} = -\frac{d}{L^2}g_{\mu\nu}. \tag{2.1.8}$$

The above two equations (2.1.7) and (2.1.8) imply AdS$_{d+1}$ is the solution of the Einstein equation (2.1.5) with negative cosmological constant Λ and scalar curvature R, given by

$$\begin{aligned} \Lambda &= -\frac{d(d-1)}{2L^2}, \\ R &= -\frac{d(d+1)}{L^2}. \end{aligned} \tag{2.1.9}$$

2.1.2 Conformal group

Conformal group are groups of conformal transformations which is larger than Poincare group and contents it as a subgroup. A conformal transformation of the spacetime coordinate is a transformation which leaves the metric invariant up to a

scaling factor given by an invertible mapping $x \to x'$,

$$g'_{\mu\nu}(x') = \Lambda(x) g_{\mu\nu}(x). \tag{2.1.10}$$

Poincare group is the sub group of Conformal group, whose transformation can be obtained by setting $\Lambda(x) = 1$. The conformal transformation preserves the angle between any curves crossing each other at some point.
In order to understand the various components in it we consider infinitesimally small confromal transformation. Under a infitesimally small general coordinate transformation $x'_\mu = x_\mu + \epsilon_\mu(x)$ the metric transforms as,

$$g'_{\mu\nu} = g_{\mu\nu} - (\partial_\mu \epsilon_\nu + \partial_\nu \epsilon_\mu). \tag{2.1.11}$$

So the transformation to be conformal we must have using (2.1.10),

$$\partial_\mu \epsilon_\nu + \partial_\nu \epsilon_\mu = f(x) g_{\mu\nu}, \tag{2.1.12}$$

where $f(x)$ is the function to be determined. For our purpose we will consider this metric to be the Minkowski metric $\eta_{\mu\nu} = \text{diag}(-1, 1, 1..., 1)$ in d-dimensional spacetime. Taking a derivative on both side in (2.1.12), permuting the indices and taking a linear combination gives,

$$2\partial_\mu \partial_\nu \epsilon_\rho = \eta_{\mu\rho} \partial_\nu f + \eta_{\nu\rho} \partial_\mu f - \eta_{\mu\nu} \partial_\rho f. \tag{2.1.13}$$

Which implies,

$$(d-1)\partial^2 f(x) = 0. \tag{2.1.14}$$

For $d \geq 3$, the solution to $f(x)$ is,

$$f(x) = A + B_\mu x^\mu, \tag{2.1.15}$$

where A and B_μ are constants. Substituting $f(x)$ in (2.1.13) and solving it, we get

$$\epsilon_\mu = a_\mu + b_{\mu\nu}x^\nu + c_{\mu\nu\rho}x^\nu x^\rho, \quad c_{\mu\nu\rho} = c_{\mu\rho\nu}. \tag{2.1.16}$$

Considering each power of x terms seperately in the above equation we can see, a_μ being unconstrained corresponds to translation. Substituting the linear term in (2.1.13) we get the following constraint on $b_{\mu\nu}$,

$$b_{\mu\nu} + b_{\nu\mu} = \frac{2}{d}b^\lambda_\lambda \eta_{\mu\nu}, \qquad b_{\mu\nu} = \alpha\eta + m_{\mu\nu}, \tag{2.1.17}$$

$b_{\mu\nu}$ comprises of a pure trace $\eta_{\mu\nu}$ which represents an infinitesimal scale transformation and the antisymmetric part $m_{\mu\nu} = -m_{\nu\mu}$ which is an infinitesimal rotation. Similarly, from the quardratic part we have

$$c_{\mu\nu\rho} = \eta_{\mu\rho}b_\nu + \eta_{\mu\nu}b_\rho - \eta_{\nu\rho}b_\mu, \quad \text{with} \quad b_\mu = \frac{1}{d}c^\sigma_{\sigma\mu} \tag{2.1.18}$$

This infintesimal transormation subjected to the above constraint is called special conformal transformation (SCT),

$$x'_\mu = x_\mu + 2x_\nu b^\nu x_\mu - b_\mu x^2 \tag{2.1.19}$$

For the finite transformation we have:

$$x'_\mu = x_\mu + a_\mu \qquad \text{translation} \tag{2.1.20}$$

$$x'_\mu = \alpha x_\mu \qquad \text{dilation} \tag{2.1.21}$$

$$x'_\mu = M\nu^\mu x^\nu \qquad \text{rotation} \tag{2.1.22}$$

$$x'_\mu = \frac{x_\mu - b_\mu x^2}{1 - 2b_\nu x^\nu + b^2 x^2} \qquad \text{SCT} \tag{2.1.23}$$

2.1.3 String theory

AdS/CFT correspondence has its origin in string theory, so in this respect, we would like to touch up on some of the relevant points. In string theory the fundamental objects are strings and the degrees of freedom are the various excitations of the strings. A string could be closed or open. As the string moves over spacetime to trace a world sheet analogous to world line in case of particles. It turns out in the low energy limit of string theory the degrees of freedom are described by massless fields. In the case of closed strings, the massless fields correspond to graviton, scalar field dilaton and various other fields with two or higher forms. In order to incorporate fermions, one needs to generalise these to the case of string theories with supersymmetry. Supersymmetry transforms a boson into its fermionic superpartner and vice versa. For the theory to be consistent all of these theories with supersymmetry require a spacetime of 10 dimensions. However, there are severe constraints arises from consistency conditions which limit the number of possible superstring theories. There are five consistent superstring theories, namely type I, heterotic, type IIA and IIB [49].

- Bosonic string theory: In this formulation of string theory one only consider bosons. There is no supersymmetry and no fermions therefore, this theory cannot describe fermionic matter. It includes both closed and open strings and for the theory to be consistent it requires 26 spacetime dimensions.

- Type I string theory: This theory includes both bosons and fermions. Particle interaction includes supersymmetry and consistent gauge group is $SO(32)$.

- Type IIA string theory: This theory includes supersymmetry open and closed strings. It gives rise to the fermionic matter as well but fermions in this theory are not chiral.

- Type IIB String theory: This theory is similar to Type IIA except it has chiral fermions.

Fields	Representation	Name
$g_{\mu\nu}$	[2, 0, 0, 0]	graviton
$B^{(2)}_{\mu\nu}$	[0, 1, 0, 0]	2 form field
ϕ	[0, 0, 0, 0]	dilaton
$C^{(0)}$	[0, 0, 0, 0]	axion
$C^{(2)}_{\mu\nu}$	[0, 1, 0, 0]	R-R 2 form field
$C^{(4)+}_{\mu\nu\rho\lambda}$	[0, 0, 0, 2]	self dual 4 form field
$\psi^{a}_{\mu\alpha}$	[1, 0, 0, 1]	Majorana Weyl gravitinos
λ^{a}_{α}	[1, 0, 0, 1]	Majorana Weyl dilatinos

Table 2.1.1: Field content of type IIB supergravity

- Heterotic string theory: This theory includes supersymmetry but only comprises of closed string. There are two heterotic string theory which are

  Heterotic $SO(32)$

  Heterotic $E_8 \times E_8$.

Except bosonic string theory all of these theroies have Supersymmetry.

AdS/CFT correspondence arises in type IIB string theory. Therefore we will discuss this theory in slightly more detail. The effective low energy theory associated with type IIB string turns out to be type IIB supergravity theory. The field content of this supergravity theory is given in table 2.1.1. Since this theory is concerned with the massless fields, they are classified by their representation under $SO(1,9)$ or $SO(8)$ group. 10 dimensional Supergravity (SUGRA) theory has 32 supercharges which are labelled by the doublet $N = N_L, N_R$, where the two doublets are the numbers of left and right handed supersymmetries respectively [50]. There are two possible theories; (1,1) which is the type IIA SUGRA and (2,0) being the type IIB SUGRA. Therefore, all the fermions in IIB are left handed which makes the theory chiral.

The bosonic part of the action for type IIB SUGRA is given by [51]

$$\begin{aligned} S = \frac{1}{4k_B^2}\int d^{10}x\sqrt{-g}(e^{-2\phi}\left(2R + 8\partial_\mu\phi\partial^\mu\phi - |H_3|^2\right) - |F_1|^2 \\ + |\tilde{F}_3|^2 + \frac{1}{2}|\tilde{F}_5|^2 - C^{(4)+}\wedge H_3 \wedge F_3), \end{aligned} \tag{2.1.24}$$

where, the field strengths are defined as,

$$\begin{aligned} F_1 &= dC^{(0)}, \quad H_3 = dB^{(2)}, \quad F_3 = dC^{(2)}, \quad F_5 = dC^{(4)+} \\ \tilde{F_3} &= F_3 - C^{(0)}H_3, \quad \tilde{F_5} = F_5 - \frac{1}{2}C^{(2)} \wedge H_3 + \frac{1}{2}B^{(2)} \wedge F_3, \\ \text{with,} & \qquad |F_p|^2 = \frac{1}{p!}g^{\mu_1\nu_1}...g^{\mu_p\nu_p}F^*_{\mu_1...\mu_p}F_{\nu_1...\nu_p}. \end{aligned} \tag{2.1.25}$$

The low energy limit of type IIB string theory also yields the same action given in (2.1.24). k_B in (2.1.24) is a free parameter which is related to α' which is a parameter in the string theory ($2k_B^2 = (2\pi)^7\alpha'^4$). α' determines the length ($l_s = \sqrt{\alpha'}$), tension ($T = 1/(2\pi\alpha')$) and the mass ($m^2 \sim 1/\alpha'$) of the fundamental string. The string coupling constant is the vacuum expectation value of the dilaton ($g_{str} =< e^{\phi} >$). Due to this fact one can consider the action (2.1.24) as an effective action with the higher powers of α' and g_{str} being neglected.

2.1.4 D-branes

An essential ingredient in the conjecture of AdS/CFT correspondence is D-brane. Supergravity theories, which can be considered as low energy effective theories in 10 dimensions admit extended object having p spatial dimension as a solution. Such solutions with p spatial dimension are called p branes. They have world volumes (p+1)-dimensional where 1 is the time dimension and p the spatial. For example, 0-brane can be considered as some kind of particles with 1-dimensional world volume. D-branes can be interpreted as some extremal limit of these p-branes. D-branes also has another description in terms of open strings [52], whose endpoints are constrained to move on the world volume of the p-brane. In other words, the endpoints satisfy Dirichlet boundary condition along the direction transverse to the world volume of the D-brane. For example, open strings which are free to move in 10 dimension represents D9 branes. However not all the extended objects are D branes, string can be regarded as a 1-brane as they are 1 dimensional extended object, but they are not D1-branes.

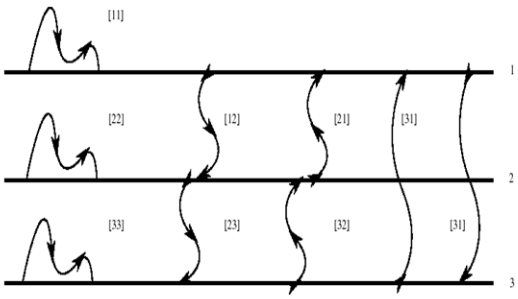

Figure 2.1: N coincident Dp brane

Dp branes are the p dimensional hyperplanes inside the d-dimensional space [49]. To specify such a hyperplane we need (d-p) number of linear conditions. We consider spacetime coordinates x^μ and split them into two groups. The first group comprises of components tangential of the brane world volume These are the p spatial coordinate plus the time coordinate. The second group comprises of (d-p) coordinates normal to the world volume.

$$\overbrace{x^0, x^1, x^2, ...x^p}^{Tangential} \underbrace{x^{p+1}, x^{p+2}, x^{p+3}, ...x^d}_{Normal} \tag{2.1.26}$$

The position of the Dp brane is specified by fixing the values of the coordinates normal to the brane. considering this split we write

$$x^a = \tilde{x}^a, a = p+1, p+2, ...d \tag{2.1.27}$$

Here $\tilde{x}^a$ are set of (d-p) constants. Similarly, the string coordinates $X^\mu(\tau, \sigma)$ split into

$$\overbrace{X^0, X^1, X^2, ...X^p}^{Tangential} \underbrace{X^{p+1}, X^{p+2}, X^{p+3}, ...X^d}_{Normal} \tag{2.1.28}$$

Since the end point of the open string must lie on the Dp brane, the string coordinates normal to the brane must satisfy Dirichlet boundary conditions

$$X^a(\tau, \sigma)|_{\sigma=0} = X^a(\tau, \sigma)|_{\sigma=\pi} = \tilde{x}^a, a = p+1, ..., d, \tag{2.1.29}$$

where X^a is called DD coordinates because both the endpoints satisfy Dirichlet boundary condition. The open string can move freely in the tangential direction with respect to D brane. Due to this, the tangential part of the string coordinate must follow the Neumann boundary conditions.

$$\partial_b X^b(\tau,\sigma)|_{\sigma=0} = \partial_b X^b(\tau,\sigma)|_{\sigma=\pi} = 0, b = p+1, ..., d \tag{2.1.30}$$

These string coordinates are known as NN coordinates as both the end of the string follows the Neumann Boundary condition. So we can also write

$$\overbrace{X^0, X^1, X^2, ...X^p}^{\text{NN coordinate}} \underbrace{X^{p+1}, X^{p+2}, X^{p+3}, ...X^d}_{\text{DD coordinate}} \tag{2.1.31}$$

Where the first part is NN coordinates, and the second part is DD coordinates. If we have N numbers of coincident Dp branes, the open string starting from one brane has a large number of choices on landing its another end, which is shown in fig.(2.1).

In the context of the correspondence D3- brane plays a crucial role. D3-branes appear as a solution of type IIB supergravity theory. The degrees of freedom associated with D3 branes corresponds to that of the open strings constrained to move on 3 dimensional hypersurface associated with the D3 brane. The massless excitations of the open strings are described by gauge fields and scalar fields. In particular, in the case of D3 brane, the dynamics of massless excitations are described by N=4 supersymmetric Yang-Mills theory (SYM) living in (3+1)-dimension. For a single D3 brane, it is described by a $U(1)$ theory. For N number of D3 branes placed on top of each other, there will be open strings beginning on one D3 brane and ending on another. So the degrees of freedom will appear as $N \times N$ matrices and the theory will be $N = 4$ $U(N)$ SYM [53]. With this brief understanding of branes, we would like to move on to our next section where we would like to discuss the origin of AdS/CFT correspondence.

2.1.5 Origin of AdS/CFT correspondence

In the context of string theory, Maldacena [2] conjectured the AdS/CFT correspondence on the basis of the following comparison. He considered a stack of N D3-Branes in Type IIB string theory (9+1 dimension) in two distinctive regimes and inquired about the decoupling of low energy physics in each of the following cases [54].

- The case with $g_s \to 0$ with N fixed, where the backreaction of the brane can be ignored. The vacuum state at that point could be a stack of D-branes in flat Minkowski space. The excitation about this state at low energy decouples into two segments. One segment corresponds to open string which starts and ends on the branes giving rise to the dynamics similar to $N = 4$ SYM gauge theory. The other segment is the massless spectrum of closed string propagating within the bulk, which is type IIB supergravity theory in the flat background. These two segments decouple in low energy limit.

- The second case that corresponds to $g_s \to 0$, $N \to \infty$ but with $g_s N$ fixed. In this case, one has to consider the backreaction from the branes. Type IIB supergravity admits black p-brane solutions which carry a charge, which acts as a source for $p + 1$ form potential. Here we would consider $p = 3$. The solution comprises of two free parameters i.e. mass (M) and charge (N). The additional constraint comes from the fact that the supergravity solution does not admit a naked sigularity [55].

$$M \geq \frac{N}{(2\pi)^p g_s l_s^{p+1}} \tag{2.1.32}$$

The low energy limit is acheived by taking the extremal solution that saturates 2.1.32, so this is related to the vacuum solution. Again there are two decoupled sectors for the low energy theory. Firstly one consider near horizon limit of these modes, then their energy measured by the observer at infinity can be considered as a low energy limit due to the redshift. We can now take an

infinitely red shifted limit, and consider modes living in the $AdS_5 \times S^5$ near extremal horizon geometry. This is type IIB string theory on$AdS_5 \times S^5$. As the low energy limit is given by the redshift rather than a long-wavelength limit, this theory comprises of the full spectrum of the massive string states and not just the massless supergravity sector. Secondly one can consider long wavelength excitations that live in the asymptotic flat spacetime away from the horizon. In this limit, the theory is described by Type IIB supergravity in Flat space. The reason why these two sectors decouple at low energy is due to the fact that infrared excitations near the extremal horizon cannot escape the gravitational well, and the supergravity modes away from the horizon have a long wavelength compared to the absorption cross-section of the black brane.

These two theories turn out to be a low energy description of the same theory in different limits. For large N limit the first case will turn out to be as one in second case i.e. $g_s \to 0$ and $N \to \infty$. Maldacena conjectured that these two low energy theories are an equivalent description of the same theory, which is written in different degrees of freedom. These two theories comprise of two decoupled sectors and share a common 9+1 dimension type IIB flat space supergravity theory. In short, type IIB string theory in $AdS_5 \times S^5$ background is equivalent to $U(N)$ SYM in 3+1 dimension. Although the assertion here is made in large N limit, Maldacena made the stronger conjecture that this equivalence, in fact, holds at any limit of N.

2.1.6 AdS/CFT statement

The correspondence mentioned above can be made more precise in terms of partition functions [4]

$$Z_{string}|_{\Phi} = Z_{SYM}[J], \tag{2.1.33}$$

where $Z_{string}|_{\Phi}$ is the partition function of Type IIB string theory on $AdS_5 \times S^5$, and $Z_{SYM}[J]$ is the partition function for $U(N)$ SYM in 4 dimension. The string theory partition function is a function of some asymptotic boundary conditions, rep-

resented by Φ. This results in fixing the spacetime to be asymptotically $\mathrm{AdS}_5 \times S^5$. In the gauge theory side, one considers the generating function, which is a function of some applied source terms J. According to the correspondence, the gravitational boundary conditions couples to the gauge theory source $\Phi \to J$. The asymptotic structure of AdS_5 at infinity happens to be a conformal boundary. The boundary conditions fix a representative of this conformal class. This metric defines the space-time of SYM, and one thinks of it as one of the sources J in the generating function. Relationship between two different parameters are given as [56–58]

$$\begin{aligned} g_s &= g_{YM}^2, \\ l^4 &= 4\pi g_s (\alpha')^2 N \end{aligned} \tag{2.1.34}$$

where g_s is the string coupling, g_{YM} is the Yang-Mills coupling and l is the AdS_5 and S_5 radius. One can consider the limit so that the gravitational theory simplifies. Firstly we consider the weak coupling i.e. $g_s \to 0$ limit of the string theory. This is the limit where $g_s \to 0$ keeping $\lambda = g_s N = g_{YM}^2 N$ fixed. Secondly, we will take large λ limit. This corresponds to strong coupling in CFT. We can see from (2.1.34), that the AdS length scale becomes large compared to the string length ($l_s = \sqrt{\alpha'}$). In this limit, we can ignore corrections arising from quantum loops on the worldsheet [56], and excited states on the string have large masses. We are left with an effective theory with only a small number of massless fields, namely classical supergravity. At this limit, one can consider the action to be that of massless supergravity sector, and the partition function is approximated by the sum of classical saddle points [59].

$$Z_{string} \sim \sum_{\phi_i | \Phi} e^{-S[\phi_i]_{sugra}} \tag{2.1.35}$$

where ϕ_i is the field configurations that solve the supergravity equations. The boundary conditions Φ for the partition function become the boundary conditions for the field equations, so the sum above is restricted to those ϕ_i which are consistent with Φ. Under the correspondence this supergravity boundary conditions that gets

mapped to the source in SYM theory. The conformal boundary is determined by the boundary condition of one of the fields which turns out to be a metric. Boundary conditions of the other fields in the supergravity side are mapped to the source terms for different local operators in the field theory. This is not a classical limit for the field theory, so this limit allows us to study a strongly coupled system in the field theory by solving the classical Supergravity theory.

In this chapter, we have presented a cursory review of AdS/CFT correspondence and its origin. In the next chapter, we will shift the gear and focus more on the strongly correlated systems arising in condensed matter. We will discuss the Fermi liquid theory, its breakdown and how one can apply AdS/CFT correspondence in such cases.

2.2 Fermi and non-Fermi liquids

AdS/CFT correspondence is useful for understanding the strongly coupled field theories and in the present case, we will be interested in such systems that appear in condensed matter. Although most of such systems are governed by strong correlation, there are non-perturbative methods designed to address their dynamics within the scope of condensed matter theories. However, with the discovery of the new materials, it has been found that there are limitations of applicability of such methods. In this section, we will briefly mention the salient features of such non-perturbative methods and their limitations, so as to set up the arena for the application of AdS/CFT correspondence.

Usually, in the condensed matter one studies the behaviour of a finite density system and when the system has less density one can study its behaviour using the statistical method. However, when one considers a large density system such that the quantum wavefunctions overlap or at low temperature when the quantum effects become important, many interesting phenomena occur. Let us focus on the latter part and study the macroscopic characteristics of low temperature ($T \to 0$) finite

density quantum system. From the past knowledge of the condensed matter, one can expect [60],

1. The system can have a gapped excitation. For a system to be gapped, a finite amount of energy is required for each of the excitations. When there is no energy density in the system ($T = 0$), the system is in the ground state and does not react to infinitesimal small perturbation.

2. Global symmetry of the system can be broken spontaneously by the ground-state. This is related to the ground state of bosons. In the case of spontaneously broken symmetry, the modes are gapless or massless Goldstone modes. The low temperature (or energy) physics is completely dominated by these modes.

3. The system can be Landau Fermi liquid if one considers a system with only fermions. This is based on the principle of Pauli exclusion. As Pauli exclusion principle forbids two fermions to be on the same quantum state, therefore they must have different momentum. The fermions start filling up the shells in the momentum space outward from the origin, with each outer shell having energy slightly larger than the former inner shell. The last added fermion gives the prefered momentum scale which is called the Fermi momentum (k_F) as shown in Fig. 2.2. The excitations of the Fermi liquid are massless which are defined by stable fermionic quasiparticle excitations. As the excitations are massless it controls the low temperature macroscopic behaviour of the system.

For a given low temperature finite density quantum system any one of the three might occur. So one can ask whether there are systems which do not fall on any of these three cases.

We can also ask the same question in a different manner but before asking the question first we have to start with a compressible state. A compressible state can be defined as a finite density state of a system having a $U(1)$ symmetry. In this system,

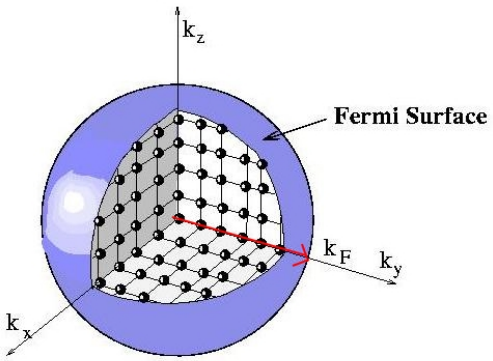

Figure 2.2: Fermi surface and Fermi momenta (k_F) denoted by a red arrow. (Image from http://www.physics.rutgers.edu/grad/620/).

the charge Q as a function of chemical potential μ is given by,

$$< Q > \equiv -\frac{\partial F}{\partial \mu} \sim \mu^{\alpha}, \quad \alpha > 0. \tag{2.2.1}$$

We can see the chemical potential is directly proportional to the charge density (upto a positive power). So small perturbation in chemical potential is enough for a system to conduct (as that in metals), which makes the compressible state a gapless. We will discuss some of the compressible states which are

- A state with broken translational symmetry is called a crystal and its state a solid.
- A state with spontaneously broken symmetry $U(1)$ symmetry. The state is known as a superconductor.
- A state which is not related with any symmetry breaking. This state is called a Fermi liquid.

Now we can ask the question that whether there can be a compressible state of matter without any symmetry breaking that is not a Fermi liquid and has a translation invariance. AdS/CFT correspondence can help us to answer this question. Understanding the breakdown of Fermi liquid theory will help us to find the answer, in this regard we will be reviewing non-Fermi liquid from [61, 62].

Fermi liquids are well understood subjects, whose behaviours are explained by excitation of long lived quasi-particles given by Landau Fermi liquid theory [63]. This theory explains the phenomenology of almost all the materials like metals, semiconductors, superconductors and superfluids. But in the 1980s there came some metallic materials whose thermodynamic and transport properties could not be understood by Landau Fermi liquid theory. These materials were called non-Fermi liquids, which incorporates high (T_c) cuprates superconductors and heavy fermions near a quantum phase transition [10, 64]. To point out the breaking of Fermi-liquid theory we start with a discussion of Fermi-liquid theory [61].

Let us first consider a system of Fermi gas, whose particles do not interact with one another. The ground state of this many particles system is given by the surface of the Fermi momentum (k_F) following the Pauli exclusion principle as explained before. Filling a state slightly outside this Fermi surface or removing a fermion from a filled state slightly inside the Fermi surface gives the low energy excitation of particle and hole respectively. These excitations are gapless and have a linear dispersion relation for $k - k_F << k_F$,

$$\epsilon(k) = E_0(k) - \mu = \frac{k_F}{m}(k - k_F) \equiv v_F(k - k_F) \tag{2.2.2}$$

where $E_0(k) = \frac{k^2}{2m}$ is the energy of a free particle. The energy of excitation is measured in terms of chemical potential $\mu = E_F = \frac{k_F^2}{2m}$. These excitations are seen as a pole of the retarded Green's function $G_R(\omega, k)$ for the electron operator in the complex frequency plane (momentum space),

$$G_R(\omega, \vec{k}) = \frac{1}{\omega - \epsilon(k) + iO_+}. \tag{2.2.3}$$

Fourier transform of $G_R(\omega, \vec{k})$ show that the propagator represents the propagation of a particle in a free space given by,

$$G_R(t, \vec{k}) \sim \theta(t) e^{-i\epsilon(k)t}. \tag{2.2.4}$$

Once the interaction between fermions is considered the notion of a single particle state becomes insignificant. One can expect that the qualitative behaviour of these interacting fermions at a very weak interaction should be same as that of non interacting fermions, but it is very hard to tell what will be the behaviour when the interaction between them is strong. According to Landau Fermi liquid theory, irrespective of interaction being weak or strong, the above qualitative behaviour does not change. Assuming that the ground state of an interacting fermionic system is characterized by a Fermi surface in momentum space at $k = k_F$ and the low energy excitation near the Fermi surface is defined by weakly interacting particles and holes called quasi-particles (quasi-particle and quasi-hole). These quasi-particles have the same charge as that of fundamental fermions and respect Pauli exclusion principle. The dispersion relation of a quasi-particle is given by,

$$\epsilon(k) = \frac{k_F}{m_*}(k - k_F) = v_F(k - k_F). \tag{2.2.5}$$

The dispersion relation looks similar to that of non-interacting fermions (2.2.2), where m_* the effective mass of the quasi-particles. The decay or scattering rate of this quasi-particle obeys

$$\Gamma \sim \frac{\epsilon^2}{\mu} << \epsilon \tag{2.2.6}$$

Though there is a strong interaction, particle or hole excitations near the Fermi surface still have a long lifetime, long enough to be approximated as a particle. The retarded Green's function is then modified to

$$G_R(t, \vec{k}) \sim e^{i\epsilon(k)t - \frac{\Gamma}{2}t}, \tag{2.2.7}$$

where $\Gamma \sim \epsilon^2(k)$. In the momentum space this retarted Green's function $G_R(\omega, \vec{k})$ takes the form

$$G_R(\omega, \vec{k}) = \frac{1}{\omega - v_F(k - k_F) + \sum(\omega, k)} + ..., \tag{2.2.8}$$

with $\sum(\omega, k) = \frac{i\Gamma}{2} \sim i\omega^2$, being the self energy. The residue $Z \leq 1$ of the pole, known as the quasi-particle weight. It is interpreted as the overlap between one quasiparticle state with the state created by the electron operator acting on a vacuum. The transport phenomenon predicted from this theory was, the linear dependence of specific heat (C_e) with temperature and the quadratically dependency of low temperature resistivity(ρ_e) with temperature.

$$\begin{aligned} C_e &= \gamma T + ..., \quad \gamma \sim m_* \\ \rho_e &= \rho_0 + AT^2 + ... \end{aligned} \tag{2.2.9}$$

This theory has been very successful in explaining almost all metallic states and also it does not require the system to be weakly coupled. The weakly coupled quasiparticles can emerge as the low energy collective excitations of a strongly interacting many-body system.

As mentioned earlier there were found some materials which did not obey Fermi liquid theory which was called non-Fermi liquids. Whose thermodynamic and transport properties could not be explained by Fermi liquid theory. One of the examples is the strange metal phase, where the electrical resistivity increases linearly with temperature and not quadratically as that of ordinary metal. In ARPES experiment, it was found that for high T_c cuprates in the strange metal region there still exists a Fermi surface. But the width of excitation is large as compared to Fermi liquids. The experiment results can be fitted to the following expression, postulated as "Marginal Fermi liquid" [61]

$$G_R(\omega, k) = \frac{h}{\omega - v_F(k - k_F) + \sum(\omega, k)}, \qquad \sum(\omega) \sim c\omega \log \omega + d\omega, \tag{2.2.10}$$

where c is real and d is complex. It can be seen from the above equation (2.2.10) that the system possesses gapless excitation with the dispersion relation $\omega = v_F(k - k_F)$. The decay rate (Γ) of the excitation which is given by the imaginary part of $\sum$, is linear in ω and not quadratic which was in case of Fermi liquid. The

decay rate Γ, which is proportional to ω, is so large, that it cannot be treated as a quasiparticle, as the excitation has already have decayed before it can propagate far enough i.e. one wavelength to show its particle-like properties. Scaling of the residue of the pole is $Z \sim 1/\log(k - k_F)$, so as one approach toward Fermi surface the quasiparticle weight vanishes logarithmically. Thus at the Fermi surface, the overlap of excitation with original electrons vanishes. The strange metals phase of cuprates has a Fermi surface but the excitation near the Fermi surface cannot be considered as a quasiparticle excitation.

From the analysis of various gravity models in top-down approach using AdS/CFT correspondence, one finds gravitational configurations predominantly correspond to states in the dual theory which are associated with such non-Fermi liquid and since the dynamics of non-Fermi liquid cannot be captured using Landau theory it makes it more interesting. In our analysis, as we will see we have obtained configurations, which are mostly in the non-Fermi regime. In some limiting values of the charge parameters, this approaches marginal Fermi liquid as well. Therefore one can expect that it will provide a further understanding of non-Fermi liquid from a different perspective. We will identify the Fermi surfaces, analyse the excitations and obtain the decay rates for those states.

2.2.1 More on Non-Fermi liquid

Before approaching these systems from a top-down perspective we would like to briefly review the behaviour of some of the materials that appear in the non-Fermi liquid phase. Such materials have been studied in the framework of condensed matter and we will take a look at the experimental and theoretical facts about them. This will provide further motivation for this work, set up the arena, and explain the scope of its further applications.

One class of materials which exhibits the non-Fermi liquid behaviour are certain phases of high temperature superconductor. BCS theory explains the superconductivity but this kind of materials, though have features of superconductors, deviates

from it. According to BCS theory, one can derive a gap equation, which defines an order parameter as a function of temperature [60]

$$\Delta(T) = \Gamma_{UV} e^{-\frac{1}{\lambda n_F T}}, \tag{2.2.11}$$

where Γ_{UV} is UV cutoff, λ a small coupling constant between the cooper pair and n_F is the number density. For normal material, there is a certain upper bound for the critical temperature which is violated by high temperature superconductors. BCS theory so fails to capture the mechanism of this high T_c superconductors.

The superconducting phase itself can be understood by the spontaneous breaking of $U(1)$ symmetry as it has no temperature bound. The main point here is why these materials become superconductors at such a high temperature. Experimentally the macroscopic characteristics of the strange metal state near the critical temperature are not as that of Fermi liquid. Also, the resistivity for non-Fermi liquids does not scale quadratically but linearly with temperature. The phase diagram for a high T_c superconductors is given in Fig. 2.3a At optimal doping (i.e. where T_c is maximum)

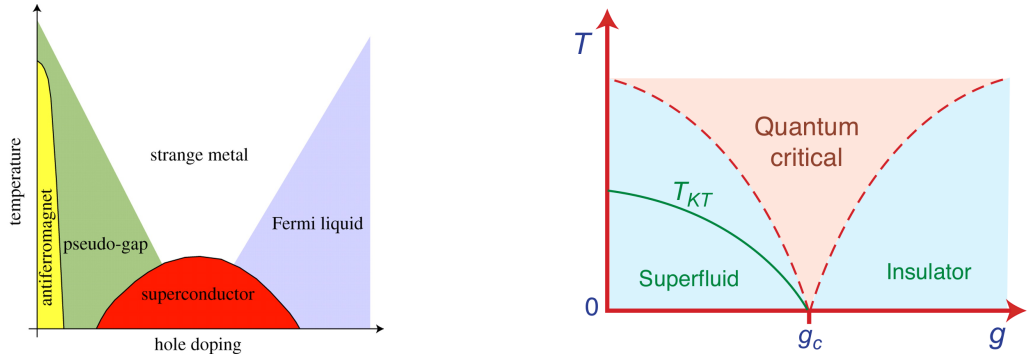

(a) Phase diagram of a high T_c superconductor (b) Phase diagram of a quantum phase transition

Figure 2.3: Typical Phase Diagrams

the material is in strange metal phase ($T > T_c$) and superconducting phase ($T < T_c$). As the doping is further increased there is a transition from strange metal to Fermi liquid regime. On decreasing the value of doping below optimal for the temperature higher than T_c, there is a phase transition to the pseudogap phase and at even lower value of doping it enters the antiferromagnetic phase.

Tremendous effort has been made in understanding the physics of strange metals and beyond the marginal Fermi liquid but the progress has been made only in one qualitative aspect. It is now believed that the phenomenon of quantum criticality leads to the behaviour of strange metals. Quantum criticality occurs near the quantum phase transition, which is a phase transition occurring at exactly zero temperature. As the transition occurs at $T = 0$, one cannot consider it to be driven by thermal fluctuation but as a quantum fluctuation. If the phase transition is of second order, the absence of scale at the critical point means that the field theory at this point is conformal. A conformal field theory at finite temperature is special in a way that its dynamics are controlled by zero temperature conformal symmetry. In general, the only aspect that changes is that all dimensionful quantities are now given in terms of the only present scale which is T.

Although the idea that the underlying mechanism of the strange metal is controlled by a finite T conformal field theory, in detail it is not so simple. This means that the phase diagram near a quantum critical point given in Fig. 2.3b (the "fan-like" region) looks similar to the phase diagram of high T_c superconductors. In particular, scaling only in terms of energy-temperature is scale invariance. In spatial directions, one still finds a distinct Fermi surface when compared to ARPES data. This feature of scale-less in the time-direction, but a distinct Fermi-momentum in the spatial directions has been known as local quantum criticality. To understand the behaviour of strange metal and its quantum criticality is to understand the role of fermionic degrees of freedom in strongly interacting CFTs.

2.3 Application of AdS/CFT to a finite density system

In previous sections, we have discussed some of the relevant aspects of condensed matter theories and the arena of applicability of AdS/CFT correspondence. We will be interested in finite density condensed matter system as our dual theory in the boundary. Though in the main text our approach will be slightly different, here we

would like to demonstrate how the gravity theory captures the various aspect of dual finite density system. For the sake of simplicity, we will begin with a simple case. After discussing this we will move to a more realistic example.

We will begin with Einstein-Hilbert action of gravity with a cosmological constant which has been discussed previously in section 2.1.2,

$$S = \frac{1}{2k^2}\int d^{d+1}x\sqrt{-g}\left(R + \frac{d(d-1)}{L^2}\right), \tag{2.3.1}$$

where L is the AdS radius.

$$\frac{2k^2}{L^{d-1}} \sim \frac{1}{N^2}, \tag{2.3.2}$$

Newton's constant is small in a large N limit of the boundary theory. The simplest solution to the above action is a pure anti-de Sitter space [55], which is given in (2.1.3) as

$$ds^2 = L^2(\frac{dz^2 + \eta_\mu\nu dx^\mu dx^\nu}{z^2}) = \frac{L^2}{z^2}(dz^2 - dt^2 + d\vec{x}^2), \tag{2.3.3}$$

where x^μ is the field theory spacetime coordinates and z is the radial or extra holographic coordinates in the gravitational theory, with the AdS boundary at $z = 0$. As (2.3.3) being the simplest and most symmetric solution in the gravity side, it represents the vacuum of the dual field theory. The vacuum of the CFT should be invariant under the conformal group in d-dimensions, which is precisely the same as the isometry group of AdS_{d+1}.

One of the aspects of this correspondence is that the renormalisation group (RG) flow of the field theory is geometrized by the spacetime of the dual gravity theory. Due to the factor $\frac{L^2}{z^2}$ given in front of the Minkowski metric in (2.3.3), local proper energy and length scales along field theory directions in AdS are related to those in the dual field theory by a z-dependent rescaling. Suppose we consider a physical process with proper energy (E_l) at some value of z in bulk (AdS). The bulk energy is measured in terms of local proper time $d\tau = \frac{L}{z}dt$ and when calculated in boundary

time t, it corresponds to an excitation of the boundary theory energy(E) given by

$$E = \frac{L}{z} E_l. \tag{2.3.4}$$

We see that physical processes in the bulk with identical proper energies but occurring at different radial positions correspond to different field theory processes with energies that scale as $1/z$. In a sense, the local bulk energies are given by the curvature scale ($E_l \sim 1/L$), then in its dual field theory side, the energy E associated with the bulk goes as $z \sim 1/E$. From this relation, one can associate z as RG scale of the boundary theory. relation implies that the z can be identified as renormalization group scale of the boundary theory. The high-energy (UV) limit $E \to \infty$ corresponds to $z \to 0$, i.e. to the near-boundary region, while the low-energy (IR) limit $E \to 0$ corresponds to $z \to \infty$, i.e. deep in the interior. As the geometry extends all the way to $z \to \infty$ the low energy excitations in the CFT is reflected in the bulk. If instead, we consider a boundary theory with a mass gap of m, the corresponding bulk geometry will then end smoothly at a finite value $z_0 \sim 1/m$. Similarly, at a finite temperature T, which provides an effective IR cutoff, the bulk spacetime will be cut off by an event horizon at a finite $z_0 \sim 1/T$.

Another aspect of the correspondence is the mapping of the field to the operator, i.e. for every (conformally primary) operator, one can find its dual field in the bulk. To show this mapping explicitly we will now consider a scalar operator $\mathcal{O}$ in the boundary theory. This operator is dual to some massive scalar field ϕ with mass m in the bulk, whose action can be written as

$$S_\phi = -\frac{1}{2} \int d^{d+1}x \sqrt{-g} \left((\nabla \phi)^2 + m^2 \phi^2 + ... \right). \tag{2.3.5}$$

Near boundary solution for the equation of motion arising from the above massive

scalar, action can be written as

$$\begin{aligned} \phi(z \to 0, x^\mu) &\sim A(x) z^{\Delta_-} + B(x) z^{\Delta_+}, \\ \text{where,} \quad \Delta_\pm &= \frac{d}{2} \pm \nu_u, \qquad \nu_u = \sqrt{\frac{d^2}{4} + m^2 L^2}. \end{aligned} \tag{2.3.6}$$

So, from the above equations (2.3.6) one can show

- Δ_+ is the comformal dimension of the dual operator $\mathcal{O}$.
- $A(x)$, which is the coefficient of the dominant term in $z \to 0$ limit, can be identified as the source term for $\mathcal{O}$. Nonzero $A(x)$ corresponds to adding a source term to the Lagrangian in field theory side.

$$\delta S_{\text{boundary}} = \int d^d x A(x) \mathcal{O}(x) \tag{2.3.7}$$

- $B(x)$, which is the coefficient of the subdominant term in $z \to 0$ limit, can be identified as the expectation value of the operator $\mathcal{O}$.

$$< \mathcal{O}(x) >= 2\nu_u B(x) \tag{2.3.8}$$

  If one finds a regular solution with $A = 0$ with $B \neq 0$ then the operator$\mathcal{O}(x)$ has developed an expectation value spontaneously, in the absence of source.

- From the above equations (2.3.7) and (2.3.8) one can write the linear response of the operator $\mathcal{O}(x)$ given by

$$G_R(\omega, k) = 2\nu_u \frac{B(\omega, k)}{A(\omega, k)} \tag{2.3.9}$$

  where $A(\omega, k)$ and $B(\omega, k)$ are the Fourier transform of the coefficients of (2.3.6) along the boundary direction. In order to determine G_R one needs an additional boundary condition at the interior of the spacetime. If the horizon develops in the interior of the spacetime, the boundary condition for comput-

ing a retarded correlator (G_R) is that the solution for ϕ should be infalling at the horizon [65].

- For a given value of $\nu = (0, 1)$, both terms in (2.3.6) are normalizable. There are two ways to quantize ϕ by imposing Dirichlet or Neumann conditions at the AdS boundary, which are called standard and alternative quantizations respectively. So depending on the boundary conditions the same gravity theory leads to two different dual CFTs. Here we have considered a standard quantization. In the alternative quantization, the role of $A(x)$ and $B(x)$ are exchanged.

2.3.1 Finite density states

In order to incorporate a finite density system, one has to consider a conformally invariant theory with $U(1)$ global symmetry. In this theory, we will turn on a nonzero chemical potential μ for the $U(1)$. The corresponding conserved current $J^\mu(x)$ is dual to a bulk gauge field $A_M(z, x)$, and the global $U(1)$ symmetry in the field theory is represented by a $U(1)$ gauge symmetry in the gravity side. Turning on a finite chemical potential for the current results in perturbing the field theory by the operator

$$\delta S_{boundary} = \mu \int d^d x J^t. \tag{2.3.10}$$

As similar to the case of the scalar, the boundary value of the gauge field A_μ is equal to the value of the field theory source for J^μ. Perturbation (2.3.10) means we should study a classical gravity solution where the gauge field $A_\mu(z)$ take some non zero value ($A_\mu(z \to 0) = \mu$) at the boundary.

Therefore to discuss finite density system in this setup we extend our earlier Einstein-Hilbert action to accommodate a Maxwell field on gravity side.

$$S = \frac{1}{2k^2} \int d^{d+1}\sqrt{-g} \left[R + \frac{d(d+1)}{L^2} + \frac{L^2}{g_f^2} F_{MN} F^{MN} \right], \tag{2.3.11}$$

where g_F is a bulk gauge coupling and F_{MN} is an electromagnetic (Maxwell) field tensor given by $F_{MN} = \partial_M A_N - \partial_N A_M$. The solution to the equation of motion for the above action with a relevant boundary condition is the Reissner-Nordstrom charged black hole (RN black hole) [66]. The metric for RN black hole is given as

$$\begin{aligned} ds^2 &= \frac{L^2}{z^2}(-f dt^2 + d\vec{x}^2) + \frac{L^2}{z^2}\frac{dz^2}{f}, \\ \text{with} \qquad f &= 1 + Q^2 z^{2d-2} - M z^d, \qquad A_t = \mu\left(1 - \frac{z^{d-2}}{z_0^{d-2}}\right), \end{aligned} \tag{2.3.12}$$

where Q, M, z_0 are constants. Nontrivial $f(z)$ means that the physics is changing with scale. The horizon lies at $f(z = z_0) = 0$. Q can be written in terms of chemical potential μ

$$Q = \sqrt{\frac{2d-2}{d-1}}\frac{\mu}{g_F z_0^{2(d-1)}}. \tag{2.3.13}$$

The temperature of the system is given by

$$T = \frac{d}{4\pi z_0}\left(1 - \frac{d-2}{d}Q^2 z_0^{2(d-1)}\right). \tag{2.3.14}$$

The solutions have two independent parameters μ and z_0. μ set the unit of the scale and the solution is characterised with dimensionless number μz_0. Thermodynamic quantities for the black hole such as charge density ρ, entropy density s and energy density ϵ are given by

$$\rho = \sqrt{2(d-1)(d-2)}\frac{L^{d-1}}{k^2}\frac{Q}{g_F}, \tag{2.3.15}$$

$$s = 2\pi\frac{L^{d-1}}{k^2}\frac{1}{z_0}^{d-1}, \tag{2.3.16}$$

$$\epsilon = \frac{d-1}{2}\frac{L^{d-1}}{k^2}M. \tag{2.3.17}$$

The charge density of the boundary theory is given by Q (upto a factor of constant). We can parameterize Q as follow

$$Q \equiv \sqrt{\frac{d}{d-2}}\frac{1}{z_*^{d-1}}, \tag{2.3.18}$$

where z_* is the length scale which is fixed by boundary charge density. Other quantities defined in terms of z_* are given as

$$\rho = \frac{L^{d-1}}{k^2}\frac{1}{e_d}\frac{1}{z_*^{d-1}}, \quad \mu = \frac{d(d-1)}{d-2}\frac{1}{z_*}\left(\frac{z_0}{z_*}\right)e_d, \quad T = \frac{d}{4\pi z_0}\left(1-\left(\frac{z_0}{z_*}\right)^{2(d-1)}\right) \tag{2.3.19}$$

where $e_d \equiv \frac{g_F}{\sqrt{2d(d-1)}}$. from the above equation (2.3.19), the zero temperature is obtained at $z = z_*$. The black hole metric at zero temperature is given by

$$f = 1 + \frac{d}{d-2}\frac{z^{2(d-1)}}{z_*^{2(d-1)}} - \frac{2(d-1)}{d-2}\frac{z^d}{z_*^d}, \quad A_t = \mu\left(1 - \frac{z^(d-2)}{z_*^{d-2}}\right)$$
$$\text{with,} \quad \mu_*\frac{1}{z_*} = 2(d-2)e^d\frac{\mu}{g_F^2} \tag{2.3.20}$$

The quantites in the field theory side will be

$$\rho = \frac{L^{d-1}}{k^2}\frac{1}{e_d}\frac{1}{z_*^{d-1}}, \quad s = \frac{L^{d-1}}{k^2}\frac{2\pi}{z_*^{d-1}}, \quad \epsilon = \frac{L^{d-1}}{k^2}\frac{(d-1)^2}{d-2}\frac{1}{z_*^d}. \tag{2.3.21}$$

For small z i.e. ($z << z_*$) we have $f \sim 1$. In this case, the black hole metric turns out to be pure AdS, which implies that physics at the energy scale much higher than the chemical potential is the conformal vacuum.

Let us focus on zero temperature limit for $z \sim z_*$ at $T = 0$. In this case, f has a double zero at the horizon ($z = z_*$),

$$f(z \to z_*) = d(d-1)\frac{(z_*-z)^2}{z_*^2} + ..., \tag{2.3.22}$$

which means that the horizon is infinitely away. Near horizon geometry now becomes $\text{AdS}_2 \times \mathbb{R}^{d-1}$ which is given by

$$ds^2 = \frac{L_2^2}{\zeta^2}(-dt^2 + d\zeta^2) + \mu_* L^2 d\vec{x}^2, \quad A = \frac{e_d}{\zeta}dt, \tag{2.3.23}$$

where L_2 is the AdS_2 curvature radius and ζ is the radial coordinate which is defined

as,

$$\zeta \equiv \frac{z_*^2}{d(d-1)(z_*-z)}, \quad L_2 = \frac{L}{\sqrt{d(d-1)}}. \tag{2.3.24}$$

In case of the finite temperature with $(z_* - z_0)/(z_*) << 1$ i.e. $T/\mu << 1$, the near horizon geometry is obtained by replacing the AdS_2 factor by AdS_2 black hole,

$$ds^2 = \frac{L_2^2}{\zeta^2}\left(-\left(1-\frac{\zeta^2}{\zeta_0^2}\right)dt^2 + \frac{d\zeta^2}{1-\frac{\zeta^2}{\zeta_0^2}}\right) + \mu_* L^2 d\vec{x}^2 \tag{2.3.25}$$

$$\text{where:} \quad A_t = \frac{e_d}{\zeta}\left(1-\frac{\zeta}{\zeta_0}\right), \quad \zeta_0 \equiv \frac{z_*}{d(d-1)(z_8-z_0)}, \quad T = \frac{1}{2\pi\zeta_0} \tag{2.3.26}$$

When the temperature of $T \sim \mu$, the AdS_2 structure is lost. As already discussed in the previous section, that RG scale of the boundary theory is determined by the radial direction z. So the near horizon AdS_2 structure plays an important role in understanding the low energy boundary theory at finite density.

These simple examples have made us familiar how the different features of finite density system get translated in terms of dual gravity theory. It enables us to address the various issues that arise in condensed matter systems as has been discussed in previous sections. However, the methodology used for this examples are bottom-up, we cooked up simple Lagrangian in the gravity theory which is tailor-made to have necessary symmetries of the field theory.

Though this method is extremely flexible and convenient, it has one limitation. Unless it can be incorporated within the framework of string theory, it is difficult to identify the exact dual field theory and operators. Instead, we will mostly use top-down approach, where we begin with know supergravity theory which can be obtained as low energy limit effective theory of string theory. The advantage is one can identify the exact dual field theory along with operators. In such a setup the analysis will provide a clearer understanding of the dynamics of field theory from the perspective of dual gravity.

Chapter 3

Holographic Fermi surfaces at zero temperature

3.1 Introduction

In the previous chapters, we have elaborately discussed the mechanism of AdS/CFT correspondence and its applicability to the study of the strongly correlated finite density system. As already been discussed in chapter 1, studies of various aspects of non-Fermi liquid using AdS/CFT correspondence in bottom-up approach have appeared in literature [15–17], such as effects of variation of mass, charge parameters, Pauli coupling as well as relation between scaling exponent of spectral function and dimension of dual operators, to name a few. In this chapter, we will discuss its application to study fermionic excitations of a specific theory in top-down approach. Since examples of pair of gravity and field theory in top-down approach are sparse not many studies have appeared in this line. We consider here a maximally gauged supergravity in seven dimension which is dual to $(2, 0)$ conformal field theory in six dimension. The dual theory is $(2, 0)$ conformal field theory in six dimensions which is world volume theory of M5 branes. As already mentioned in chapter 1, this theory is interesting in its own right, as this is one of the three maximally superconformal field theories. The other two, namely $N = 4$ SYM and ABJM theory have been

studied in [29, 31, 36]. This theory consists of tensor multiplet in six dimension and in that respect, the field content is different from the others. In particular, the gaugino appears as symplectic Majorana-Weyl spinors. So from such a study, we expect to learn something new about this theory and this will improve our understanding of the Fermi surface behaviour in general.

As we mentioned earlier the gravity dual of a finite temperature finite density system is a black hole. Black hole solution in a truncated version of this maximal gauged supergravity was already obtained in the literature and we will consider it as the background. On the dual side, this should correspond to a specific state of the system. This black hole background is characterised by two chemical potentials and at zero temperature gives rise to a one parameter family. The fermionic content of this supergravity theory consists of 16 spin-1/2 fermions which can be classified according to their charge with respect to $SO(5)$ R-symmetry group. For convenience, we have studied only those modes that do not couple to the gravitino. We find each mode admits Fermi surface over a range of parameter unless they vanish inside the oscillatory region where Green's function displayed log oscillatory behaviour. We also find excitations in the Fermi liquid and non-Fermi regime. In some cases, it approaches marginal Fermi-liquid behaviour near the boundary of the range. In the next section, we discuss the charged black hole solution. Section 3 and 4 are devoted to fermionic fluctuations and solution of Dirac equations respectively. Section 5 and 6 discuss the results. The contents of this chapter have been published in [44].

3.2 Bosonic Action

M-theory is a supersymmetric theory which lives in 11 dimensions. As conjectured in [2], compactification of M-theory on $\text{AdS}_7 \times S^4$ is dual to a conformal field theory in six dimensions. One can consider a consistent truncation of 11 dimensional supergravity to the maximal ($N = 4$) gauged supergravity in seven dimension keeping only the lowest massless modes [67]. This can be considered as a dual to the six

dimensional conformal field theory at the appropriate limit [2–4].

The field contents of the supergravity theory on the bosonic side of the action are as follows [67–69]. It involves two groups, a gauged $SO(5)_g$ and a composite $SO(5)_c$. It comprises of a gravitational field, Yang-Mills gauge fields, fourteen scalars and five rank-3 tensor fields. The gauge fields are in the adjoint representation of $SO(5)_g$ gauge group and the scalars parametrise $SL(5,R)/SO(5)_c$ coset. The rank-3 tensor fields are in the representation $\mathbf{5}$ of $SO(5)_g$. The fermionic sector contents are sixteen spin-half fields which transform as the $\mathbf{16}$ of $SO(5)_c$ and four gravitini transforming as $\mathbf{4}$ of $SO(5)_c$.

In order to describe the action we introduce the following notation. We denote $SO(5)_g$ and $SO(5)_c$ indices by $I, J = 1, 2, .., 5$ and $i, j = 1, 2, .., 5$ respectively. We represent fourteen scalar degrees of freedom by V_I^i. They transform as $\mathbf{5}$ under both $SO(5)_g$ and $SO(5)_c$ and parametrise $SL(5,R)/SO(5)_c$ coset. With these scalar fields one can construct tensor T_{ij} as $T_{ij} = V_i^{-1\ I} V_j^{-1\ J} \delta_{IJ}$ consisting of $SO(5)_c$ indices only.T denotes the trace of T_{ij} as given by $T = T_{ij}\delta^{ij}$. The potentials for the scalar fields are given in terms of T_{ij}. The kinetic term for the scalar fields involve covariant derivatives given by $\mathcal{D}_\mu V_I^i = \partial_\mu V_I^i - igA_\mu^a\ (J^a)_I^J\ V_J^i$, where $(J^a)_I^J$ are the generators of $SO(5)$ in the $\mathbf{5}$ representation. Kinetic terms are written in terms of symmetric and antisymmetric parts of the covariant derivative, given by P_μ and Q_μ. Their expression may be obtained from $V_i^{-1I}\mathcal{D}_\mu V_I^k \delta_{kj} = (Q_\mu)_{[ij]} + (P_\mu)_{(ij)}$.

With these notations the bosonic part of the lagrangian is given as:

$$\begin{aligned} 2\kappa^2 e^{-1}\mathcal{L}_{boson} =& R + \frac{1}{2}m^2(T^2 - 2T_{ij}T^{ij}) - tr(P_\mu P^\mu) - \frac{1}{2}(V_I^i V_J^j F_{\mu\nu}^{IJ})^2 + m^2(V_i^{-1I}C_{\mu\nu\rho I})^2 \\ &+ e^{-1}\left(\frac{1}{2}\delta^{IJ}(C_3)_I \wedge (dC_3)_J + m\epsilon_{IJKLM}(C_3)_I F_2^{JK} F_2^{LM} + m^{-1}p_2(A,F)\right) \end{aligned} \tag{3.2.1}$$

To obtain a black hole solution the above action can be further simplified in the following manner [70,71]. We keep only two gauge fields $A_\mu^{(1)}$ and $A_\mu^{(2)}$ along two of the Cartan generators J^{12} and J^{34} respectively of $SO(5)_g$ and set other components

to be zero. In addition, we set three-form potential $C^I_{\mu\nu\rho}$ to zero as well. We further make a gauge choice to identify $SO(5)_g$ with $SO(5)_c$ by restricting the vielbein to the following

$$V^i_I = \text{diag}(e^{-\phi_1} \quad e^{-\phi_1} \quad e^{-\phi_2} \quad e^{-\phi_2} \quad e^{2\phi_1+2\phi_2}). \tag{3.2.2}$$

This truncation of field contents leads to the following reduced bosonic Lagrangian [70]

$$\begin{aligned} 2\kappa^2 e^{-1}\mathcal{L} =& R - \frac{1}{2}m^2\nu(\phi_1,\phi_2) - 6(\partial\phi_1)^2 - 6(\partial\phi_2)^2 - 8(\partial_\mu\phi_1)(\partial^\mu\phi_2) \\ & -e^{-4\phi_1}F^{(1)2}_{\mu\nu} - e^{-4\phi_2}F^{(2)2}_{\mu\nu} + m^{-1}p_2(A,F), \\ \text{where} \quad \nu(\phi_1,\phi_2) =& -8e^{2(\phi_1+\phi_2)} - 4e^{-2\phi_1-4\phi_2} - 4e^{-4\phi_1-2\phi_2} + e^{-8\phi_1-8\phi_2}. \end{aligned} \tag{3.2.3}$$

With the above truncated bosonic lagrangian one can obtain an asymptotically AdS black hole solution[1] which is charged with respect to the two gauge fields [70, 71]. The black hole solution is given by

$$\begin{aligned} ds^2 &= e^{2A(r)}(h(r)dt^2 - d\vec{x}^2) - \frac{e^{2B(r)}}{h(r)}dr^2, \\ A^{(1)}_\mu dx^\mu &= A^{(1)}(r)dt, \quad A^{(2)}_\mu dx^\mu = A^{(2)}(r)dt, \quad \phi_1 = \phi_1(r), \quad \phi_2 = \phi_2(r). \end{aligned} \tag{3.2.4}$$

The metric functions, scalar fields and gauge fields have only r dependence and their

[1] [71] gave $k = 0, \pm 1$ solutions of the bosonic action of which we consider $k = 0$

expressions are as follows:

$$
\begin{aligned}
e^{2A(r)} &= \frac{m^2}{4} r^2 \left(1+\frac{Q_1^2}{r^4}\right)^{\frac{1}{5}} \left(1+\frac{Q_2^2}{r^4}\right)^{\frac{1}{5}}, \quad e^{2B(r)} = \frac{4}{m^2}\frac{1}{r^2}\left(1+\frac{Q_1^2}{r^4}\right)^{-\frac{4}{5}} \left(1+\frac{Q_2^2}{r^4}\right)^{-\frac{4}{5}}, \\
h(r) &= \left(1-\frac{r^2}{r_h^2}\frac{(r_h^4+Q_1^2)(r_h^4+Q_2^2)}{(r^4+Q_1^2)(r^4+Q_2^2)}\right), \\
A^{(1)}(r) &= \frac{1}{2}\frac{m}{2}\frac{Q_1}{r_h}\left(\frac{r_h^4+Q_2^2}{r_h^4+Q_1^2}\right)^{\frac{1}{2}}\left(1-\frac{r_h^4+Q_1^2}{r^4+Q_1^2}\right), \quad A^{(2)}(r) = \frac{1}{2}\frac{m}{2}\frac{Q_2}{r_h}\left(\frac{r_h^4+Q_1^2}{r_h^4+Q_2^2}\right)^{\frac{1}{2}}\left(1-\frac{r_h^4+Q_2^2}{r^4+Q_2^2}\right), \\
e^{2\phi_1(r)} &= r^{\frac{4}{5}}\frac{(r^4+Q_2^2)^{\frac{2}{5}}}{(r^4+Q_1^2)^{\frac{3}{5}}}, \quad e^{2\phi_2(r)} = r^{\frac{4}{5}}\frac{(r^4+Q_1^2)^{\frac{2}{5}}}{(r^4+Q_2^2)^{\frac{3}{5}}}.
\end{aligned}
\tag{3.2.5}
$$

the remaining parameter of the background m and g are fixed by the radius of AdS L as $m/2 = 1/L$ and $g = 2m$. The thermodynamic property of the black hole i.e. temperature and entropy density are given by are given by [31]

$$
T = \frac{m^2}{4}\frac{r_h}{2\pi}\frac{3+\frac{Q_1^2}{r_h^4}+\frac{Q_2^2}{r_h^4}-\frac{Q_1^2Q_2^2}{r_h^8}}{\sqrt{1+\frac{Q_1^2}{r_h^4}}\sqrt{1+\frac{Q_2^2}{r_h^4}}}, \quad s = (m/2)^5\frac{r_h}{4G}\sqrt{(r_h^4+Q_1^2)(r_h^4+Q_2^2)}. \tag{3.2.6}
$$

The charge density and chemical potentials become

$$
\mu_1 = \frac{1}{2}\frac{m^2}{4}\frac{Q_1}{r_h}\left(\frac{r_h^4+Q_2^2}{r_h^4+Q_1^2}\right)^{\frac{1}{2}} \quad , \quad \mu_2 = \frac{1}{2}\frac{m^2}{4}\frac{Q_2}{r_h}\left(\frac{r_h^4+Q_1^2}{r_h^4+Q_2^2}\right)^{\frac{1}{2}} \quad , \quad \rho_i = \frac{Q_i s}{2\pi r_h^2}. \tag{3.2.7}
$$

From the above equations, one can note that this black hole characterised by two charges has an extremal limit where $T = 0$,

$$
3+\frac{Q_1^2}{r_h^4}+\frac{Q_2^2}{r_h^4}-\frac{Q_1^2Q_2^2}{r_h^8} = 0. \tag{3.2.8}
$$

One can observe that the black hole is characterised by a zero-point entropy i.e. at zero temperature the entropy of this black hole solution does not vanish. In the following sections, we will introduce fermions on this background to study its fluctuations and analysis whether the boundary theory admits a Fermi surface/s or not.

3.3 Fermionic Action

The field content on the fermionic sector of this supergravity theory are spin-3/2 gravitini ψ_μ^A and spin-1/2 field λ_i^A which transforms as **4** and **16** under the group of $SO(5)_c$ respectively [67–69]. The spinor indices is given by A and i represents vector indices of $SO(5)_c$ and they satisfy $\gamma^i\lambda_i = 0$.

Spinor indices are lowered and raised by antisymmetric matrices Ω_{AB} and $\tilde{\Omega}^{AB}$ where $\Omega_{AB} = \text{antidiag}(\mathbf{1}, -\mathbf{1})$, $\tilde{\Omega}^{AB}\Omega_{AC} = \delta^B_C$. Both ψ and λ are eight-dimensional symplectic Majorana spinors obeying $\bar{\lambda}^A = \lambda^\dagger_A\Gamma^0$ and $\bar{\lambda}_A = \lambda^T_A C_7$, where C_7 is charge conjugation matrix in seven Minkowski dimension, satisfying $C_7\Gamma^\mu C_7^{-1} = -(\Gamma^\mu)^T$ and is symmetric. These relations hold for gravitino as well.

We have adopted the notation given in [68] with the negative sign of metric. For convenience we have chosen the two generators of Cartan as J^{12} and J^{34} and the five components of a vector v^i in the vector representation is rewritten as

$$v^{1\pm} = \frac{1}{\sqrt{2}}(v^1 \pm iv^2), \quad v^{2\pm} = \frac{1}{\sqrt{2}}(v^3 \pm iv^4), \quad v^0 = v^5. \tag{3.3.1}$$

Under these new notations the charges under $U(1) \times U(1)$ are given by $(\mp 1, 0)$, $(0, \mp 1)$ and $(0, 0)$ for $v^{1\pm}$, $v^{2\pm}$ and v^0 repectively.

One can use the gamma matrices γ of $SO(5)$ to produce the spin reprsentations of these two generators of $SO(5)$ group. They are given by $\psi(s_{12}, s_{34})$, where $s_{12}, s_{34} = \pm\frac{1}{2}$ acts as the respective charges.

$$S^{12} = -(i/2)\gamma^1\gamma^2, \quad S^{34} = -(i/2)\gamma^3\gamma^4, \tag{3.3.2}$$

The Lagrangian for spin-1/2 fields λ^i is as follows

$$e^{-1}\mathcal{L}_{fermion} = \frac{i}{2}\bar{\lambda}_i(\Gamma^\mu D_\mu\lambda^i) - \frac{m}{8}\bar{\lambda}_i(8T^{ij} - T\delta^{ij})\lambda_j - \frac{1}{32}\bar{\lambda}_i\gamma^j\gamma^{kl}\gamma^i\Gamma^{\mu\nu}\lambda_j(F_{\mu\nu})_{kl}, \tag{3.3.3}$$

where the first term in the Lagrangian is a kinetic term, second a mass term and the last term is Pauli or dipole coupling term. The covariant derivatives the kinetic term

are given by

$$D_\mu \lambda^i = \nabla_\mu \lambda^i - ig[(A^{(1)}_\mu (J^{12})^i_j + A^{(2)}_\mu (J^{34})^i_j)\lambda^j + (A^{(1)}_\mu S^{12} + A^{(2)}_\mu S^{34})\lambda^i], \quad (3.3.4)$$

where covariant derivative ∇_μ consists of spin connection which is given by

$$\nabla_\mu = \partial_\mu - \frac{1}{4}(\omega_\mu)_{ab}\Gamma^{ab}. \quad (3.3.5)$$

with J^{12} and J^{34} being the vector representation of the generators in $U(1) \times U(1)$. S^{12} and S^{34} are spinor representations of the generators in this group.

The Lagrangian consists of the coupling between gravitino ψ_μ and spin-1/2 fields λ^i which is given by

$$e^{-1}\mathcal{L}_{int} = \bar{\psi}_\mu(-m\Gamma^\mu T_{ij}\gamma^i\lambda^j + \Gamma^\nu\Gamma^\mu(P_\nu)_{ij}\gamma^i\lambda^j + \frac{1}{2}\Gamma^{\nu\sigma}\Gamma^\mu(F_{\nu\sigma})_{ij}\gamma^i\lambda^j), \quad (3.3.6)$$

For our purpose, we would like to study the fermions with only spin 1/2 field. So in this regards, we will be only considering those components of λ which decouples from gravitino [30]. As one can observe that the gravitino is charged $\pm\frac{1}{2}$ with respect to two Cartans of $SO(5)$. Therefore all the λ's which have charge $\pm\frac{3}{2}$ under any one of the two generators cannot couple to gravitino. From equation (3.3.6) one finds that λ and gravitino couples in the following manner: $\gamma^{1+}\lambda^{1-}$, $\gamma^{1-}\lambda^{1+}$, $\gamma^{2+}\lambda^{2-}$ and $\gamma^{2-}\lambda^{2+}$. Therefore, we will consider only the following eight components of λ, given in this notation by $\lambda^{1+}(-\frac{1}{2}, s_{34})$, $\lambda^{1-}(\frac{1}{2}, s_{34})$, $\lambda^{2+}(s_{12}, -\frac{1}{2})$ and $\lambda^{2-}(s_{12}, \frac{1}{2})$ with $s_{12}, s_{34} = \pm 1/2$, each of which has at least one of the charges equals $\pm\frac{3}{2}$ in our notation.

The dual field theory for this maximally gauged supergravity theory corresponds to six dimensional $(2, 0)$ conformal field theory. It has $SO(5)$ group with an R-symmetry. The field contents in this dual theory which are relevant in this case are tensor multiplet comprising of a self-dual 2-form potential $B_{\mu\nu}$ which transforms as

1 , five scalars Σ^i and four symplectic Majorana-Weyl spinors [2] ψ^A transforming as **5** and **4** under the group of R-symmetry respectively. All the fields are in the adjoint representation of $U(N)$. As mentioned above $U(1)\times U(1)$ charges related to the various fields are Σ^0, $\Sigma^{1\pm}$ and $\Sigma^{2\pm}$ with charges $(0,0)$, $(\mp 1,0)$ and $(0,\mp 1)$ respectively. For the spinors the representations are given as $\psi(s_{12},s_{34})$ with $s_{12},s_{34}=\pm 1/2$. The operators dual to the spinor which transforms under **16** in the supergravity theory are of the form $tr(\Sigma\psi)$ [72, 73]. So counting the charges of $U(1)\times U(1)$, the operators which are considered here can be written as $tr(\Sigma^{1\pm}\psi(s_{12},s_{34}))$ and $tr(\Sigma^{2\pm}\psi(s_{12},s_{34}))$ with $s_{12},s_{34}=\pm 1/2$. All these operators with their corresponding charges are given in table 3.4.1.

3.4 Dirac Equations

To examine Fermi surfaces in the boundary theory, we will consider arrangements of Dirac equations for the eight spinors that don't couple to the gravitino. The Dirac equations that pursue from the fermionic lagrangian (3.3.3), on setting the parts of fermions that couple to gravitino equivalent to zero, gives the following equation of motion:

$$\begin{aligned}&[i\Gamma^\mu\nabla_\mu - m(m_1e^{2\phi_1}+m_2e^{2\phi_2}+m_3e^{-4(\phi_1+\phi_2)})+2m(q_1A^{(1)}_\mu+q_2A^{(2)}_\mu)\\&+i(p_1e^{-2\phi_1}F^{(1)}_{\mu\nu}+p_2e^{-2\phi_2}F^{(2)}_{\mu\nu})\Gamma^{\mu\nu}]\lambda^i(s_{12},s_{34})=0,\end{aligned}\tag{3.4.1}$$

where values of all the parameters m_1, m_2, m_3, q_1, q_2, p_1 and p_2 are summerised in table 3.4.1. One can see the top four columns are traded with base four lines under $(m_1,q_1,p_1)\leftrightarrow(m_2,q_2,p_2)$ thus the Dirac conditions stay unaltered given one exchanges the charge parameters Q_1 and Q_2 too. Under $q_i\to -q_i, p_i\to -p_i$, (1,4), (2,3), (5,8) and (6,7) will be traded between one another.

In the black hole background (3.2.4 we will consider the Dirac equations (3.4.1).

[2] One may not get confused from ψ_μ with ψ^A. ψ with superscript correspond to spinor in dual field theory, whereas ψ with subscript represent grivitino in supergravity theory.

Table 3.4.1: Parameters and dual operators correponding to various fermionic modes

No.	$\lambda^I(s_{12}, s_{34})$	m_1	m_2	m_3	q_1	q_2	p_1	p_2	dual operator
1	$\lambda^{1-}(\frac{1}{2},\frac{1}{2})$	$\frac{3}{2}$	-$\frac{1}{2}$	-$\frac{1}{4}$	$\frac{3}{2}$	$\frac{1}{2}$	-$\frac{1}{4}$	-$\frac{1}{4}$	$tr(\Sigma^{1-}\psi(\frac{1}{2},\frac{1}{2}))$
2	$\lambda^{1-}(\frac{1}{2},-\frac{1}{2})$	$\frac{3}{2}$	-$\frac{1}{2}$	-$\frac{1}{4}$	$\frac{3}{2}$	$-\frac{1}{2}$	-$\frac{1}{4}$	$\frac{1}{4}$	$tr(\Sigma^{1-}\psi(\frac{1}{2},-\frac{1}{2}))$
3	$\lambda^{1+}(-\frac{1}{2},\frac{1}{2})$	$\frac{3}{2}$	-$\frac{1}{2}$	-$\frac{1}{4}$	-$\frac{3}{2}$	$\frac{1}{2}$	$\frac{1}{4}$	-$\frac{1}{4}$	$tr(\Sigma^{1+}\psi(-\frac{1}{2},\frac{1}{2}))$
4	$\lambda^{1+}(-\frac{1}{2},-\frac{1}{2})$	$\frac{3}{2}$	-$\frac{1}{2}$	-$\frac{1}{4}$	- $\frac{3}{2}$	-$\frac{1}{2}$	$\frac{1}{4}$	$\frac{1}{4}$	$tr(\Sigma^{1+}\psi(-\frac{1}{2},-\frac{1}{2}))$
5	$\lambda^{2-}(\frac{1}{2},\frac{1}{2})$	-$\frac{1}{2}$	$\frac{3}{2}$	-$\frac{1}{4}$	$\frac{1}{2}$	$\frac{3}{2}$	-$\frac{1}{4}$	-$\frac{1}{4}$	$tr(\Sigma^{2-}\psi(\frac{1}{2},\frac{1}{2}))$
6	$\lambda^{2-}(-\frac{1}{2},\frac{1}{2})$	-$\frac{1}{2}$	$\frac{3}{2}$	-$\frac{1}{4}$	$-\frac{1}{2}$	$\frac{3}{2}$	$\frac{1}{4}$	-$\frac{1}{4}$	$tr(\Sigma^{2-}\psi(-\frac{1}{2},\frac{1}{2}))$
7	$\lambda^{2+}(\frac{1}{2},-\frac{1}{2})$	-$\frac{1}{2}$	$\frac{3}{2}$	-$\frac{1}{4}$	$\frac{1}{2}$	-$\frac{3}{2}$	-$\frac{1}{4}$	$\frac{1}{4}$	$tr(\Sigma^{2+}\psi(\frac{1}{2},-\frac{1}{2}))$
8	$\lambda^{2+}(-\frac{1}{2},-\frac{1}{2})$	-$\frac{1}{2}$	$\frac{3}{2}$	-$\frac{1}{4}$	$-\frac{1}{2}$	-$\frac{3}{2}$	$\frac{1}{4}$	$\frac{1}{4}$	$tr(\Sigma^{2+}\psi(-\frac{1}{2},-\frac{1}{2}))$

The Γ-matrices in tangential space indices are choosen as follows:

$$\Gamma^{\hat{t}} = \begin{pmatrix} \Gamma_1^{\hat{t}} & 0 \\ 0 & \Gamma_1^{\hat{t}} \end{pmatrix}, \qquad \Gamma^{\hat{r}} = \begin{pmatrix} \Gamma_1^{\hat{r}} & 0 \\ 0 & \Gamma_1^{\hat{r}} \end{pmatrix}, \qquad \Gamma^{\hat{i}} = \begin{pmatrix} \Gamma_1^{\hat{i}} & 0 \\ 0 & \Gamma_1^{\hat{i}} \end{pmatrix}$$
$$\Gamma_1^{\hat{t}} = \begin{pmatrix} \sigma_1 & 0 \\ 0 & \sigma_1 \end{pmatrix}, \qquad \Gamma_1^{\hat{r}} = \begin{pmatrix} i\sigma_3 & 0 \\ 0 & i\sigma_3 \end{pmatrix}, \qquad \Gamma_1^{\hat{i}} = \begin{pmatrix} i\sigma_2 & 0 \\ 0 & -i\sigma_2 \end{pmatrix}, \tag{3.4.2}$$

where σ_1, σ_2 and σ_3 are Pauli spin matrices.

We have redefined λ^i to get rid of the spin connection in the covariant derivative $\nabla_\mu\lambda^i = (\partial_\mu - \frac{1}{4}(\omega_\mu)_{ab}\Gamma^{ab})\lambda^i$

$$\lambda^i = e^{-A(r)}h(r)^{-1/4}\chi^i. \tag{3.4.3}$$

χ^i depends on r, time t and space x as

$$\chi^i(t, r, x) = e^{-i\omega t+ikx}\chi^i(r). \tag{3.4.4}$$

χ^i can be written in form of two 4-component spinors, Ψ^i and η^i as follows:

$$\chi^i = \begin{pmatrix} \Psi^i \\ \eta^i \end{pmatrix}. \tag{3.4.5}$$

As one can check from the Γ matrices (3.4.2) that the block diagonal structure of Γ

matrices gives the same equations for both Ψ^i and η^i. So it is sufficient to consider only one of the four component spinors, therefore we will be considering Ψ^i. We have chosen

$$\Psi^i = \begin{pmatrix} \Psi^i_1 \\ \Psi^i_2 \end{pmatrix}, \quad \Psi^i_\alpha = \begin{pmatrix} \Psi^i_{\alpha-} \\ \Psi^i_{\alpha+} \end{pmatrix}, \quad \alpha = 1, 2. \tag{3.4.6}$$

With these notations considering the bosonoic background (3.2.4, 3.2.5) the Dirac equations reduce to

$$\begin{aligned} \left(\partial_r + m\frac{e^B}{\sqrt{h}}M(\phi_1,\phi_2)\right)\Psi_{\alpha-} &= \frac{e^{B-A}}{\sqrt{h}}[u(r) + (-1)^\alpha k - v(r)]\Psi_{\alpha+} \\ \left(\partial_r - m\frac{e^B}{\sqrt{h}}M(\phi_1,\phi_2)\right)\Psi_{\alpha+} &= \frac{e^{B-A}}{\sqrt{h}}[-u(r) + (-1)^\alpha k - v(r)]\Psi_{\alpha-}, \end{aligned} \tag{3.4.7}$$

where we have introduced other functions as follows:

$$\begin{aligned} M(\phi_1,\phi_2) &= (m_1 e^{2\phi_1} + m_2 e^{2\phi_2} + m_3 e^{-4(\phi_1+\phi_2)}) \\ u(r) &= \frac{1}{\sqrt{h}}[\omega + 2m(q_1 A^{(1)}_t + q_2 A^{(2)}_t)] \\ v(r) &= 2e^{-B}[p_1 e^{-2\phi_1} F^{(1)}_{rt} + p_2 e^{-2\phi_2} F^{(2)}_{rt}] \end{aligned} \tag{3.4.8}$$

These are two first order coupled equations, and we can decoupl these equations by arranging them in second order form:

$$\begin{aligned} &\partial_r^2\Psi_{\alpha\pm} - \partial_r \log\left(\frac{e^{B-A}}{\sqrt{h}}[v - (-1)^\alpha k \pm u]\right)\partial_r\Psi_{\alpha\pm} + [\mp\partial_r\left(\frac{e^B}{\sqrt{h}}mM\right) - \frac{m^2M^2e^{2B}}{h} \\ &+\frac{e^{2(B-A)}}{h}[u^2 - (v-(-1)^\alpha k)^2] \pm \frac{e^B}{\sqrt{h}}mM\partial_r \log\left(\frac{e^{B-A}}{\sqrt{h}}[v-(-1)^\alpha k \pm u]\right)]\Psi_{\alpha\pm} = 0 \end{aligned} \tag{3.4.9}$$

Flipping sign of k gives a relation between $\alpha = 1, 2$. Flipping sign of q_i, p_i, ω and k does not yield any change in the equations (3.4.9). Therefore the spinors and their conjugates, which are related to each other through flipping of signs of q_i, p_i will have solutions related through a change of signs of k and ω.

• **Asymptotic limit:**

Following [30] we will expand (3.4.9) in asymptotic limit. In this limit $r \to \infty$,

the scalar fields are given by $e^{2\phi_1} = e^{2\phi_2} = 1$ which fix $M(\phi_1, \phi_2) = (m_1 + m_2 + m_3)$. Substituting this in (3.4.9) and expanding the other values near asymptotics we obtain

$$\partial_r^2 \Psi_{\alpha\pm} + \frac{2}{r}\partial_r \Psi_{\alpha\pm} - \frac{(2M_0)^2 \pm 2M_0}{r^2}\Psi_{\alpha\pm} = 0, \tag{3.4.10}$$

where we use $M_0 = m_1 + m_2 + m_3$, solutions for the above differential equation is,

$$\Psi_{\alpha+} = A_\alpha(k) r^{2M_0} + B_\alpha(k) r^{-2M_0-1}, \qquad \Psi_{\alpha-} = C_\alpha(k) r^{2M_0-1} + D_\alpha(k) r^{-2M_0}. \tag{3.4.11}$$

The first order dirac equations (3.4.7) gives a relation between $A_\alpha(k)$ ($B_\alpha(k)$) and $C_\alpha(k)$ ($D_\alpha(k)$) [30, 31, 74],

$$C_\alpha = \frac{\tilde{\omega} + (-1)^\alpha k}{2(2M_0) - 1} A_\alpha, \quad B_\alpha = \frac{\tilde{\omega} - (-1)^\alpha k}{2(2M_0) + 1} D_\alpha, \quad \text{where} \quad \tilde{\omega} = \omega + 4\sum_{i=1}^{2} q_i A_t^{(i)}(r \to \infty). \tag{3.4.12}$$

Given $M_0 > 0$, the source and response term are given by A iand D respectively. The retarded Green's function for dual fermionic operator can be obtained by

$$D_\alpha = (G_R)_{\alpha\beta} A_\beta, \tag{3.4.13}$$

where the solution is obtained by considering the infalling boundary condition at the horizon. In this case, the Green's function becomes diagonal due to the fact that these differential equations (3.4.7) do not mix different α components.

• **Near Horizon Limit**

In order to obtain infalling boundary condition we expand Dirac equations (3.4.9) around near horizon [30] in the extremal limit. For the extremal case, ($T = 0$) metric develops a pole of second order at the horizon. We expand the metric and other bosonic fields near horizon upto leading order which are given below. In addition to this, we have introduced [15,30] parameters which are required for examining Dirac

equation in the near horizon limit.

$$
\begin{aligned}
g_{ii} &\sim k_0^2 = \frac{m^2}{4} r_h^{-8/5} 2^{3/5} \frac{(Q_1^2 + r_h^4)^{4/5}}{(Q_1^2 - r_h^4)^{2/5}}, \\
g_{tt} &\sim \tau_0^2 = \frac{m^2}{4} r_h^{-4/5} 2^{6/5} \frac{(Q_1^4 + 6Q_1^2 r_h^4 - 3r_h^8)}{(Q_1^2 + r_h^4)^{8/5}(Q_1^2 - r_h^4)^{1/5}} \\
g_{rr} &\sim L_2^2 = \frac{4}{m^2} 2^{-9/5} r_h^{16/5} \frac{(Q_1^2 + r_h^4)^{2/5}(Q_1^2 - r_h^4)^{4/5}}{(Q_1^4 + 6Q_1^2 r_h^4 - 3r_h^8)} \\
A_t^{(i)} &\sim \beta_i (r - r_h), \qquad \beta_1 = \frac{m}{2} \frac{4\sqrt{2} r_h^4 Q_1}{(Q_1^2 + r_h^4)\sqrt{(Q_1^2 - r_h^4)}}, \qquad \beta_2 = \frac{m}{2} \frac{\sqrt{2}}{r_h^2} \frac{(Q_1^2 + 3r_h^4)^{1/2}(Q_1^2 - r_h^4)}{(Q_1^2 + r_h^4)} \\
e^{2\phi_1} &\sim e^{2\phi_{10}} = \frac{2^{2/5} r_h^{12/5}}{(Q_1^2 - r_h^4)^{2/5}(Q_1^2 + r_h^4)^{1/5}} \qquad e^{2\phi_2} \sim e^{2\phi_{20}} = \frac{1}{2^{3/5} r_h^{8/5}} \frac{(Q_1^2 - r_h^4)^{3/5}}{(Q_1^2 + r_h^4)^{1/5}}
\end{aligned}
\tag{3.4.14}
$$

At the near horzon limit Dirac equation simplifies into following [30]:

$$
\begin{aligned}
&\partial_r^2 \Psi_{\alpha\pm} + \frac{1}{r - r_h} \partial_r \Psi_{\alpha\pm} - \frac{\nu_k^2}{(r - r_h)^2} \Psi_{\alpha\pm} = 0, \\
\text{where,} \quad &\nu_k^2 = (mM(\phi_{10}, \phi_{20}))^2 L_2^2 + (\tilde{k}/k_0))^2 L_2^2 - (2m)^2 (q_1 e_1 + q_2 e_2)^2, \\
\text{and,} \quad &\tilde{k} = k - (-1)^\alpha \frac{2k_0}{L_2^2} [p_1 e^{-2\phi_{10}} e_1 + p_2 e^{-2\phi_{20}} e_2], \quad e_i = (L_2/\tau_0)\beta_i,
\end{aligned}
\tag{3.4.15}
$$

where expressions for various parameters are given in (3.4.14).

We need to analyse solutions to (3.4.15) following [15, 30] to determine appropriate boundary condition. It admits two solutions

$$
\Psi \sim (r - r_h)^{\pm \nu_k}, \tag{3.4.16}
$$

of which we choose

$$
\Psi \sim (r - r_h)^{+\nu_k}, \tag{3.4.17}
$$

which corresponds to infalling boundary condition at the horizon. We impose this boundary condition at the near horizon and scan the value of momentum to find the Fermi momentum $k = k_F$ where the source term $A_\alpha(k_F)$ vanishes in (3.4.11)

As one can readily check from the second condition of (3.4.15), where the mass and shifted momentum gives the positive contributions to the square of the exponent ν_k^2 while negative contribution comes from the coupling to electric fields. When the electric field dominates ν_k will end up being imaginary for an extent of values of momentum [30] which is called oscillatory region. Over this extend Green's function gets to be oscillatory with oscillatory peaks periodic in $\log|\omega|$ [14, 15]. For scalar particles, this compares to instability towards pair production in AdS_2 region. For spinors, in any case, it does not suggest an instability as there's no singularity of Green's function within the upper-half of the complex ω-plane [15]. On the field theory side, Oscillatory region implies that effective dimension of the operator within the boundary Conformal Field Theory will end up being complex [15].

Boundary of oscillatory region is given by $\tilde{k} = \tilde{k}_{osc}$, where

$$\tilde{k}_{osc}^2 = k_0^2[(\frac{g}{L_2})^2(q_1e_1 + q_2e_2)^2 - m^2M_0^2], \tag{3.4.18}$$

as it is prominent from the above equation, the oscillatory region depends on the competition between charges and the masses.

For a small ω one can write the retarded Green's function near Fermi surface in terms of $k_\perp = k - k_F$ and ω as [15, 30]

$$G_R(k,\omega) \sim \frac{h_1}{k_\perp - \omega/v_F - h_2e^{i\gamma_{k_F}}(2\omega)^{2\nu_{k_F}}}, \qquad \gamma_k = arg[\Gamma(-2\nu_k)(e^{-2\pi i\nu_k} - e^{-2\pi g(q_1e_1+q_2e_2)})], \tag{3.4.19}$$

where ν_k is given in (3.4.15), γ_k is as given above and h_1, h_2 are positive constants. For $\nu_{k_F} > 1/2$, the leading real part comes from $\mathcal{O}(\omega)$ correction, given by $1/v_F$ term. The ratio of excitation width to excitation energy $\dfrac{\Gamma}{\omega_*}$ becomes vanishing as Fermi surface is approached. Quasiparticles are stable and the system behaves as Fermi liquid.

For $\nu_{k_F} < 1/2$, one ignores v_F term the dispersion relation becomes

$$\omega_* \sim (k_\perp)^z, \quad \text{where} \quad z = \frac{1}{2\nu_{k_F}}, \tag{3.4.20}$$

and ratio of excitation width to energy is

$$\frac{\Gamma}{\omega_*} = \begin{array}{cc} \tan(\frac{\gamma_{k_F}}{2\nu_{k_F}}) & k_\perp > 0 \\ \tan(\frac{\gamma_{k_F}}{2\nu_{k_F}} - \pi z) & k_\perp < 0 \end{array}. \tag{3.4.21}$$

For $\nu_{k_F} = 1/2$, is the marginal Fermi liquid, where $\dfrac{\Gamma}{\omega_*}$ vanishes logarithmically in ω as one approaches Fermi surface. We find Fermi surfaces for our cases corresponding to $\nu_{k_F} > 1/2$, $\nu_{k_F} = 1/2$ and $\nu_{k_F} < 1/2$.

3.5 Fermi Surfaces

In order to study Fermi surface and its nature we have considered Dirac equation (3.4.15) subjected to infalling boundary condition (3.4.17). We tend to numerically solve it for various values of k to find k_F where $A_\alpha(k_F)$ given in (3.4.11) vanishes. We considered $\alpha = 1$ for Ψ in (3.4.15) as similar results are expected from other components.

As it is evident from the table I, under interchange of two generators of Cartan, top four rows are exchanged with four rows in the bottom so interchanging charge parameters $Q_1 \leftrightarrow Q_2$ will provide the identical equations. In this manner, it is adequate to consider just four top modes. Moreover, flipping the sign of q_i and p_i will exchange spinors with its conjugates. As we have already mentioned, from the symmetry of Dirac Eq.(3.4.9), that amounts to flipping the sign of k and ω. So if a fermion with (q_i and p_i) contains a Fermi surface singularity as k_F, its conjugate one with ($-q_i$ and $-p_i$) will have Fermi surface singularity at $-k_F$. Under flipping the sign of q_i and p_i, rows (1,2) will be interchanged with rows (3,4) in Table I. Therefore, in this case, we have only considered row 3 and 4 of Table I. We numerically

searched for Fermi momentum for these two spinors for $\omega = 0$ and have plotted the k vs square of inverse charge parameter, given by $x = r_h^4/Q_1^2$. Range of x is limited to $(0, 1)$ as $Q_1^2/r_h^4 < 1$ at $T = 0$ will make Q_2^2/r_h^4 negative. At $x = 1/3$, $Q_1 = Q_2$ and two chemical potentials will be equal to each other. We introduce $\tilde{Q}_1 = Q_1/r_h^2$, which is the value of the charge parameter in units of r_h^2. It is related to x through $x = 1/\tilde{Q}_1^2$. For simplicity, $m/2$ is set to be equal to 1 in the numerical computation. Discussions are given below for each of these cases.

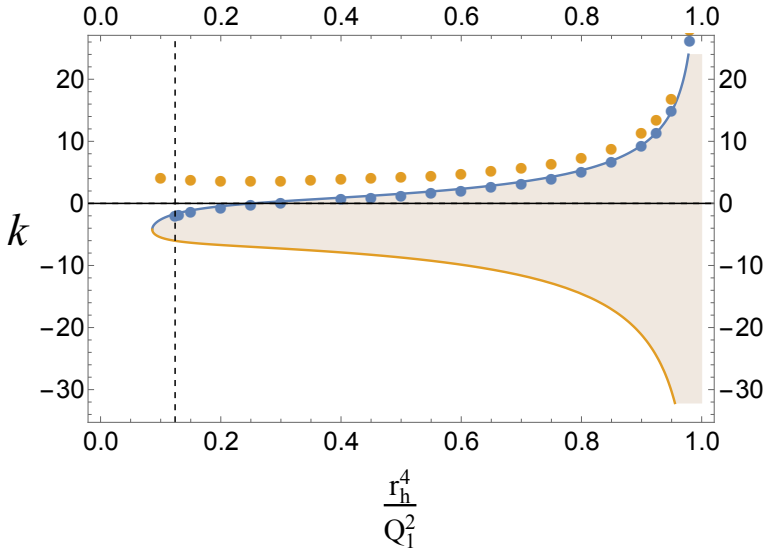

Figure 3.1: Case 1: k vs r_h^4/Q_1^2. The shaded bell-shaped area represents oscillatory region. It shows two branches; Dashed line show where the lower branch enters oscillatory region

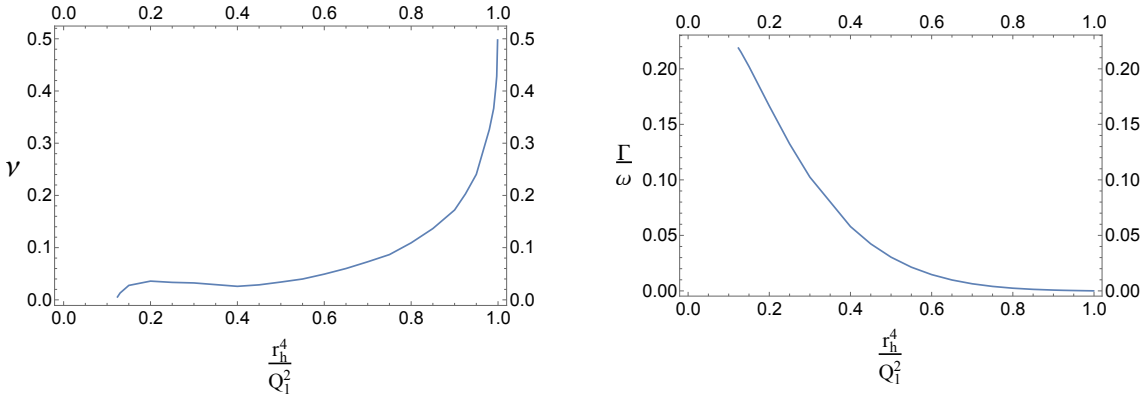

Figure 3.2: Case 1: ν vs r_h^4/Q_1^2 and Γ/ω vs r_h^4/Q_1^2 for lower branch.

In general, we have two cases one with total net charge $|q_1 + q_2| = 2$ and another with total net charge $|q_1 + q_2| = 1$.

• Case 1: $\lambda^{1+}(-\frac{1}{2},-\frac{1}{2})$, $q_1 = -\frac{3}{2}$, $q_2 = -\frac{1}{2}$ where the dual operator is given by $tr(\Sigma^{1+}\psi(-\frac{1}{2},-\frac{1}{2}))$: This case corresponds to higher net charge $|q_1+q_2| = 2$ and has more chances of forming Fermi surface/s. In fact, we find Fermi surface singularities with two branches, as shown in Fig. 3.1. We find that one of them lies on the non-Fermi liquid regime, while the other one is in the regime of Fermi liquid. Beginning from left, as $\tilde{Q}_1$ decreases from ∞ to 3.356 there is no oscillatory region. It first shows up at $\tilde{Q}_1 = 3.356$ and expands as charge parameter decreases till $\tilde{Q}_1 = 1$ forming a bell-shaped region.

The branch for which Fermi surface is in the non-Fermi regime, the Fermi surface singularities appear along the boundary of the oscillatory region. It begins at $\tilde{Q}_1 = 2.887$, on the left, it enters the oscillatory region, which means that the dual operator has developed a complex dimension. As $\tilde{Q}_1$ decreases, we find that Fermi momenta are very close to the boundary of the oscillatory region, almost traces the boundary itself and continues till $\tilde{Q}_1 = 1$. Looking at ν and Γ/ω for this branch (Fig. 3.2), we see that ν is small where it has entered the oscillatory region on the left, increases as $\tilde{Q}_1$ decreases and approaches 0.5 as $\tilde{Q}_1 = 1$. Therefore, the Fermi surface remains in the non-Fermi region for the entire range in the parameter space, while it approaches marginal Fermi liquid at $\tilde{Q}_1 = 1$, which corresponds to $Q_2^2/r_h^4 \to \infty$.

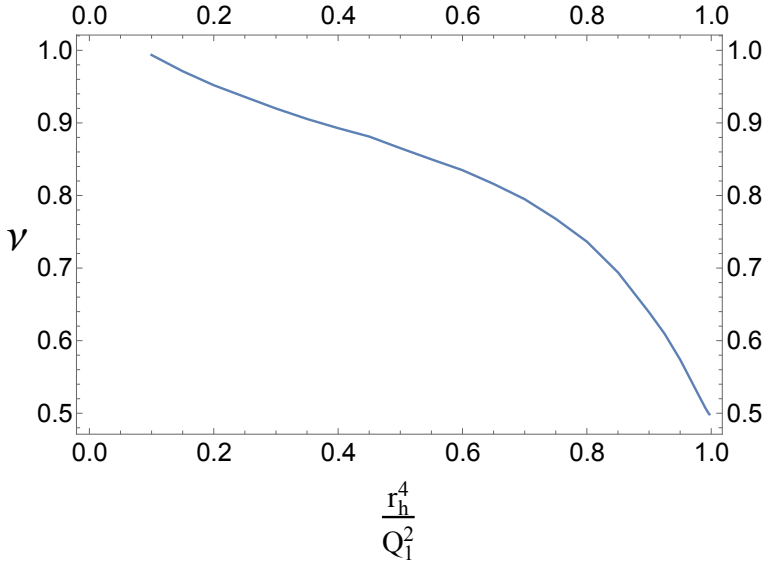

Figure 3.3: Case 1: ν vs r_h^4/Q_1^2 for upper branch.

The excitation width decreases steadily with $\tilde{Q}_1$ implying that the quasiparticle becomes more and more stable and approaches zero at the limit of marginal Fermi liquid, where $\tilde{Q}_1$ tends to 1. This branch cross zero at around $\tilde{Q}_1 = 2$, which may be associated with a transition between Fermi surfaces of particles to antiparticles [30].

The other branch also begins on the same side of the oscillatory region and the corresponding Fermi momenta have a larger value. In the case of this branch, it remains completely outside the oscillatory region. Plot of ν is shown in Fig. 3.3 and as one may observe ν decreases with the decrease in charge parameter. On the left extreme, where $\tilde{Q}_1$ approaches ∞, ν approaches 1 whereas at the other extreme with $\tilde{Q}_1$ approaches 1, ν approaches 0.5, indicating that the system is driven toward the marginal Fermi liquid regime. For the entire range of the parameter, it remains in Fermi liquid regime and approaches marginal at the limit of $\tilde{Q}_1 = 1$.

Taking both the branches in an account, one may see that there are two Fermi surfaces over a range of $\tilde{Q}_1$ in Fig. 3.1. Signs of the Fermi momenta for these two surfaces are same for $\tilde{Q}_1 < 2$ and opposite for $\tilde{Q}_1 > 2$. This corresponds to the dual field theory admitting two different excitations for this range of charge parameter, hence resulting in two different Fermi surfaces. As $\tilde{Q}_1$ approaches 1, these two branches approach each other and merge, leading to marginal Fermi liquid in the limiting case.

• Case 2: $\lambda^{1+}(-\frac{1}{2}, \frac{1}{2})$ and $q_1 = \frac{1}{2}, q_2 = -\frac{3}{2}$ with the dual operator given by $tr(\Sigma^{1+}\psi(-\frac{1}{2}, \frac{1}{2}))$: This case has a lower net charge in comparison to case 1 (total charge $|q_1 + q_2| = 1$) and in this case, we have only one branch of Fermi surface as shown in Fig. 3.4. As comparable to case 1, there is no oscillatory region on the left side corresponding to a large value of charge parameter. As $\tilde{Q}_1$ decreases from ∞, oscillatory region appears at around $\tilde{Q}_1 = 2.04$ and expands till $\tilde{Q}_1 = 1$.

In this case, the branch appears throughout the entire range and does not enter the oscillatory region. Plots for ν and Γ/ω for this branch are given in Fig. 3.5. On the far left, where the charge parameter approaches ∞, ν is greater than 0.5, which indicates the Fermi liquid regime. As $\tilde{Q}_1$ decreases, ν decreases at a steady

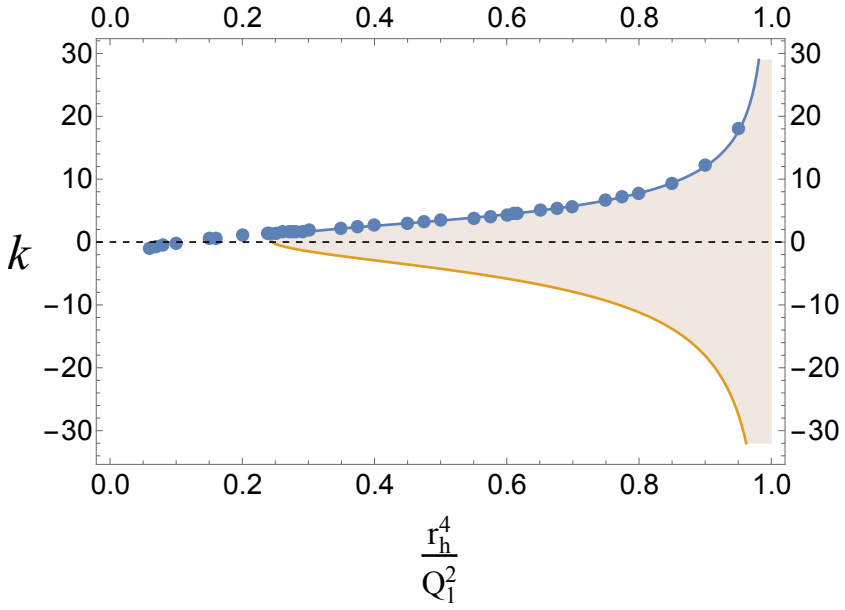

Figure 3.4: Case 2: k vs r_h^4/Q_1^2. The shaded bell-shaped area represents oscillatory region.

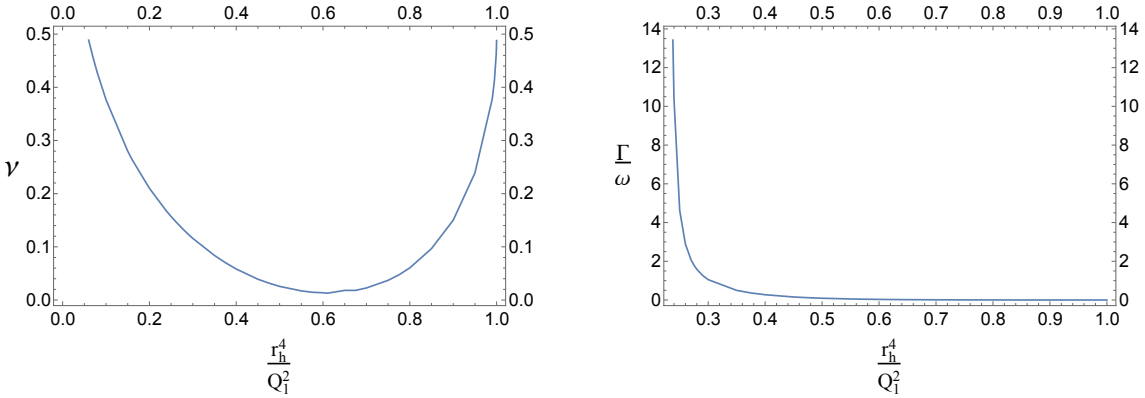

Figure 3.5: Case 2: ν vs r_h^4/Q_1^2 and Γ/ω vs r_h^4/Q_1^2

rate and at $\tilde{Q}_1 = 4.23$, ν becomes equal to 0.5, which corresponds to marginal Fermi liquid. As $\tilde{Q}_1$ decreases further ν reaches a minimum and then increases with decreasing $\tilde{Q}_1$, reaching 0.5 again at the right extreme where $\tilde{Q}_1 = 1$. The width of excitation decreases with a decrease of $\tilde{Q}_1$ and it becomes very small at $\tilde{Q}_1 = 1$, making the excitation stable. However, with increasing $\tilde{Q}_1$ it shoots up before it reaches marginal Fermi liquid state. For most of the range, the Fermi momentum sign remains positive, as it passes through zero at $\tilde{Q}_1 = 3.01$ and becomes negative at higher values, again indicating a transition between Fermi surfaces of particles and antiparticles. This branch exhibits a transition from non-Fermi liquid to Fermi

liquid behaviour, with a variation of charge parameter. Similar kind of transition has been observed in [75] in a different context, where the system moves from Fermi liquid to non-Fermi liquid as one changes some impurity parameter.

3.6 Discussion

In this chapter, we have used Gauge/Gravity duality to study the Fermi surfaces in six dimensional $(2,0)$ theory. We consider seven dimensional gauged supergravity where it admits an asymptotically AdS black hole solution, using this as the background we have analysed fermionic modes which decouple from gravitino. We considered two sorts of such fermionic modes; with net charge $q = |q_1 + q_2| = 1$ and 2 , where q_1 and q_2 are the two $U(1)$ gauge fields charges. We find both fermionic modes admit Fermi surface/s. In particular, fermions with higher net charge $q = 2$ gives two branches of Fermi surfaces, where one remains in the regime of Fermi liquid, while the other lie in the non-Fermi regime. For the other fermionic mode with lower net charge $q = 1$ we find that the existence of Fermi surface which lies in the regime of Fermi liquid for a range of charge parameter while for the rest it is in the non-Fermi regime.

In the current model, we find one of the fermionic modes lie on Fermi liquid regime. Comparing this result to other maximal supersymmetry models, the present model gives new results which were absent in the case of $N = 4$ SYM and ABJM theory. The other Fermi surface is completely in the non-Fermi regime and at the extreme value of the charge parameter, it approaches marginal Fermi liquid, which is very similar to the cases obtained on those models. As explained in chapter 2 such marginal Fermi liquid appear in the strange metal phase of high T_c superconductor. We have also found a branch which changes from Fermi liquid to non-Fermi liquid, which is different from $N = 4$ SYM and ABJM theory. For two of our branches the Fermi momenta lies along the boundary of the oscillatory region, which is again very similar to results obtained in [30, 31]. Looking at the structure of the dual operator,

for all the fermions that we have considered, $U(1) \times U(1)$ charge of fermions in the boundary theory plays a prominent role in determining the nature of Fermi surface while the scalars do not play any role. On comparison with $N = 4$ SYM, this kind of behaviour is different as in their case the nature of the Fermi surface also depends on the boundary theory scalars.

In the present work, we have considered Fermi momentum in extremal limit at $\omega = 0$. A full-fledged study of spectral functions and transport phenomena at finite temperature and over a range of ω may provide a more elaborate picture of the field theory. We have observed fermionic modes shows marginal Fermi liquid behaviour for certain values of charge parameter, for example in the limit of $Q_1/r_h^2 = 1$ which at zero temperature corresponds to Q_2/r_h^2 approaching ∞. Marginal Fermi liquid was proposed to describe optically doped cuprates [76] and it may be interesting to further explore the model for these values of charge parameter. The present model with a single charge by setting other charge density to zero would also be a natural extension, which cannot be obtained as a limiting case of this study. Considering the quasi-particles on the field theory side, operators are given by $tr(\Sigma\psi)$ in our case and we have observed that the nature of Fermi surface changes only when charge of the gaugino (ψ) in the operator changes, while it remains the same with the change of the scalar (Σ). This is consistent with the argument [29] that gaugino itself generates the Fermi surface. However, in $N = 4$ SYM it was found nature of Fermi surface may depend on bosons as well and so this issue requires a better understanding.

The limiting factor for the zero temperature case was that we could not analysis the Fermi surface in case of single charge case. As for the zero temperature with a single charge the chemical potential turns out to be complex. So to address this problem, we will extend our work in finite temperature regime and analysis the full spectral function. In the next chapter, we will consider the finite temperature regime for this model and analysis the Fermi surface in case of two charge parameters together with a one charge parameter.

Chapter 4

Holographic Fermi surface at finite temperature

4.1 Introduction

In the previous chapter, we have considered maximally gauged supergravity theory. Using AdS/CFT correspondence we have studied different aspects of Fermi surfaces and the excitations associated with the fermionic operators in the dual theory at zero temperature. We considered two charge black hole solution as the background and analysed the behaviour of the fermionic operators. Looking at the poles of the Green's function we identified the Fermi surfaces and also studied the nature and the decay width of excitations with a variation of the charge parameters of the background.

In this chapter, we will extend our analysis to finite temperature. Usually, zero temperature is the correct setting for studying Fermi surfaces, however extending this study to the finite temperature will give more specific pieces of information of the various excitations of this theory. In particular, in the previous chapter, we have considered a background with two charge parameters. We will like to consider a background with a single charge parameter by setting one of them to be zero. This case cannot be analysed in zero temperature, so by extending this to a finite

temperature allow us to study this limiting case as well.

In order to extend the zero-temperature analysis to the finite temperature, we will obtain the expression for full Green's function of the dual theory. This will be our main tool in the subsequent analysis, as an imaginary part of it provides the spectral function that can capture the behaviour of different fermionic modes at a non-zero temperature. As we will see in the case of two non-zero charge parameters, finite temperature results precisely agree with zero temperature analysis. Since the dual field theory is known, it enables us to study the role of the operators in the dual field theory in determining the nature of the Fermi surface. The contents of this chapter have been published in [45].

The following is the plan of the chapter. The black hole solution that we use as a background has already been discussed in detail in the previous chapter. In section 4.2, we have set up the equations to calculate Green's function for the dual operator. In section 4.3, the numerical computation of Green's function is done for various modes and backgrounds. We end with a discussion of the findings in section 4.4.

4.2 Green's Function

In order to study the dual fermionic operators, we will compute the Green's function using the techniques of AdS/CFT correspondence. We will consider black hole solution given in 3.2.4 as our background and obtain the Dirac equations for spin 1/2 fermions λ^i in supergravity theory in this background for studying Fermi surfaces in the boundary theory. The Dirac equation [44] for the 8 spinors in the theory of supergravity is given in 3.4.1. These equations can be further simplified as discussed in the previous chapter. Each spinor consists of a pair of four component spinors Ψ^i and η^i. By appropriate selection of Γ matrices and choosing t and x dependences for λ^i as $\lambda^i = e^{-A(r)}h(r)^{-1/4}e^{-i\omega t+ikx}\begin{pmatrix}\Psi^i\\ \\ \eta^i\end{pmatrix}$, one can make the four-component spinors, Ψ^i and η^i to satisfy the same equation. In this regard, we will be only considering Ψ^i for our calculations as η^i will have the same behaviour. The four

component spinor Ψ^i can be written in terms of a pair of 2-components spinors Ψ^i_α, as follows:

$$\Psi^i = \begin{pmatrix} \Psi^i_1 \\ \Psi^i_2 \end{pmatrix}, \quad \Psi^i_\alpha = \begin{pmatrix} \Psi^i_{\alpha-} \\ \Psi^i_{\alpha+} \end{pmatrix}, \quad \alpha = 1, 2. \tag{4.2.1}$$

With this notation, Dirac equations (3.4.1) reduce to (i index has been supressed),

$$\begin{aligned} &(\partial_r + X\sigma_3 + Yi\sigma_2 + Z\sigma_1)\Psi_\alpha = 0, \\ \text{where} \quad &X = m\frac{e^B}{\sqrt{h}}M(\phi_1,\phi_2), \quad Y = -\frac{e^{B-A}}{\sqrt{h}}u(r), \quad Z = -\frac{e^{B-A}}{\sqrt{h}}[(-1)^\alpha k - v(r)], \\ \text{and} \quad &M(\phi_1,\phi_2) = (m_1 e^{2\phi_1} + m_2 e^{2\phi_2} + m_3 e^{-4(\phi_1+\phi_2)}) \\ &u(r) = \frac{1}{\sqrt{h}}[\omega + 2m(q_1 A^{(1)}_t + q_2 A^{(2)}_t)] \\ &v(r) = 2e^{-B}[p_1 e^{-2\phi_1} F^{(1)}_{rt} + p_2 e^{-2\phi_2} F^{(2)}_{rt}]. \end{aligned} \tag{4.2.2}$$

One can see that if one changes the value of α than there is a relative flip in the sign of k. Therefore, for a given value of α if a system admits a Fermi surface at $k = k_F$, for the other value of α, Fermi surface is at $k = -k_F$, provided all other parameters are unaltered. Thus, a specific value of α can be selected without any loss in generality.

Near horizon behaviour of these fermions are oscillatory. To get rid of this oscillatory behaviour we will follow [32] and introduce the following quantities, termed as generalised fluxes. On the introduction of these generalised fluxes one can get rid of this oscillatory behaviour at near horizon limit.

$$\begin{aligned} &U_\pm = \Psi_- \pm i\Psi_+, \quad \mathcal{F} = |U_+|^2 - |U_-|^2 \\ &\mathcal{I} = U_+U_-^* + U_+^*U_-, \quad \mathcal{J} = i(U_+U_-^* - U_+^*U_-), \quad \mathcal{K} = |U_+|^2 + |U_-|^2. \end{aligned} \tag{4.2.3}$$

Dirac equation (4.2.2) can be now written in terms of these generalised fluxes,

with the equations given as

$$\begin{aligned} \partial_r \mathcal{F} = 0, \quad \partial_r \mathcal{I} = 2Y\mathcal{J} - 2X\mathcal{K}, \\ \partial_r \mathcal{J} = -2Y\mathcal{I} + 2Z\mathcal{K}, \quad \partial_r \mathcal{K} = -2X\mathcal{I} + 2Z\mathcal{J}. \end{aligned} \tag{4.2.4}$$

For a given value of α the near horizon behaviour of the fermion fields [74] are given by,

$$\Psi_- = i\Psi_+ = \frac{i}{2}(r - r_h)^{-\frac{i\omega}{4\pi T}}, \tag{4.2.5}$$

along with corrections of order $\sqrt{r - r_h}$. The near horizon behaviour of the generalized fluxes can be evaluated from (4.2.5). Considering upto the leading order in expansion of X, Y and Z at near horizon limit these fluxes at this limit is given by,

$$\mathcal{F} = 1, \quad \mathcal{I} = i_1\sqrt{r - r_h}, \quad \mathcal{J} = j_1\sqrt{r - r_h}, \quad \mathcal{K} = 1, \tag{4.2.6}$$

where i_1 and j_1 depends on ω, k, r_h and parameters related with fermions.

At the asymptotic limit $r \to \infty$, behaviour of the fermions are given by [44]

$$\Psi_+ = Ar^{\frac{3}{2}} + Br^{-\frac{5}{2}}, \qquad \Psi_- = Cr^{\frac{1}{2}} + Dr^{-\frac{3}{2}}. \tag{4.2.7}$$

Using (4.2.3), one can relate generalised fluxes to the coefficients A, B, C and D given in (4.2.7). The expression for these fluxes at asymptotic limit is given by,

$$\mathcal{F}_0 = 2i(AD^* - A^*D) = 1, \quad \mathcal{J}_0 = -2(A^*D + AD^*), \quad \mathcal{K}_3 = 2|A|^2 = -\mathcal{I}_3, \tag{4.2.8}$$

where the subscript in coefficient in the above equation shows the power of r in the asymptotic expansion.

The ratio of the coefficients in the asymptotic limit (4.2.7) gives the relation of Green's function.

$$G_R = \frac{D}{A}, \tag{4.2.9}$$

due to infalling boundary condition, the Green's function becomes retarded. The

imaginary and real part of Green's function are given by

$$\begin{aligned}\mathcal{I}m(G_R) &= \frac{1}{2i}\frac{A^*D - AD^*}{|A|^2} = \frac{1}{2\mathcal{K}_3},\\ \mathcal{R}e(G_R) &= \frac{1}{2}\frac{A^*D + AD^*}{|A|^2} = -\frac{\mathcal{J}_0}{2\mathcal{K}_3}.\end{aligned} \tag{4.2.10}$$

The Green's function turns out to be a 2×2 matrix $G_{\alpha\beta}$ in case of our notation. However, it turns out to be diagonal in the present case. We will be considering G_{11}, corresponding to $\alpha = 1$. Changing the α value would equate to the reversal of the Fermi momentum sign, as previously mentioned.

4.3 Results

In this section, we have analysed the dual fermionic operator in the supergravity theory, given in Table 3.4.1 by studying the spectral function related to it. All eight fermions are charged under $U(1) \times U(1)$ gauge field. As explained in [44], these various fermionic modes are related to each other by interchanging the charge parameters Q_1 and Q_2 and flipping the sign of q_i and p_i associated with flipping the signs of k and ω. In general, we have a background with two non zero charge parameter Q_1 and Q_2. We have only considered two different modes, namely $q_1 = -3/2$, $q_2 = -1/2$ and $q_1 = -3/2$, $q_2 = 1/2$ as the behaviour of other modes in this background are similar. We have referred to these as two-charge cases. For each of the two modes, we numerically solve (4.2.2) subject to the infalling boundary condition (4.2.6) and obtain the spectral function ImG_R using (4.2.10), throughout the result we will set $m = 2$. In addition, to the general background, we have studied spectral function for fermions in the background with a single charge, as well. This background can be realised by setting one of the charge parameters, $Q_2 = 0$ and then following the previous procedure we examined the modes with $q_1 = 3/2$, $q_2 = 1/2$ and $q_1 = 1/2$, $q_2 = 1/2$. Due to the symmetry, once again the other modes in table 3.4.1 have similar behaviours. We have termed these as one-charge cases. It may be mentioned that, since $Q_2 = 0$ does not admit an extremal limit, Fermi surfaces

of one-charge cases can only be studied at finite temperature. We have followed the criteria given in [32] to verify the existence of Fermi surface at finite temperature. If there is a Fermi surface for a certain value of $k = k_F$, it appears as a peak in the spectral function for $\omega = 0$ around k_F, which has a width small enough compared to the temperature. In addition to that, if we plot the spectral function vs. ω at $k = k_F$ that should show a peak near $\omega = 0$, which is consistent with quasi-particle. Furthermore, the height of the peak of spectral function at $\omega = 0$ should be large enough. We have considered ratio of spectral function and $\mu^* = \sqrt{T^2 + \mu_1^2 + \mu_2^2}$ in the plots as the underlying theory is conformal.

In chapter 3 we have studied Fermi surfaces for the two-charge cases at zero temperature [44]. We found two kinds of solution one with a higher net charge, where dual operator admits two Fermi surfaces with one Fermi surfaces lying in the regime of Fermi liquid and the other being in the non-Fermi liquid regime, both approaches marginal Fermi liquid as Q_1 approaches infinity. Operator dual to the mode with lower net charge admits one Fermi surface, which is partly in both Fermi liquid and non-Fermi liquid regime.

We begin our analysis for finite temperature by taking $q_1 = -3/2$, $q_2 = -1/2$ at $T = 0.0005$. To study the charge parameter dependence on the Fermi surface we have taken two different values, $Q_1^2/r_h^4 = 10$ and $Q_1^2/r_h^4 = 2$. In Fig. 4.1 we have plotted spectral function at $\omega = 0$ for $Q_1^2/r_h^4 = 10$, as we see there are two peaks around two different k values, $k_1 = -2.6$ and $k_2 = 4.3$. The former peak is quite broad which does correspond to the Fermi surface while the latter is sharp indicating a Fermi surface. Comparing this to our previous results in chapter 3 we can observe at that value of charge parameter, there is only one branch that admits Fermi surface, while the other branch has already entered the oscillatory region. The existence of the Fermi surface is confirmed by spectral function vs. ω plots for $k_1 = -2.6$ and $k_2 = 4.3$ given in Fig. 4.1 where we can see, the former does not have a sharp peak around $\omega = 0$. Next for $Q_1^2/r_h^4 = 2$, the plot of spectral function vs. k is given in Fig. 4.2, where we can see two sharp peaks at $k_1 = 1.177$ and $k_2 = 4.5$, indicating

existence of two Fermi surfaces. Plots of spectral function vs. ω at those values of k are given in Fig. 4.2, where we can see peaks around $\omega = 0$, adding to the fact that both correspond to Fermi surfaces. These results for two different charge parameter support the previous results in chapter 3 obtained at $T = 0$ [44], that at this value of charge parameter, there exist two Fermi surfaces.

Taking the same temperature $T = .0005$ next we will consider the fermionic mode with charges $q_1 = -3/2$, $q_2 = 1/2$ which correspond to lower net charge in case of zero temperature. For $Q_1^2/r_h^4 = 10$ and $Q_1^2/r_h^4 = 2$ plots are given in Fig. 4.3 and Fig. 4.4 respectively. It is clear from the figures that in both the cases it has a single peak, at $k = -.1572$ and at $k = 3.054$ for $Q_1^2/r_h^4 = 10$ and $Q_1^2/r_h^4 = 2$ respectively. For both the values of charge parameter, it shows a peak of spectral function around $\omega = 0$ at respective k values. Due to the single peak for each value of charge parameter, this specific mode admits only a single Fermi surface for each of the cases. This feature is seen in the zero temperature case in chapter 3 as well.

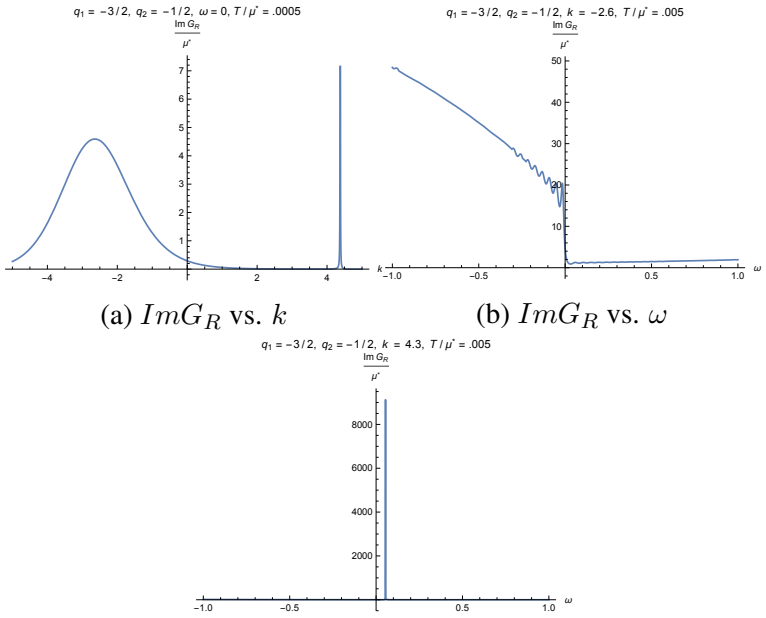

(a) ImG_R vs. k (b) ImG_R vs. ω

(c) ImG_R vs. ω

Figure 4.1: Spectral function for fermionic mode with $q_1 = -3/2, q_2 = -1/2, Q_1^2/r_h^4 = 10$

As mentioned earlier we could not find any extremal limit for one-charge cases in zero temperature so we extend our analysis to one-charge cases, by setting one

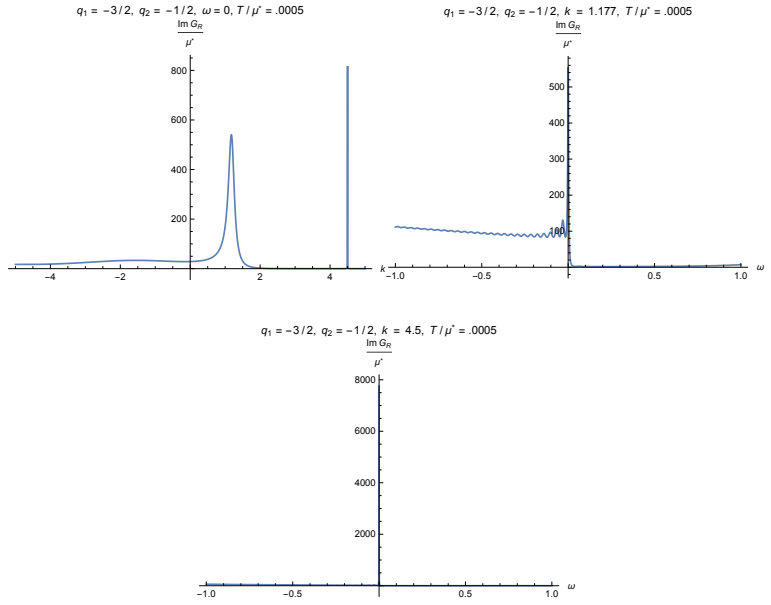

Figure 4.2: Spectral function for fermionic mode with $q_1 = -3/2, q_2 = -1/2$ for $Q_1^2/r_h^4 = 2$

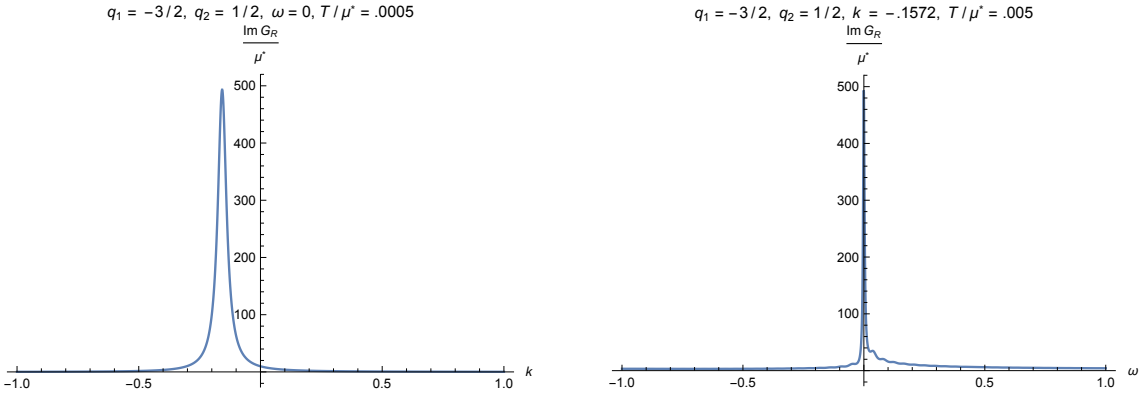

Figure 4.3: Spectral function for fermionic mode with $q_1 = -3/2, q_2 = 1/2$ for $Q_1^2/r_h^4 = 10$

of the charge parameters to be zero $Q_2 = 0$. First we start with operator dual to the mode with $q_1 = 3/2$, $q_2 = 1/2$, for this case we have plotted spectral function vs. k at $\omega = 0$. One can clearly see from Fig. 4.5, it shows a peak at around $k = -0.899$. Taking this value $k = -0.899$ we have plotted the spectral function vs. ω, where we see a peak of around $\omega = 0$. From this, we conclude that this mode admits a Fermi surface. Similarly we will consider the operators, dual to the fermionic mode with $q_1 = 1/2$, $q_2 = 3/2$ where the corresponding plots are given in Fig. 4.6. We can see a peak in spectral function vs. k at $k = 0.451$ but the spectral function vs ω-plot at $k = 0.451$ does not give any peak around $\omega = 0$. Therefore we can conclude that

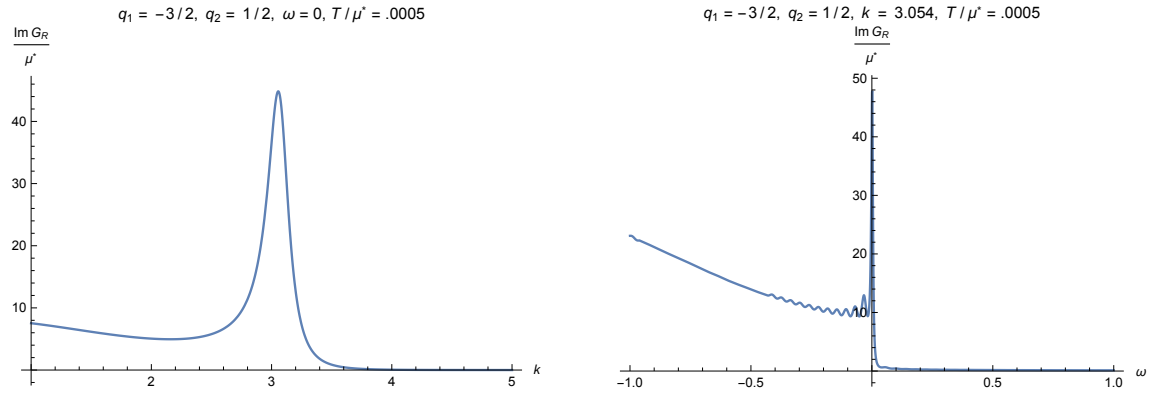

Figure 4.4: Spectral function for fermionic mode with $q_1 = -3/2, q_2 = 1/2$ for $Q_1^2/r_h^4 = 2$

the operator dual to the fermionic mode with charges $q_1 = 1/2$, $q_2 = 3/2$ no Fermi surface exists.

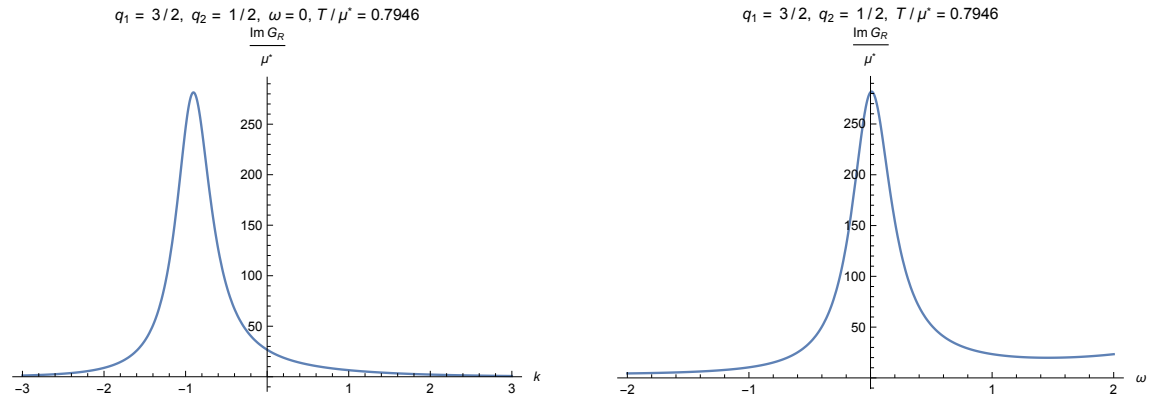

Figure 4.5: Spectral function $q_1 = 3/2$, $q_2 = 1/2$. Left figure is at $\omega = 0$ and right figure is the plot vs. ω..

In two-charge cases, fermions with higher charges have more tendency of forming Fermi surfaces. From the dual field theory perspective, operators with gauginos $\psi(\pm 1/2, \pm 1/2)$ have two Fermi surfaces, while operators involving gauginos $\psi(\pm 1/2, \mp 1/2)$ have a single Fermi surface. So it seems that it is the gauginos that determine the nature of the Fermi surface admitted by the operator. To determine the role of the scalars toward the nature of the Fermi surface in the dual field theory, we consider the relation between ϕ_1 and ϕ_2 in the supergravity and the scalar operator in the dual field theory. Our solution has a symmetry group of $U(1) \times U(1)$ which rotates phases of $\Sigma^{1\pm}$ and $\Sigma^{2\pm}$ respectively. This means that $M5$-branes are distributed in a symmetrical manner in the large N limit. In terms of Σ^i, $i = 1, 2, ..5$

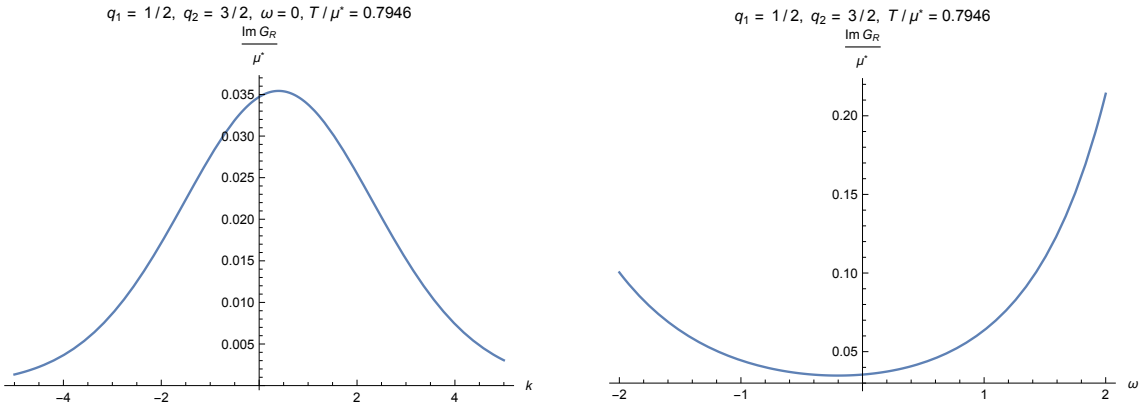

Figure 4.6: Spectral function $q_1 = 1/2$, $q_2 = 3/2$. Left figure is at $\omega = 0$ and right figure is the plot vs. ω.

(they are related to $\Sigma^{1\pm}$ and $\Sigma^{2\pm}$ through $\Sigma^{1\pm} = \Sigma^1 \pm i\Sigma^2, \Sigma^{2\pm} = \Sigma^3 \pm i\Sigma^4$) [44] this means that dual field theory scalar operators satisfy $tr((\Sigma^1)^2) = tr((\Sigma^2)^2)$ and $tr((\Sigma^3)^2) = tr((\Sigma^4)^2)$, which we would refer as $tr(\Sigma_A^2)$ and $tr(\Sigma_B^2)$ respectively, while we write $(\Sigma^5)^2 = \Sigma_C^2$. Taking this symmetry in the account, the operators dual to the supergravity field ϕ_1 and ϕ_2 can be written as by [77],

$$\mathcal{O}_{\phi_1} \sim \frac{1}{5} tr(-3\Sigma_A^2 + 2\Sigma_B^2 + \Sigma_C^2) \quad \text{and} \quad \mathcal{O}_{\phi_2} \sim \frac{1}{5} tr(2\Sigma_A^2 - 3\Sigma_B^2 + \Sigma_C^2). \quad (4.3.1)$$

From the asymptotic expansion of ϕ_1 and ϕ_2, as given in supergravity solution (3.2.5), one can see for the one-charge cases, where we set $Q_2 = 0$, $\langle \mathcal{O}_{\phi_1} \rangle$ is negative and $\langle \mathcal{O}_{\phi_2} \rangle$ is positive. This implies Σ_A, or in other words, $\Sigma^{1\pm}$ has a non-zero expectation value. From our analysis given above, we find that the operators involving $\Sigma^{1\pm}$ give rise to Fermi surface, while operators involving $\Sigma^{2\pm}$ does not admit one. It suggests that expectation values of the scalars appearing in the dual operator play a role in determining the Fermi surface. A similar result has been found in N=4 SYM and ABJM model [32]. It may be mentioned that in the present case the near horizon geometry is AdS_2 with a non-zero entropy at $T = 0$, while the models discussed in [32] have vanishing zero entropy, and so this feature seems to be quite general. In the cases where both the charge parameters are non-zero, it is plausible to assume that both $\Sigma^{1\pm}$ and $\Sigma^{2\pm}$ have non-zero expectation value in general, giving rise to Fermi surface(s) for all the operators.

4.4 Discussion

To summarise, Fermi surface has been studied for two charge parameters and one charge parameter in the six dimensional $(2, 0)$ theory at finite temperature. For two charge parameters, operators which are dual to the fermionic modes with higher net charge are most probable of admitting Fermi surface, confirming the result of zero temperature analysis. We find the one with higher charge admits two Fermi surfaces, while the one with less charge admits one. For our results, we can see the nature of the Fermi surface depends on the charge of the gaugino ψ of the dual operator which is of the form $tr(\Sigma\psi)$. The analysis was extended at finite temperature to the single-charge cases, which were obtained with the charge parameter set to zero. We have taken all fermionic modes into consideration and found that only operators dual to certain modes admit Fermi surface, whereas others do not. By analysing the dual field theory, we find the corresponding operator admits Fermi surface if the background corresponds to the non-zero expectation of the scalar. However, if both the charge parameters are non-zero, all scalars will probably have expectation values and dual operators associated with all fermionic modes, as we saw in the current model, admit one or more Fermi surface/s. If that is the case as explained in [32], then Fermi surface singularity is related to the coloured gaugino. Nevertheless, the $N = 4$ SYM [30] analysis gives counter examples [32], therefore understanding the roles of scalar operators requires a further study.

As already described, it is necessary to consider models which can be analyzed in more detail to obtain a clear overview of the roles played by various operators in dual field theory in the context of Fermi surfaces. One can also shed some light on it by using Luttinger count of charge density [29]. In this current chapter, we have only considered those fermionic modes, which decouples from gravitini in supergravity theory. A study of other modes and that of the gravitini itself could provide further insight into the dual field theory. In previous chapter 3, we have observed that the dual field theory is in the marginal Fermi liquid regime in the two-charge cases for limiting values of the charge parameters [44]. This marginal Fermi

liquid behaviour is shown by cuprates at the limit of optimally doped [76] and so the study of such limiting value of charge parameters will be interesting to extend. A finite temperature study of transport phenomena for the current model could also lead to a better understanding.

Finally, a thermodynamic analysis could illuminate the stability issues of the present model. In five dimensions similar black hole solutions show instability through the development of charge density resulting in spontaneous breaking of $SU(2) \subset SO(6)$ and translational invariance [78]. In the present case, the theory has an $SO(5)$ symmetry and it might be interesting to see if it becomes unstable with the similar breaking of symmetry.

Chapter 5

Fermionic spectrum with spontaneous symmetry breaking

5.1 Introduction

So far we have studied the fermionic response of black hole solutions which corresponds to specific states in the dual system. Using AdS/CFT correspondence we have analysed the behaviour of the Fermi surface and excitations around it. Being dual to a finite density system, such solutions are characterised with one or more $U(1)$ symmetries. However, in specific circumstances these systems develop instabilities toward decay into a more stable configuration, which spontaneously break one or more $U(1)$ symmetry. The canonical example is a holographic superconductor, where $U(1)$ symmetry is broken spontaneously by condensation of the scalar field. It is interesting to study how the fermionic spectrum changes as the consequence of such symmetry breaking.

In this chapter, we will consider a domain wall geometry which breaks one of the $U(1)$ spontaneously. They are natural candidates for zero temperature limit of holographic superconductors [37,38]. Study of fermions for such a condensed phase of holographic superconductor at zero temperature [39] shows a spectrum similar to that obtained in APRES experiment. Other works in this line include [41], who

considered a generic fermion in a domain wall background and found normalisable modes. On the other hand [42] discussed, ABJM theory with symmetry breaking source and found both gapped and gapless spectrum. [43] also considered a similar solution in ABJM theory and obtained a gapped spectrum, where the gaps in the spectra have been attributed to low fermionic charge and particle-hole interaction.

In this chapter, we will look for such a domain wall solution in a maximally symmetric gauged supergravity theory in seven dimensions.

The field content of this theory has been elaborately discussed in chapter 3. It has an R symmetry group $SO(5)$ of which domain wall solution breaks one of the $U(1)$ in the Cartan while retaining the other and thus may correspond to zero temperature of holographic superconductor. The solution interpolates between two AdS geometries. We have obtained the optical conductivity numerically and find that in the low frequency limit it behaves as $\omega^{2\triangle_B+3}$ for certain constant $\triangle_B$, while for the high frequency it goes as ω^3. The fermionic content of the supergravity theory consists of 16 spin-1/2 fermions and we have considered only those modes, which do not couple to gravitino. In the background of the domain wall solutions, we find there are only four such modes. We have studied spectral function for the operators dual to those modes and find in the spectrum there is a depleted region around $\omega = 0$. We have also artificially dialled the value of the charges to study its effect on the spectrum and find the gap persists. The contents of this chapter have been published in [46].

The plan of this chapter is as follows. In the next section, we describe the domain wall solution and study the optical conductivity. In section 5.3 we present Green's function while section 5.4 consists of the numerical result. We conclude with a discussion in section 5.5.

5.2 Domain Wall solution

The truncated part of the bosonic action of maximally gauged supergravity has been discussed in chapter 3. Apart from the black hole solution for this truncated theory, we can obtain a different class of solution namely domain wall solution. The Lagrangian for this theory is given in (3.2.1), where we have considered only two Cartan gauge fields $A^{12}_\mu = A^{(1)}_\mu$ and $A^{34}_\mu = A^{(2)}_\mu$. Considering a diagonal scalar vielbein V^i_I will lead to $U(1)^2$ gauge symmetry which leads to the case given in chapter 3 and 4. In this particular model, we want a background that would break one of the $U(1)$, so in this regard, we consider the following ansatz for the scalar vielbein

$$\begin{aligned} &V^i_I = \exp[\phi_2 Y_2]\exp[\phi_1 Y_1 + \phi_3 Y_3], \qquad && Y_1 = \text{diag}(1,-1,0,0,0), \\ &Y_2 = \begin{pmatrix} 0 & 1 \\ -1 & 0 \end{pmatrix} \oplus \text{diag}(0,0,0), \qquad && Y_3 = \text{diag}(0,0,1,1,-2), \end{aligned} \tag{5.2.1}$$

where Y_1, Y_2 and Y_3 are generators of $SL(5)$ group. For such a choice the bosonic action turns out to be

$$\begin{aligned} 2\kappa^2 e^{-1}\mathcal{L} =& R - \frac{m^2}{2}V(\phi_1,\phi_3) - 2(\partial\phi_1)^2 - 2\sinh^2 2\phi_1(\partial_\mu\phi_2 + gA^{(1)}_\mu)^2 - 6(\partial_\mu\phi_3)^2 \\ & -(F^{(1)}_{\mu\nu})^2 - e^{4\phi_3}(F^{(2)}_{\mu\nu})^2, \end{aligned}$$

$$\text{where} \quad V(\phi_1,\phi_3) = -(e^{2\phi_1} + e^{-2\phi_1} + 2e^{-2\phi_1} + e^{4\phi_3})^2 + 2(e^{4\phi_1} + e^{-4\phi_1} + 2e^{-4\phi_3} + e^{8\phi_3}). \tag{5.2.2}$$

To break one of the $U(1)$ symmetry we will set $\phi_2 = 0$ in the above Lagrangian which breaks the $U(1)$ symmetry associated with $A^{(1)}_\mu$. From (5.2.1) we can observe that this is equivalent to a choice of unitary gauge for the coset. From the equations ensuing from the Lagrangian (5.2.2) we can further simplify the action by setting $\phi_3 = 0$ and $A^{(2)}_\mu = 0$. From the equations of motion, that follows from the above Lagrangian one can see that these correspond to a consistent solution. The potential

$V(\phi_1, \phi_3)$ will reduce to

$$V(\phi_1) = (2\cosh 2\phi_1 - 3)^2 - 16. \tag{5.2.3}$$

The extrema of this potential (5.2.3) lies at $\phi_1 = 0$ and $\phi_1 = \frac{1}{2}Log(\frac{3\pm\sqrt{5}}{2})$. We will consider a domain wall solutions such that the scalar ϕ_1 interpolates between these two extrema. To obtain such an interpolating solution, the ansatz for the metric and the gauge field are chosen as follows

$$ds^2 = e^{2A}(-hdt^2 + d\vec{x}_5^2) + \frac{dr^2}{h}, \qquad A^{(1)} = B_1 dt. \tag{5.2.4}$$

With this ansatz, we find the equations of motion to be

$$\begin{aligned}
-5A'' &= 2\frac{e^{-2A}}{h^2}g^2\sinh^2 2\phi_1 B_1^2 + 2\phi_1'^2, \\
h'' + 6A'h' &= 4\frac{e^{-2A}}{h}g^2\sinh^2 2\phi_1 B_1^2 + 4e^{-2A}B_1'^2, \\
4h[\phi_1'' + (6A' + \frac{h'}{h})\phi_1'] &= -4\frac{e^{-2A}}{h}\sinh 4\phi_1 g^2 B_1^2 + \frac{m^2}{2}\frac{\partial V}{\partial \phi_1}, \\
B_1'' + 4A'B_1' &= \frac{1}{h}g^2\sinh^2 2\phi_1 B_1, \\
30(A')^2 + 5\frac{h'}{h}A' &= 2\frac{e^{-2A}}{h^2}g^2\sinh^2 2\phi_1 B_1^2 + 2\phi_1'^2 - 2\frac{e^{-2A}}{h}B_1'^2 - \frac{m^2}{2}\frac{1}{h}V(\phi_1),
\end{aligned} \tag{5.2.5}$$

the last equation is a constraint, which remains valid for a range of r given it is satisfied at some value of r where all other remaining equations are satisfied. We're looking for a solution of the above equations (5.2.5) where the scalar field $\phi_1 = \phi_{IR} = \frac{1}{2}Log(\frac{3\pm\sqrt{5}}{2})$ at IR ($r \to -\infty$) and $\phi_1 = 0$ at UV ($r \to \infty$). Considering the above equation in IR limit, we find the following solution

$$\phi_1 \sim \phi_{IR}, \quad h = 1, \quad B_1 = 0, \quad A = \frac{r}{L_{IR}}, \tag{5.2.6}$$

with exponentially suppressed corrections. With the above solution, the geometry at IR turns out to be AdS with a radius $L_{IR} = \frac{\sqrt{15}}{2m}$. Similarly, at the UV limit, the

geometry is also AdS with radius $L_{UV} = \frac{2}{m}$ with $A = \frac{r}{L_{UV}}$. In both the limit we have AdS geometry with different radius.

In order to obtain a solution which interpolates between these two limits, we need to consider the first corrections to the scalar and the gauge fields at IR which follows from (5.2.6). Where the corrections are given as [79–82]

$$\phi_1(r) = \phi_{IR} + a_\phi e^{\triangle_\phi (r/L_{IR})}, \qquad B_1(r) = a_B e^{\triangle_B (r/L_{IR})}, \tag{5.2.7}$$

where $\triangle_\phi = \frac{\sqrt{111}}{2} - 3$ and $\triangle_B = \frac{\sqrt{91}}{2} - 2$, are obtained from the IR limit analysis of ϕ and B. We will set a_b to be 1 which can be obtained from shifting r and scaling t and x as given in [81]. Therefore, we will be left out with only a single parameter a_ϕ for the solution.

At the UV limit from the equation of motion of ϕ_1 we get the leading behaviour as e^{-2A} and e^{-4A}, which represents the source and expectation value of the dual operator respectively. As we have already mentioned that we are interested in the solution which would break the symmetry spontaneously. Further we impose the additional condition that $\lim_{r\to\infty} \phi_1 \sim e^{-4A}$, under this condition, the parameter a_ϕ can take only discrete values.

Taking boundary condition (5.2.7) into consideration we have numerically solved the equations (5.2.5). The value of a_ϕ was chosen to be 1.717. We have taken that specific value (1.717) for a_ϕ as it provided a scalar field with the least number of nodes. So it may correspond to a solution which is most likely to be stable. In fig.(5.1) we have given the solutions of different fields. The refractive index which is given by the ratio between the relative speed of propagation of light in the ultraviolet and the infrared $n = \sqrt{h_{UV}/h_{IR}}$ [80–82], turns out to be 2.10845 in this case.

We examine the behaviour of conductivity with variation in frequency after obtaining the domain wall solution [80–83]. To do so we consider the gauge fields as $A_x = a_x(r)e^{-i\omega t}$, where we have added a time dependent perturbation in x direction. Due to this a metric perturbation in g_{tx} arises in presence of finite gauge field.

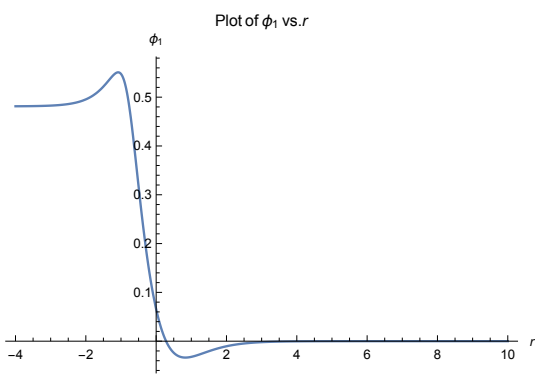

(a) ϕ_1 vs. r

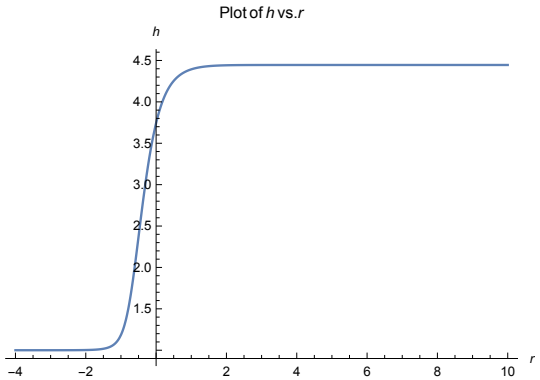

(b) h vs. r

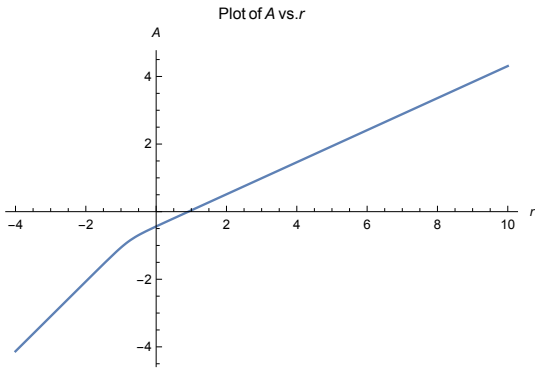

(c) A vs. r

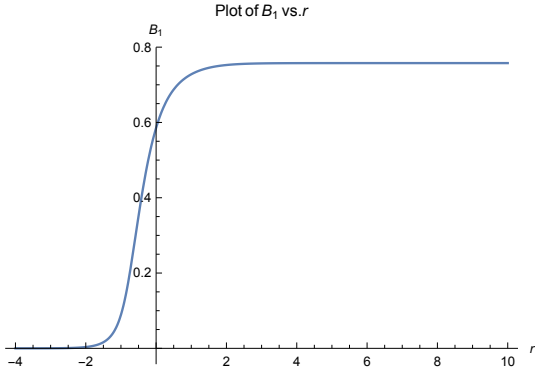

(d) B_1 vs. r

Figure 5.1: Plots of different fields for domain wall solution

From Maxwell's equation and Einstein equation, we will get two coupled linearised equation involving the perturbations, a_x and δg_{tx}, which give rise to the following equation for a_x,

$$a_x'' + (4A' + \frac{h'}{h})a_x' + \frac{\omega^2}{h^2}e^{-2A}a_x - \frac{4}{h}e^{-2A}(B_1')^2 a_x = \frac{g^2}{h}\sinh^2 2\phi_1 a_x. \tag{5.2.8}$$

The asymptotic behaviour of a_x is given by

$$a_x(r) \sim a_x^{(0)} + a_x^{(4)}e^{-4A} + ..., \tag{5.2.9}$$

where the ellipses denote higher order terms. The expression of conductivity is obtained by solving the equation (5.2.8) together with infalling boundary condition which is given by

$$\sigma \sim \frac{-i}{\omega}\frac{a_x^{(4)}}{a_x^{(0)}}, \tag{5.2.10}$$

where the constant of proportionality is independent of ω.

At IR the infalling solution is given by

$$a_x(r) = e^{-2r/L_{IR}} H^{(1)}_{\triangle_B+2}(\omega L_{IR} e^{-r/L_{IR}}), \tag{5.2.11}$$

where $H^{(1)}$ is Hankel function of first kind.

We have numerically solved (5.2.8) subject to the boundary condition (5.2.11) and evaluate conductivity by using the expression given (5.2.10). In Fig. 5.2 we have plotted conductivity vs. frequency. In order to study the behaviour of conductivity for small frequency ω, following [81, 82] we will introduce $\mathcal{F}$,

$$\mathcal{F} = -he^{4A} \frac{a_x^* \partial_r a_x - a_x \partial_r a_x^*}{2i}, \tag{5.2.12}$$

where $\partial_r \mathcal{F} = 0$, as follows from (5.2.8). At IR limit, $\mathcal{F}$ is independent of ω which follows from (5.2.11). The real part of the conductivity is given by

$$Re(\sigma) = \frac{\mathcal{F}}{4h_{UV}} \frac{1}{\omega |a_x^{(0)}|^2}, \tag{5.2.13}$$

and so in order to determine ω dependence we need to find out how $a_x^{(0)}$ depends on ω. For the region $L_{IR} Log(\omega L_{IR}) << r << r_{IR}$ where deviation of geomtry from AdS_{IR} is negligible one can show,

$$a_x \sim -i \frac{\Gamma(\triangle_B + 2)}{\pi} (\frac{2}{\omega L_{IR}})^{\triangle_B+2} Z_x(r), \tag{5.2.14}$$

where at the IR region, $\lim_{r\to-\infty} e^{-\triangle_B r/L_{IR}} Z_x(r) \to 1$. For large r the ω^2 term in (5.2.8) is negligible and on this basis, if we assume that even at large r the ω dependence of a_x remains unaltered, then $a_x^{(0)} = \lim_{r\to\infty} a_x(r) \sim \omega^{-(\triangle_B+2)}$ [81, 82]. From (5.2.13) it follows

$$Re(\sigma) \sim \omega^{2\triangle_B+3}. \tag{5.2.15}$$

From figure 5.2 one can observe that ω dependence of $Re(\sigma)$ agrees with this for

small ω. For large ω limit, the real part of conductivity goes as ω^3, which is its behaviour for ultraviolet AdS_7 geometry.

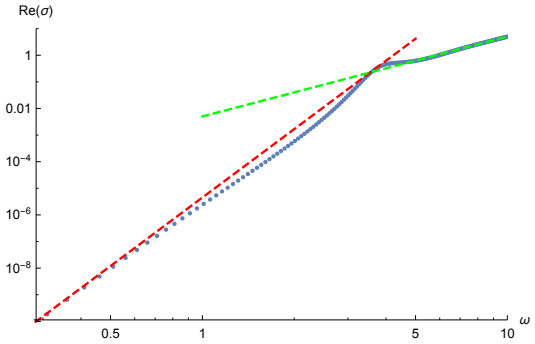

Figure 5.2: Re(σ) vs. ω

5.3 Fermionic Action

We have already discussed the fermionic content of $N = 4$ gauged supergravity in seven dimensions [67–69] in previous chapters, which comprises of gravitino ψ_μ^A and spin-1/2 field λ_i^A. In this domain wall background, we will be only considering those fermions which do not couple with gravitino. The Lagrangian consisting of only spin-1/2 fields λ^i are given in (3.3.3). The covariant derivatives differs from the previous as in chapter 3 and 4 due to the fact that we have a different background compaired to previous ones. The covariant derivatives in this background are given by

$$D_\mu \lambda^i = \nabla_\mu \lambda^i - ig \cosh 2\phi_1 [A_\mu^{(1)} (J^{12})^i_j \lambda^j + (A_\mu^{(1)} S^{12}) \lambda^i], \tag{5.3.1}$$

where J^{12} and S^{12} are generators of the $U(1)$ gauge group for vector and spinor representations respectively. the covariant derivative ∇_μ comprises of the spin connection as follows

$$\nabla_\mu = \partial_\mu - \frac{1}{4}(\omega_\mu)_{ab} \Gamma^{ab}. \tag{5.3.2}$$

The terms in the Lagrangian corresponds to coupling between gravitino Ψ_μ and spin-1/2 fields λ^i are given in (3.3.6).

In order to simplify the notation we will use for $SO(5)$ vector indices as ex-

plained in chapter 3 and 4. With this $SO(5)$ notation, 16 independent components of λ can be organised as $\lambda^{1\pm}(s_{12}, s_{34})$ and $\lambda^{2\pm}(s_{12}, s_{34})$.

We are interested in the fermions which do not couple to gravitino. The second $U(1)$ (associated with $A^{(2)}_\mu$) remains unbroken and gravitino has charges $\pm\frac{1}{2}$ with respect to it. Therefore spinor components with total charge $\pm\frac{3}{2}$ with respect to second $U(1)$ do not couple to gravitino. So $\lambda^{2-}(s_{12}, \frac{1}{2})$ and $\lambda^{2+}(s_{12}, -\frac{1}{2})$, with $s_{12} = \pm\frac{1}{2}$ are decoupled from gravitino and we restrict ourselves to the case of these four fermions only. An explicit computation shows, for the present choice of V^i_I, all the other fermions in **16** couple to gravitino.

Dirac equation for these fermions λ_i can be written as

$$\begin{aligned} &(\Gamma^\mu D_\mu + \frac{m}{4}(5 - 2\cosh 2\phi_1) + i\frac{s_{12}}{2}\Gamma^{\mu\nu}F^{(1)}_{\mu\nu})\lambda = 0, \\ \text{where,} \quad &D_\mu\lambda = \partial_\mu\lambda - ig(q\cosh 2\phi_1 A^{(1)}_\mu)\lambda, \quad F^{(1)}_{\mu\nu} = \partial_\mu A^{(1)}_\nu - \partial_\nu A^{(1)}_\mu, \end{aligned} \tag{5.3.3}$$

the charges q related to the gauge field is given by s_{12}, but for our analysis, we have kept it generic. The scalar field ϕ_1 determines both the mass and charge term. At IR limit the mass is given by $m/2$ where the scalar $\phi_1 = \phi_{IR}$, while at the UV limit $\phi_1 = 0$ and the mass turns out to be $3m/4$.

Γ-matrices are chosen as follows

$$\begin{aligned} &\Gamma^{\hat{t}} = \begin{pmatrix} \Gamma^{\hat{t}}_1 & 0 \\ 0 & \Gamma^{\hat{t}}_1 \end{pmatrix}, \qquad \Gamma^{\hat{r}} = \begin{pmatrix} \Gamma^{\hat{r}}_1 & 0 \\ 0 & \Gamma^{\hat{r}}_1 \end{pmatrix}, \qquad \Gamma^{\hat{i}} = \begin{pmatrix} \Gamma^{\hat{i}}_1 & 0 \\ 0 & \Gamma^{\hat{i}}_1 \end{pmatrix} \\ &\Gamma^{\hat{t}}_1 = \begin{pmatrix} 0 & i\sigma_2 \\ i\sigma_2 & 0 \end{pmatrix}, \qquad \Gamma^{\hat{r}}_1 = \begin{pmatrix} I & 0 \\ 0 & -I \end{pmatrix}, \qquad \Gamma^{\hat{i}}_1 = \begin{pmatrix} 0 & \sigma_1 \\ \sigma_1 & 0 \end{pmatrix}, \end{aligned} \tag{5.3.4}$$

where I is 2×2 is identity matrix, σ_1, σ_2 and σ_3 are Pauli spin matrices. Due to the identical nature of the block diagonal in the relevant Γ-matrices, we can choose, $\lambda = (\Psi, \chi)^T$ where both the 4-component spinors Ψ and χ satisfies the same equation. In this regard, we will consider only the upper component Ψ. One can get rid of the spin connection by redefining the spinors with appropriate prefactor and choose the

$\Psi = (\Psi^+, \Psi^-)^T$, with each components satisfying the following equation:

$$(\sqrt{h}\partial_r + \frac{m}{4}(5 - 2\cosh 2\phi_1))\Psi^+ + ie^{-A}[k\sigma_1 - (\frac{\omega + gq\cosh 2\phi_1 B_1}{\sqrt{h}} - s_{12}B_1')i\sigma_2]\Psi^- = 0,$$
$$(-\sqrt{h}\partial_r + \frac{m}{4}(5 - 2\cosh 2\phi_1))\Psi^- + ie^{-A}[k\sigma_1 - (\frac{\omega + gq\cosh 2\phi_1 B_1}{\sqrt{h}} + s_{12}B_1')i\sigma_2]\Psi^+ = 0. \tag{5.3.5}$$

These two component spinors are further written as $\Psi^\pm = (\Psi_1^\pm, \Psi_2^\pm)$ and obtain the equations for each individual components,

$$(\sqrt{h}\partial_r - \frac{m}{4}(5 - 2\cosh 2\phi_1))\Psi_1^- - ie^{-A}[k - (\frac{\omega + gq\cosh 2\phi_1 B_1}{\sqrt{h}} + s_{12}B_1')]\Psi_2^+ = 0,$$
$$(\sqrt{h}\partial_r + \frac{m}{4}(5 - 2\cosh 2\phi_1))\Psi_2^+ + ie^{-A}[k + (\frac{\omega + gq\cosh 2\phi_1 B_1}{\sqrt{h}} - s_{12}B_1')]\Psi_1^- = 0. \tag{5.3.6}$$

As one can observe, the Dirac equation reduces to coupled equations for the two components (Ψ_1^-, Ψ_2^+). A similar set of equations follows for the other two components,

$$(\sqrt{h}\partial_r - \frac{m}{4}(5 - 2\cosh 2\phi_1))\Psi_2^- - ie^{-A}[k + (\frac{\omega + gq\cosh 2\phi_1 B_1}{\sqrt{h}} + s_{12}B_1')]\Psi_1^+ = 0,$$
$$(\sqrt{h}\partial_r + \frac{m}{4}(5 - 2\cosh 2\phi_1))\Psi_1^+ + ie^{-A}[k - (\frac{\omega + gq\cosh 2\phi_1 B_1}{\sqrt{h}} - s_{12}B_1')]\Psi_2^- = 0. \tag{5.3.7}$$

These two sets of equations can be made identical by changing the signs of ω, q and s_{12}. So it is sufficient to consider only one set of equations and we will be considering the first set of equations (5.3.6). We will be using a numerical method with appropriate boundary conditions to solve these equations as we could not find any analytic solution for it. Nevertheless, one can find analytic expressions for the behaviour of the solutions at IR and UV limits.

IR limit: At the IR limit above equation gets simplified with the fields and metric coefficient reduces to $A \sim r/L_{IR}$, $h \sim 1$, $B_t^{(1)} \sim 0$, $\phi_1 \sim \phi_{IR}$. The geometry is AdS with radius L_{IR} and the mass is given by $m_{IR} = m/2$. The equation (5.3.6)

is solved by using the infalling boundary condition given in [74]. The solutions get split into two regions which are space-like and time-like momenta region. For space-like momenta, $k^2 \geq \omega^2$:

$$\begin{aligned} \Psi_1^-(r) &= e^{-r/2L_{IR}} K_{m_{IR}L_{IR}+\frac{1}{2}}(\sqrt{k^2-\omega^2}L_{IR}e^{-r/L_{IR}}), \\ \Psi_2^+(r) &= i\sqrt{\frac{k+\omega}{k-\omega}} e^{-r/2L_{IR}} K_{-m_{IR}L_{IR}+\frac{1}{2}}(\sqrt{k^2-\omega^2}L_{IR}e^{-r/L_{IR}}), \end{aligned} \tag{5.3.8}$$

where $K_{\pm m_{IR}L_{IR}+\frac{1}{2}}$ represents modified Bessel function. For time-like momentum we have two parts with, $\omega > |k|$ we get a solution which is expressed in terms of Hankel function of first kind,

$$\begin{aligned} \Psi_1^-(r) &= e^{-r/2L_{IR}} H^{(1)}_{m_{IR}L_{IR}+\frac{1}{2}}(\sqrt{\omega^2-k^2}L_{IR}e^{-r/L_{IR}}), \\ \Psi_2^+(r) &= -i\sqrt{\frac{\omega+k}{\omega-k}} e^{-r/2L_{IR}} H^{(1)}_{m_{IR}L_{IR}-\frac{1}{2}}(\sqrt{\omega^2-k^2}L_{IR}e^{-r/L_{IR}}), \end{aligned} \tag{5.3.9}$$

Similarly, for the other half, $\omega < -|k|$ they are expressed in terms of Hankel function of second kind.

UV limit: At the UV limit, the fields and metric coefficient are given by $A \sim r/L_{UV}$, $h \sim h_{UV}$, $\phi_1 \sim 0$. The geometry is once again AdS with radius $L_{UV} = 2/m$ and the mass reduces to $m_{UV} = 3m/4$. In this limit equations (5.3.6) has only mass terms dependence and the asymptotic limit of the solutions are given by,

$$\begin{aligned} \Psi_1^-(r) &\sim C_1^- e^{m_0 r} + D_1^- e^{-(m_0+1)r}, \\ \Psi_2^+(r) &\sim C_2^+ e^{(m_0-1)r} + D_2^+ e^{-m_0 r}, \end{aligned} \tag{5.3.10}$$

where we have set $m = 2$ and defined $m_0 = m_{UV}/\sqrt{h_{UV}}$.

For this set of fermions (Ψ_1^-, Ψ_2^+) Green's function is given by the following [14].

$$G_R(\omega, k) = i\frac{D_2^+}{C_1^-}. \tag{5.3.11}$$

while for the other set (Ψ_1^+, Ψ_2^-) we have a similar expression. These two components of Green's function form the two diagonal object of Green's function. For

our purpose, we will consider only the one given in (5.3.11). The spectral function evaluated from the expression of Green's function as $A(\omega, k) = Im[G_R(\omega, k)]$. We will study the behaviour of the spectral function with respect to frequency and momenta. In the next section, using the boundary conditions at IR we will solve the Dirac equations numerically.

We conclude this section with the discussion of the dual field theory. The operators dual to the spinor fields in the supergravity transforming under **16** are of the form $tr(\Sigma\psi)$, as already mentioned in chapter 3. For our purpose we organise them as $tr(\Sigma^{1\pm}\psi(s_{12}, s_{34}))$ and $tr(\Sigma^{2\pm}\psi(s_{12}, s_{34}))$ with $s_{12}, s_{34} = \pm 1/2$.

The identification of the operators dual to the 14 scalars appearing in the coset is slightly more subtle. We have already mentioned about these identification in terms of position of M5 branes in chapter 4. A more precise identification of the 14 scalars in cosets is given by [77]. In the dicussion of bosonic action in chapter 3 we introduced the symmetric tensor, $T^{ab} = V_I^{-1\ a} V_J^{-1\ b} \delta^{IJ}$, where V^{-1} is the inverse of the coset and $a, b = 1, 2.., 5$. This tensor can be written in terms of another symmetric tensor $(e^S)_{ab}$, where S_{ab} is a 5×5 traceless matrix. The operators dual to S_{ab} are given by $\mathcal{O}_{ab} = \Sigma_a \Sigma_b - \frac{1}{5}\delta_{ab}(\Sigma_c \Sigma^c)$. For our choice of scalars,

$$S_{ab} = (-2\phi_1, 2\phi_1, 2\phi_3, 2\phi_3, -4\phi_3), \quad \mathcal{O}_{\phi_1} \sim -(\Sigma_1^2 - \frac{1}{5}(\Sigma_1^2 + ... + \Sigma_5^2)) \quad \text{etc.} \tag{5.3.12}$$

Let us also recall that we begin with two $U(1)$ symmetry for the choice of our coset one of the $U(1)$ is broken. The surviving $U(1)$ symmetry corresponds to rotation between Σ_3 and Σ_4. We also note for the latter purpose that the fermionic operators dual to the four fermionic modes in the supergravity that we are considering involve Σ_3 and Σ_4 only.

5.4 Numerical Result

In this section we have considered fermions $\lambda^{2\pm}(\frac{1}{2}, \pm\frac{1}{2})$ and plotted the spectral function corresponding to its operator in the boundary dual CFT. The charges for

first $U(1)$ is given by $q = \pm\frac{1}{2}$ and the coefficient of the Pauli term is $\pm\frac{1}{2}$. In Fig. 5.3 we have plots of spectral function $Im(G_R)$ vs. ω for several values of k with two distinct charges $q = 1/2$ and $-1/2$.

For positive q, which can be observed in Fig. 5.3a, all peaks lie on the positive side of ω. Height of the peak is highest for $k = 0.11$, as k moves away from it, the height of the peak decreases. It develops a hump on the negative side of ω. For the negative value of q, the peaks appear on the negative side of ω which is given in Fig. 5.3b with the height of peak being highest at $k = -0.12$. The peak's height becomes smaller as k deviates from this value of k. Once again humps appear, this time on the positive side of ω. As the humps in the main figure are not visible, we have created an enlarged figure for positive ω in the inset. In both of the cases, spectral function shows a depletion around $\omega = 0$ indicating a gapped spectrum. We have inspected the spectral function for further higher values of q. We find that the depleted region still survives for this higher value of the charge. However, on increasing the charge q, a larger number of peaks seem to appear and the heights of the peaks appear to increase

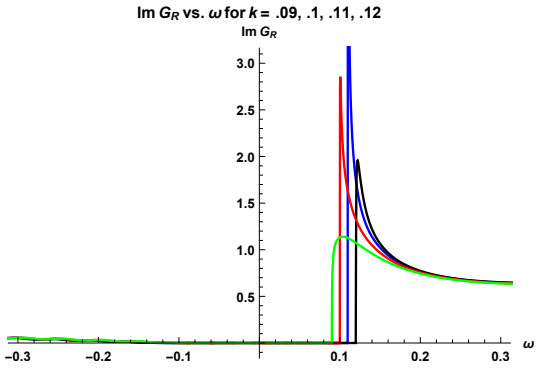

(a) ImG_R vs. ω for $q = 1/2$

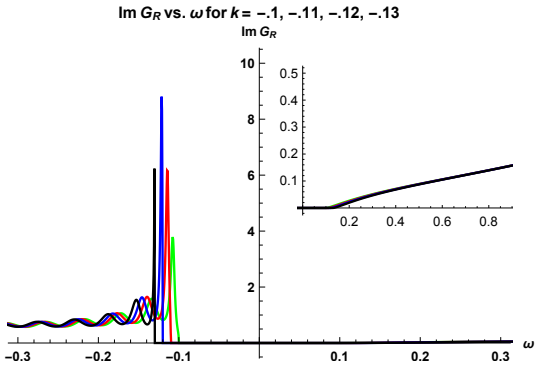

(b) ImG_R vs. ω for $q = -1/2$

Figure 5.3: Spectral function for fermionic mode with: Left: $k = .09$ (green), $k = .1$ (red), $k = .11$ (blue), $k = .12$ (black). Right: $k = -.1$ (green), $k = -.11$ (red), $k = -.12$ (blue), $k = .13$ (black).

The presence of gapped spectrum for the fermionic operators may be due to insufficient charge or due to the presence of Pauli term. In the present case, charges of fermions under the $U(1)$ gauge group at the asymptotic limit is given by $q = \pm\frac{1}{2}$. We have artificially tuned q to $q = -2$ and set the Pauli term as zero to prevent its

effect, in order to check whether that gap in the spectrum depends on the charge of the fermion. The gap still remains which can be seen from Fig. 5.5. When $|q|$ is higher, the peaks start to appear on the positive side of ω and those peaks are sharper and higher than $q = \pm 1/2$. On the negative side, for this value of q, humps continue to exist along with small peaks.

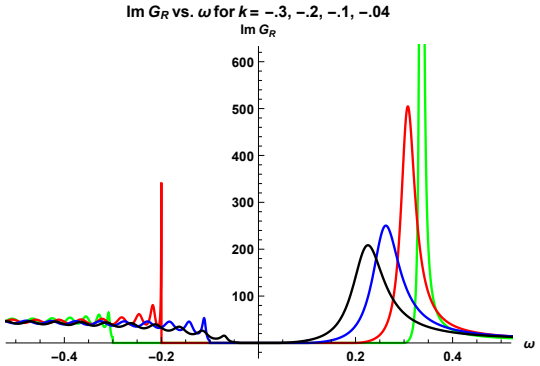

Figure 5.4: ImG_R vs. ω for $q = 2$

Figure 5.5: Spectral function for fermionic mode with $k = -.3$ (green), $k = -.2$ (red), $k = -.1$ (blue), $k = -.04$ (black)

5.5 Discussion

In seven dimensional gauged supergravity theory we have obtained a domain wall solution, which interpolates between two AdS geometries which have different radii. These two AdS geometry lies on extrema of the scalar potential, where one extrema is the IR limit where we have a non-zero value of the scalar field and the other extrema corresponds to UV limit where scalar field vanishes. Non zero expectation value of the scalar field on the extrema breaks one of the $U(1)$ symmetry spontaneously in the Cartan of $SO(5)$, due to this one can consider this to be similar to a holographic superconductor. We have studied the behaviour of optical conductivity with variation in frequency where we find that the real part of conductivity obeys a power law with certain exponent for small frequency, while for the large frequency it depends on the cubic power of frequency.

In the background of domain wall, we have considered the fermions. It turns

out, there are four fermionic modes (out of total 16) in the supergravity theory, that does not couple to the gravitino in this background. We have studied the spectral function associated with the dual operators to those modes and find all of them leads to gapped spectra. Since inadequate charge or presence of Pauli term often leads to gapped spectrum. we have artificially increased the charges and set the Pauli term equals zero, though the gap remains in the spectral function. Similar gapped spectrum was obtained in [39] for fermionic quasi-particles in the presence of condensate at zero temperature. Gapped spectra were also found in four dimensional gauged supergravity dual to ABJM model [42, 43], where the gap has been attributed to the low charge or particle-hole interaction.

The present solution corresponds to the expectation value of dual operator $\mathcal{O}_{\phi_1}$ to be negative. Therefore. from (5.3.12) it implies $\langle tr(\Sigma_1^2)\rangle > 0$. Furthermore, since $\phi_3 = 0$ for our solution, from $\mathcal{O}_{\phi_3} = 0$ one can conclude that $\langle tr(\Sigma_3^2) + tr(\Sigma_4^2)\rangle > 0$. As has already been pointed out, the operators dual to the fermionic modes considered here involves Σ_3 and Σ_4. So the fermionic operators involving bosons with non zero expectation value gives rise to gapped spectrum in this case. It will be interesting to understand the essential field theory mechanism that determines the appearance of the gap in the spectrum.

The domain wall we have considered interpolates between two conformal field theories and in that sense, it is similar to a renormalisation group flow. However, in this case, it has a spontaneously generated expectation value of a symmetry breaking operator rather than adding relevant deformation. It may be interesting to address the stability issues associated with this domain wall solution. It would also be interesting to obtain this solution as a zero temperature limit of holographic superconductor. Regarding the fermionic spectrum, a clear picture of the roles played by various operators in the dual field theory would be quite useful, which requires models that can provide more precise and detailed analysis. In order to keep the analysis simple, we have set one of the gauge fields and scalar fields to be zero. Considering a more general background may be more informative. We have not considered the

fermionic modes coupled to gravitini and a full fledged analysis of all the modes including gravitini may lead to further insight.

Chapter 6

Fermionic spectrum from a domain wall in five dimensions

6.1 Introduction

In last chapter we have studied the behaviour of fermions in the background of domain wall solution arising in a maximally symmetric theory. This domain wall soution arises due to particular choice of scalar vielbiens in truncated bosonic action of maximally gauged supergravity theory. Due to presence of large symmetry one can have a better control. Also it makes the theory simpler involving less number of fields. Though it is suitable to study some of the aspects, a realistic model would have less symmetry and lower dimension.

In view of this, we would like to extend this analysis to a gavity theory with less supersymmetry in five dimension. This theory can be obtained [81] by compactification of type IIB supergravity on a five dimensional Sasaki-Einstein manifold [80,84] after making suitable truncations. Solution of equation of motion of this truncated theory can be expected to remain a solution when uplifted to the full theory. The field contents and the dynamics of this model has been elaborately discussed in [84]. The bosonic part of this theory admits a domain wall solution, which interpolates between two AdS geometries. It leads to spontaneously breakdown of a $U(1)$ sym-

metry and in that respect, it may correspond to zero temperature of holographic superconductor. This domain wall solution corresponds to some state in the dual field theory. Studying fermions in the gravity theory in this background can shed light on the behaviour of fermionic operators in the dual theory.

So we consider dynamics of the fermionic modes of this truncated five dimensional theory in this domain wall background. It turns out [84] that after suitable truncation, the fermionic modes can be organised in different sectors.In addition, this five dimensional theory demonstrates a different kind of couplings between fermions and charged scalars which may have some phenomenological interest [84]. For convenience, we have chosen most suitable sector for our purpose; the sector consisting of a single fermion, which does not couple to fermions in other sectors or gravitini. As we have explained in detail this fermion can be considered as dual to fermion of a supermultiplet, arising in a quiver gauge theory. We have used holographic method to study the spectral function of this dual operator. Furthermore, in order to keep our study flexible we analyse fermions with different values of charges.

We have analysed behaviour of fermions for two different distinct fermionic charges. From the study of the fermionic spectrum we find higher fermionic charge leads to a gapless spectrum, while for lower charge it develops a gap. We have also studied behaviour of the gap with variation of Pauli term. We obtained the dispersion relation of excitations for these two charges as well. The contents of this chapter has been published in [47]. In the next section, we briefly describe the domain wall solution that we use as the background. In section 6.3 and 6.4 we present Green's function and its numerical computation for different charges respectively. We conclude with a discussion in section 6.5.

6.2 Domain Wall solution

In this section we will start with a brief review of the domain wall solution which was obtained in [81]. We consider compactification of type IIB string theory on a

product of an anti-de Sitter space and a Sasaki-Einstein manifold, $AdS_5 \times Y$. A consistent truncation gives rise to a five-dimensional theory with bosonic content consisting of metric, a $U(1)$ gauge field and a complex scalar. The action is given by [81]

$$\begin{aligned} S =& \frac{1}{2\kappa_5^2}\int d^5x\sqrt{-g}(R - \frac{1}{4}F_{\mu\nu}F^{\mu\nu} \\ & - \frac{1}{2}[(\partial_\mu\eta)^2 + \sinh^2\eta(\partial_\mu\theta - \frac{\sqrt{3}}{L}A_\mu)^2] + \frac{3}{L^2}\cosh^2\frac{\eta}{2}(5-\cosh\eta) \end{aligned} \tag{6.2.1}$$

where $\eta e^{i\theta}$ represents the complex scalar field and also there is an additional Chern-Simons term. The potential $V(\eta) = -\frac{3}{L^2}\cosh^2\frac{\eta}{2}(5-\cosh\eta)$ has two extrema, $\eta = 0$ and $\eta = Log(2+\sqrt{3})$

Similar to previous domain wall solution in chapter 5, we will consider following ansatz for the metric, gauge field and scalar field in order to obtain domain wall solution,

$$ds^2 = e^{2A}\left(-hdt^2 + d\mathbf{x}^2\right) + \frac{dr^2}{h}, \quad A = A_t dt, \quad \theta = 0. \tag{6.2.2}$$

The equations of motion obtained from the above action (6.2.1) together with of the ansatz (6.2.2) are given by [82]

$$\begin{aligned} 3hA'' &= -\frac{3}{2L^2}\frac{e^{-2A}}{h}\sinh^2\eta A_t^2 - \frac{1}{2}h(\eta')^2, \\ h'' + 4A'h' &= e^{-2A}(A_t')^2 + 2\frac{3}{2L^2}\frac{e^{-2A}}{h}\sinh^2\eta A_t^2, \\ \eta'' + (4A' + \frac{h'}{h})\eta' &= -2\frac{3}{2L^2}\frac{e^{-2A}}{h^2}A_t^2\sinh\eta\cosh\eta + \frac{1}{h}V'(\eta), \\ A_t'' + 2A'A_t' &= \frac{3}{L^2h}\sinh^2\eta A_t, \\ \frac{3}{2}[4h(A')^2 + A'h'] &= \frac{1}{2h}[\frac{1}{2}h^2(\eta')^2 + \frac{3}{2L^2}e^{-2A}\sinh^2\eta A_t^2 - \frac{1}{2}e^{-2A}h(A_t')^2 - hV(\eta)], \end{aligned} \tag{6.2.3}$$

the last equation is a constraint which has been explained in previous chapter 5.

The domain wall solution once again interpolates between two extrema of scalar potential, $\eta = 0$ at UV and $\eta = Log(2+\sqrt{3})$ at IR. At both the limits of IR and UV we have a AdS_5 geometry with radii of curvature $L_{IR} = 2\sqrt{2}\frac{L}{3}$ and L respectively.

The boundary conditions are chosen in the following manner. At IR, A_t vanishes and $A \sim r/L_{IR}$, $h \sim 1$. At IR limit the asymptotic behaviour of the gauge field and the scalar field are given by,

$$\eta \sim Log(2+\sqrt{3}) + a_\eta e^{(\triangle_{IR}-4)r/L_{IR}}, \quad A_t \sim a_{A_t} e^{(\triangle_{A_t}-3)r/L_{IR}}. \tag{6.2.4}$$

With $\triangle_{IR} = 6-\sqrt{6}$ and $\triangle_{A_t} = 5$ which follows from the IR limit of the equations. The parameter a_{A_t} can be set to 1 [81] by shifting r. That would introduce a multiplicative factor in e^{2A} in the metric, which can be reabsorbed by rescaling t and $\vec{x}$ appropriately. So we are left with a single parameter a_η.

At UV, $\eta = 0$, $h = h_{UV}$, $A \sim \frac{r}{\sqrt{h_{UV}}L}$. From the equation of motion, it follows that asymptotic behaviour of η is given by e^{-A} and e^{-3A}. Solution with spontaneous breaking of symmetry is ensured by setting $\eta \sim e^{-3A}$ at UV, which corresponds to an expectation value for the dimension 3 operator dual to η. This condition allows a_η to have only the discrete values. Equations (6.2.3) can be solved numerically by choosing a suitable value of the parameter a_η, which leads to a domain wall solution. $a_\eta = 1.866$ gives the least number of nodes for the range we have considered, so we have chosen that value of a_η for our further calculations. This solution is expected not to be supersymmetric and so there are possibilities of instabilities. An analysis of thermodynamic stability of the numerical solution is required to settle stability related issue. Our choice corresponds to the fact that for other values of a_η would give solutions with a higher number of nodes with same boundary condition and so have higher free energy and can be considered as less favourable thermodynamically. Profiles of the various fields are given in Fig. 6.1.

6.3 Green's Function

In this section considering domain wall solution as our background, we will study the fermionic spectrum A consistent truncation of bosonic theory in a compactification of type IIB theory on AdS_5 times a Sasaki-Einstein manifold gives domain

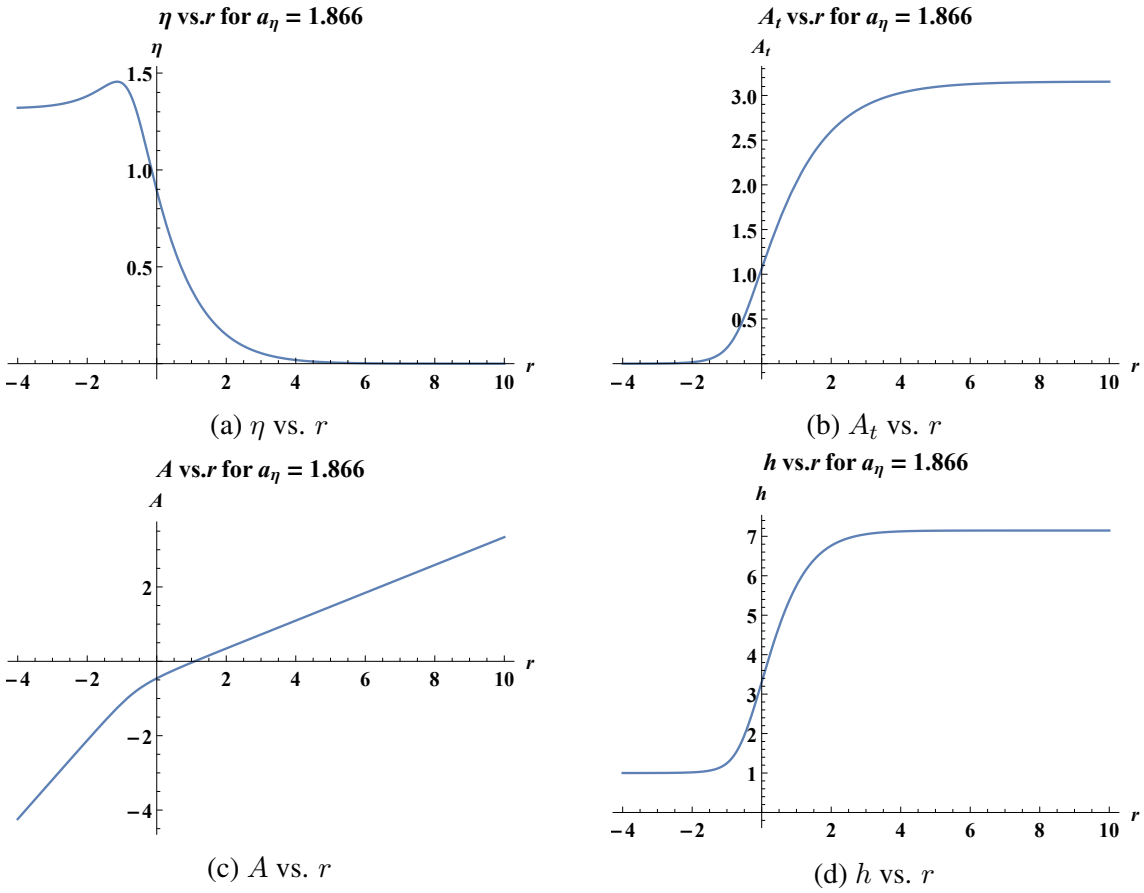

(a) η vs. r

(b) A_t vs. r

(c) A vs. r

(d) h vs. r

Figure 6.1: Plots of different fields for domain wall solution

wall as a solution. The fermionic part of this truncated theory has been studied in a detailed manner in [84]. As given there, one can get a decoupled sector for the fermionic fields with the suitable truncation of the fermionic sector of this theory. To make our analysis simple in the present case, we will be only considering a single fermionic mode, which decouples from gravitino and any other fermionic modes. The action for this particular single fermionic mode is given by

$$S = \int d^5x\,\sqrt{-g}\,\frac{1}{2}\bar{\lambda}(\Gamma^\mu D_\mu + i\frac{\sqrt{3}}{2}\sinh^2\frac{\eta}{2}\Gamma^\mu A_\mu - \frac{1}{2}(7+\sinh^2\frac{\eta}{2}) - ip\frac{\sqrt{3}}{4}\Gamma^{\mu\nu}F_{\mu\nu})\lambda, \tag{6.3.1}$$

where $D_\mu = \partial_\mu + \frac{1}{4}\omega_{\mu ab}\Gamma^{ab} - i\frac{\sqrt{3}q}{2}A_\mu$ and $\omega_{\mu ab}$ is the spin connection. We have set $L = 1$. The asymptotic charge and the coefficient of Pauli term evaluated from the supergravity action are given by $q = 1$ and $p = \frac{1}{6}$ respectively, but we have kept

these as a free parameter. The Dirac equation following from the action is given by

$$[\Gamma^{\mu}(\partial_{\mu} - i\frac{\sqrt{3}Q}{2}A_{\mu}) - M - ip\frac{\sqrt{3}}{4}\Gamma^{\mu\nu}F_{\mu\nu}]\lambda = 0, \tag{6.3.2}$$

where $Q = q + \sinh^2\frac{\eta}{2}$ and $M = \frac{1}{2}(7 + \sinh^2\frac{\eta}{2})$ are charge and mass terms which depends on the scalar. Contribution from spin connection in the Dirac equation can be removed by redefining λ as $\lambda \to h^{-1/8}\,\lambda$.

We choose the following γ-matrices in 2×2 block form,

$$\Gamma^{\widehat{t}} = \begin{pmatrix} 0 & i\sigma_2 \\ i\sigma_2 & 0 \end{pmatrix}, \quad \Gamma^{\widehat{r}} = \begin{pmatrix} 1 & 0 \\ 0 & -1 \end{pmatrix}, \quad \Gamma^{\widehat{x}} = \begin{pmatrix} 0 & \sigma_1 \\ \sigma_1 & 0 \end{pmatrix}. \tag{6.3.3}$$

Spinors are chosen to be $\lambda = e^{-i\omega t + ikx}(\Psi^+, \Psi^-)^T$, where each of the $\Psi^{\pm}$ are two component spinors. Dirac equations reduce to

$$(\pm\sqrt{h}\partial_r - M)\Psi^{\pm} + ie^{-A}(k\sigma_1 - \frac{\omega + \frac{\sqrt{3}Q}{2}A_t}{\sqrt{h}}i\sigma_2 \mp \frac{\sqrt{3}p}{2}A_t' i\sigma_2)\Psi^{\mp} = 0. \tag{6.3.4}$$

Writing $\Psi^{\pm} = (\Psi_1^{\pm}, \Psi_2^{\pm})^T$, equations for the individual components becomes

$$\begin{aligned} (\sqrt{h}\partial_r - M)\Psi_1^+ + ie^{-A}[k - \frac{\omega + \frac{\sqrt{3}Q}{2}A_t}{\sqrt{h}} - \frac{\sqrt{3}p}{2}A_t']\Psi_2^- = 0, \\ (\sqrt{h}\partial_r + M)\Psi_2^- - ie^{-A}[k + \frac{\omega + \frac{\sqrt{3}Q}{2}A_t}{\sqrt{h}} - \frac{\sqrt{3}p}{2}A_t']\Psi_1^+ = 0. \end{aligned} \tag{6.3.5}$$

The other two components satisfy the following equations,

$$\begin{aligned} (\sqrt{h}\partial_r - M)\Psi_2^+ + ie^{-A}[k + \frac{\omega + \frac{\sqrt{3}Q}{2}A_t}{\sqrt{h}} + \frac{\sqrt{3}p}{2}A_t']\Psi_1^- = 0, \\ (\sqrt{h}\partial_r + M)\Psi_1^- - ie^{-A}[k - \frac{\omega + \frac{\sqrt{3}Q}{2}A_t}{\sqrt{h}} + \frac{\sqrt{3}p}{2}A_t']\Psi_2^+ = 0. \end{aligned} \tag{6.3.6}$$

(Ψ_1^+, Ψ_2^-) and (Ψ_2^+, Ψ_1^-) are two set of coupled equations. Each set can be interchanged by flipping the signs of ω, Q and p. In this respect it is sufficient to consider only one set of equations, so we will confine ourselves to the case of (Ψ_1^+,

Ψ_2^-) only. From (6.3.5) we can get the IR and UV behaviour of these fermions. At the IR limit, $\eta = Log(2+\sqrt{3})$, which sets $Q = q + 1/2, m_{IR} = 15/4$ and $h = 1$. The geometry at this limit is AdS with radius L_{IR}. The behaviour of fermions that match the in-falling boundary condition depends on whether the momentum is time-like or space-like after [74]. In the following, we discuss the two individual cases.

We start with space-like momenta, where $k^2 \geq \omega^2$. In this case, in-falling boundary conditions at IR is defined in terms of modified Bessel functions given as

$$\begin{aligned}\Psi_1^+(r) &\sim U_1^+ e^{-r/2L_{IR}} K_{m_{IR}L_{IR}+\frac{1}{2}}(\sqrt{k^2-\omega^2}L_{IR}e^{-r/L_{IR}}),\\ \Psi_2^-(r) &\sim U_2^- e^{-r/2L_{IR}} K_{m_{IR}L_{IR}-\frac{1}{2}}(\sqrt{k^2-\omega^2}L_{IR}e^{-r/L_{IR}}),\end{aligned} \tag{6.3.7}$$

where $U_2^- = -i\sqrt{\frac{k+\omega}{k-\omega}}U_1^+$. We have chosen $U_1^+ = 1$.

For time-like momentum, where $\omega| > |k|$ the solutions are given in terms of Hankel function of first kind,

$$\begin{aligned}\Psi_1^+(r) &\sim U_1^+ e^{-r/2L_{IR}} H^{(1)}_{m_{IR}L_{IR}+\frac{1}{2}}(\sqrt{\omega^2-k^2}L_{IR}e^{-r/L_{IR}}),\\ \Psi_2^-(r) &\sim U_2^- e^{-r/2L_{IR}} H^{(1)}_{m_{IR}L_{IR}-\frac{1}{2}}(\sqrt{\omega^2-k^2}L_{IR}e^{-r/L_{IR}}),\end{aligned} \tag{6.3.8}$$

where $U_2^- = i\sqrt{\frac{\omega+k}{\omega-k}}U_1^+$. We have chosen $U_1^+ = 1$. Similarly, for $\omega < -|k|$ they are expressed in terms of Hankel function of second kind.

At UV limit, for both time-like and space-like region, $\eta = 0$, $Q = q$ and $M_{UV} = 7/2$. The metric coefficient $h(r)$ and the gauge field A_t approaches h_{UV} and $A_t(UV)$ respectively, with h_{UV} being a constant. The geometry is AdS with radius L_{UV}. At asymtotic limit $r \to \infty$ fermions depend only on mass terms and are given by

$$\begin{aligned}\Psi_1^+(r) &\sim C_1^+ e^{M_{UV}r/\sqrt{h_{UV}}} + D_1^+ e^{-(M_{UV}+1)r/\sqrt{h_{UV}}},\\ \Psi_2^-(r) &\sim C_2^- e^{(M_{UV}-1)r/\sqrt{h_{UV}}} + D_2^- e^{-M_{UV}r/\sqrt{h_{UV}}}.\end{aligned} \tag{6.3.9}$$

The Green's function is given by

$$G_R(\omega, k) = \frac{D_2^-}{C_1^+}. \tag{6.3.10}$$

The Green's function in the present case is diagonal and the other component can be obtained from (Ψ_2^+, Ψ_1^-) in a similar manner. The imaginary part of the retarded Green's function represents the spectral function. In the next section, we study the behaviour of spectral function for fermions for different choices of charges. In this case, the Green's function is diagonal, and the other component (Ψ_2^+, Ψ_1^-) can be obtained similarly. The spectral function is given by the imaginary part of the retarded Green's function. In the following section, we examine the behaviour of spectral function for fermions with the variation of charge.

6.4 Result

In this section, we will study the behaviour of the dual operators of these fermionic modes. As mentioned earlier, we will be only considering the modes corresponding to (Ψ_1^+, Ψ_2^-) which is sufficient as the behaviour for the other two fermionic modes will be similar. In this model both charges and masses depend on the scalar field η as $Q = q - \sinh^2 \frac{\eta}{2}$ and $M = \frac{1}{2}(7 + \sinh^2 \frac{\eta}{2})$ which is not seen in the case any other generic fermions.

We will analyse two different cases which correspond to spacelike and timelike region. For the spacelike region taking the boundary condition (6.3.7) we will solve Dirac equations (6.3.5) numerically and look for normal modes. The normal modes are given by the zeroes of C_1^+ in (3.4.11) which leads to singularities in the Green's function. We fix the value of charge q and we scan the value of k for different value of ω to find the zeroes of C_1^+. We begin with $q = 1$ which follows from the supergravity model, which does not yield any normal mode. We could not find any normal mode with the charge of this supergravity model which is consistent with [41] as the asymptotic charge ($q = 1$) is quite small and also has a non-zero

asymptotic mass ($m = \frac{7}{2}$), as the mass increases the probability of finding a normal mode decreases.

We find the normal modes for $\omega \geq \omega_c$ in this region by artificially increasing the value of the charge. As charge increases the value of ω_c decreases and becomes $\omega_c = 0$. To show this we have considered two different value of charges, $q = 4.5$ and $q = 10$. Unless mentioned otherwise, the value of the mass and Pauli coupling are set to be equal to the one obtained from supergravity. The plots of ω vs. k for normal modes for those two charges are given in Fig. 6.2a and Fig. 6.2b respectively. For $q = 4.5$ we find the appearance of normal modes at $\omega \geq \omega_c = 0.761$, whereas for $q = 10$ the minimum value for ω to show normal modes is $\omega_c = 0$ indicating the spectrum to be gapped and gapless respectively.

The supergravity Lagrangian in the present model has a Pauli term with a coefficient of $p = \frac{1}{6}$ and as shown in [17, 20] Pauli term may have a significant effect on the spectral function. As observed in [20], in particular, the large value of Pauli term may give rise to gapped spectrum. To examine the effect of Pauli coupling keeping the charge q fixed at 4.5 we have dialled its value of coefficient p manually and plotted the gap δ vs. p in Fig 6.3b. We find the gap is maximum at a small negative value of p (around -0.3). As we depart from this value, the gap generally decreases in either side of it, except around $p = -3.55$ where we get a local maxima. Since the gap is non-zero at $p = 0$ for a lower charge, so one cannot comprehend the gap as a result of Pauli coupling.

From the semi-classical analysis [41], $\frac{(\omega+q\phi_{UV})^2}{h_{UV}} - k^2 = m_{eff}^2$ can be considered as dispersion relation satisfied by the normal modes, where the constant on the right hand side is related to the number of nodes of the fermion wave-function associated with normal mode. The normal modes shown in Fig. 6.2a for $q = 4.5$ correspond to zero node wave functions. We have given a plot in Fig. 6.3a representing a typical wavefunction. As the value of charge q is increased to $q = 10$, more normal modes start to appear. These are arranged along different curves as shown in Fig. 6.2b, where associated wavefunctions of the modes lying on a curve have the same

number of nodes.

In Fig. 6.2b, the normal modes with the lowest number of nodes lie on the extreme right curve where the number of nodes is zero, as one moves from right to left the number of nodes increases. We have tried one parameter fit for these point with the relation $\frac{(\omega+q\phi_{UV})^2}{h_{UV}} - k^2 = m_{eff}^2$, with the values of ϕ_{UV} and h_{UV} fixed by the equation and varied m_{eff}. But this one parameter fit could not properly fit these points. Due to this we tried a three parameter fit where we varied ϕ_{UV}, h_{UV} and m_{eff} as arbitrary parameters, which reproduced the shape of the curves in a proper manner as given in Fig. 6.2a and Fig. 6.2b. Introducing $k_{UV}^2 = k^2 - \frac{(\omega+qA_t(UV))^2}{h_{UV}}$ we find that, all the normal modes appear inside the region $k \leq \frac{(\omega+qA_t(UV))^2}{h_{UV}}$ which was also observed in [41].

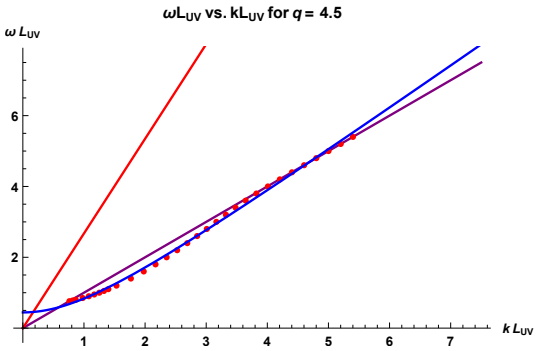

(a) ωL_{UV} vs. kL_{UV} for $q = 4.5$

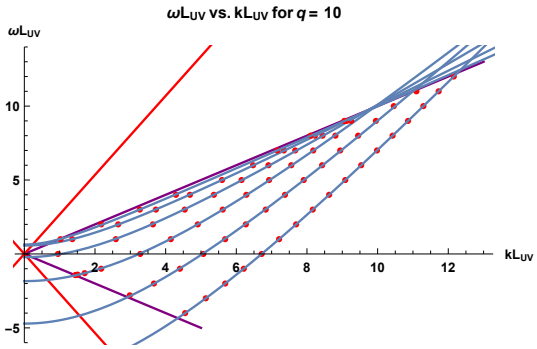

(b) ωL_{UV} vs. kL_{UV} for $q = 10$

Figure 6.2: Normal modes in the space-like region for $q = 4.5$ and $q = 10$. The solid purple lines and red lines represents boundaries of IR and UV lightcones respectively. Blue lines show the fits.

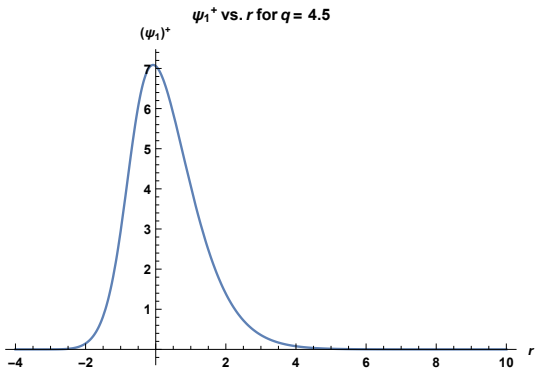

(a) Ψ_1^+ vs. r for $q = 4.5$ for a typical normal mode.

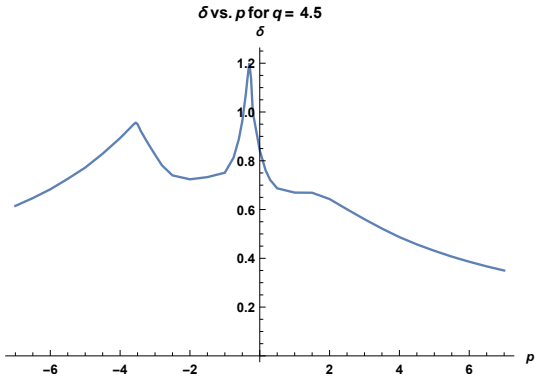

(b) Gap vs. Pauli term coefficient in spacelike region for $q = 4.5$

Figure 6.3

Next, we look at the complementary timelike region where taking boundary condition (6.3.8) we solve the Dirac equation (6.3.5) numerically to study the behaviour of the spectral function. As mentioned above the spectral function is given by the imaginary part of the Green's function given in (6.3.10). First, we start with the massless case of the Dirac equation together with the absence of Pauli term with charge $q = 10$ and plot the spectral function vs. ω for different values of k which are given in Fig.s 6.4a and 6.4b. We plotted ω and k values for the peaks for $k < 0$

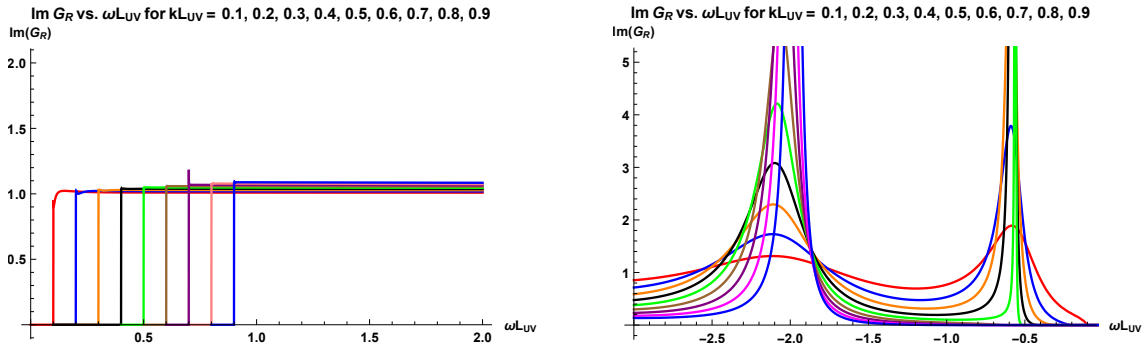

(a) Spectral function for $q = 10, \omega > k$

(b) Spectral function for $q = 10, \omega < -k$

Figure 6.4: Spectral function for fermionic mode in absence of mass term. kL_{UV} = 0.1(red), 0.2(blue), 0.3(orange), 0.4(black), 0.5(green), 0.6(brown), 0.7(purple), 0.8(pink), 0.9(blue)

in Fig. 6.7a to find dispersion relationship for these excitations. As one can observe from the figure the set of points in UV region and the set of points for the normal mode in IR connects smoothly which are separated by the IR light cone (purple line). A numerical three parameter fit with expression $\frac{(\omega+q\phi_{UV})^2}{h_{UV}} - k^2 = m_{eff}^2$ reproduces shape of the curve. For $k > 0$ one finds a similar kind of plot.

Next, we look at the cases with both mass term and Pauli terms in place for two different values of charge ($q = 4.5$ and $q = 10$) and plot the spectral vs. ω for five and eight different values of k respectively. The plots are given for $q = 4.5$ in the Fig. 6.5b and $q = 10$ in the Fig. 6.6. The heights of the peaks increase as the charge increases. However, as k increases the peak position in ω does not vary monotonically.

The position of these peaks gives the associated ω value for a given value of k, from these k and ω value one can get a dispersion relation and plot ω vs. k. For

modes within the time-like region for $q = 10$ are given in Fig. 6.7b. Using three parameter fit with $\frac{(\omega+q\phi_{UV})^2}{h_{UV}} - k^2 = m_{eff}^2$ and varying all the 3 parameters ϕ_{UV}, h_{UV} and m_{eff} the fit did not agree with the numerical data. Instead, a quadratic fit, with a relation like $\omega - \omega_0 = \frac{(k-k_0)^2}{2m_{\text{eff}}}$ gave a correct fit fot the data points in this region, as shown in the figure 6.7b. Similar relation holds for $q = 4.5$ too. Fig. 6.8 shows that for both $q = 4.5$ and $q = 10$ the modes appearing in the timelike region and the modes corresponding to the normal modes in the space-like region connects smoothly. For $q = 4.5$ the modes are trailing along the boundary of IR lightcone for positive k, while for $q = 10$ modes for large frequency appears in the timelike region. However, the modes are outside the UV lightcone in both the cases for timelike region. A three parameter fit $\frac{(\omega+q\phi_{UV})^2}{h_{UV}} - k^2 = m_{eff}^2$ (green curve in the figure) was used to fit all the data for entire region which gave a proper fit.

In addition, the dispersion relation for $q = 4.5$ given in Fig. 6.8 shows a similar kind of relation as expected from BCS theory where the modes lying on the positive ω region gives an upward concave pattern. For $q = 10$, however, a similar kind of pattern emerges on the negative ω region as well, which is different from the one obtained for gapped spectrum in [43]. The reason for this could be that as the value of the charge has been increased the modes has been shifted downwards in ω. However, for the actual charge of this supergravity model i.e. $q = 1$ we could not find any peak as given in Fig. 6.5a. This could be due to the fact that the charge of this mode is too small. Regardless of this, the large frequency behaviour shows a similar nature as that of other charges. For the charge $q = 1$, which follows from the supergravity, however, we have not found any peak as shown in Fig. 6.5a. This may be attributed to the fact that charge of this mode is too small. This can be seen in the inset figure in Fig. 6.5b for $q = 4.5$.

This is interesting to consider the implications in the dual field theory. For the present five dimensional supergravity model, the dual theory is given by a four dimensional superconformal quiver gauge theory, depending on the compactification manifold. We are interested in the chiral primary operators in the dual field the-

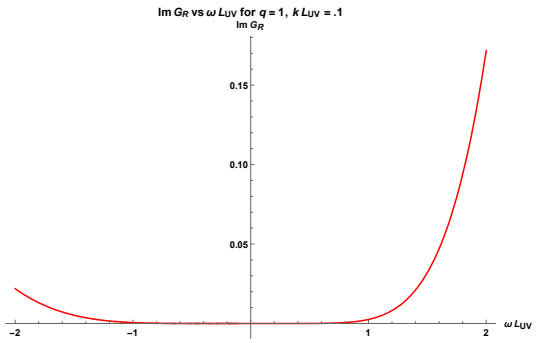

(a) Spectral function for $q = 1$; $kL_{UV} = 0.1$

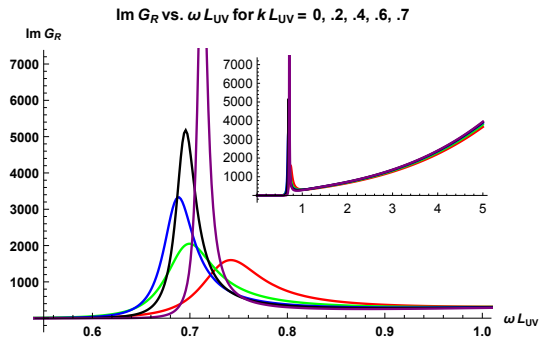

(b) ImG_R vs. ωL_{UV} for $q = 4.5$

Figure 6.5: Spectral function for fermionic mode. Left $q = 1$. Right $q = 4.5$ with kL_{UV}=0 (red), 0.2(green), 0.4(blue), 0.6(purple) and 0.7(brown). The inset figure shows the behaviour at large frequency.

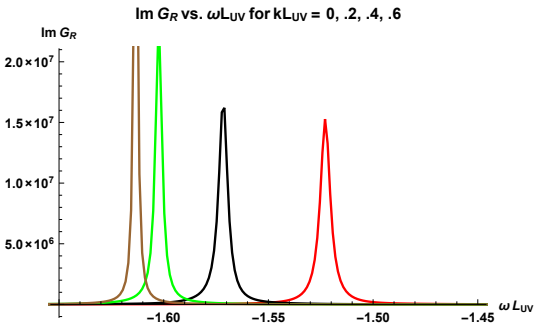

(a) ImG_R vs. ωL_{UV} for $q = 10$

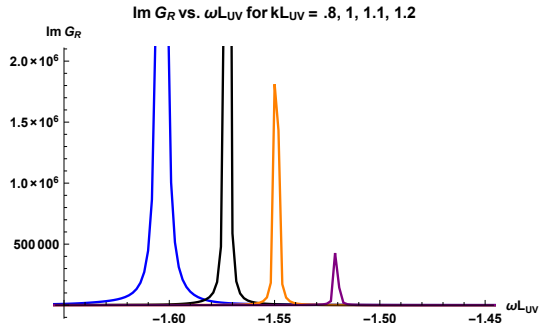

(b) ImG_R vs. ωL_{UV} for $q = 10$

Figure 6.6: Spectral function for fermionic mode for $q = 10$. On left with kL_{UV}=0(red), .2(black), .4(green), .6(brown). On right with kL_{UV}=.8(blue), 1(black), 1.1(orange), 1.2(purple).

ory. The pertinent field on the gravity side is the scalar field η. Since the mass of the scalar field is $m^2 = \triangle(\triangle - 4) = -3$ the dual operator $\mathcal{O}_\eta$ has a conformal dimension $\triangle = 3$ with R-charge 2 and so it is chiral primary. In order to identify this dual chiral primary operator, we observe that for IIB theory compactified on S^5 there are two such possible candidates. One is given by the superpotential $\mathcal{W}$ and the other operator involves the gauge field strength superfield W_α and is written as $tr(W_\alpha W^\alpha)$. It turns out that the chiral primary is a linear combination of these two operators, which is orthogonal to chiral superfield associated with Konishi multiplet [85]. The operator dual to $\mathcal{O}_\eta$ can be identified as the lowest component of that linear combination of these two [80].

One can associate a critical temperature with chiral primary, below which it will

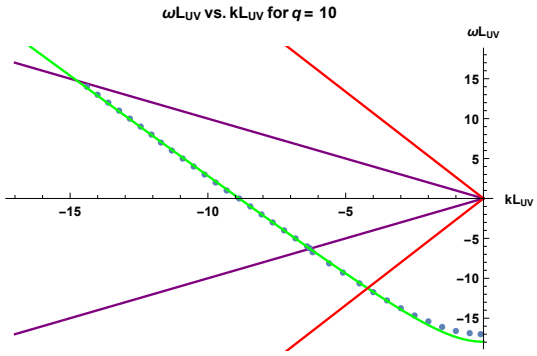

(a) Without mass and Pauli term

(b) With mass and Pauli term.

Figure 6.7: Dispersion relation for $q = 10$ in time-like region. The solid purple lines and red lines represent boundaries of IR and UV lightcones respectively. Green lines show the fits. Left figure shows all regions in $k < 0$. Right figure shows timelike region.

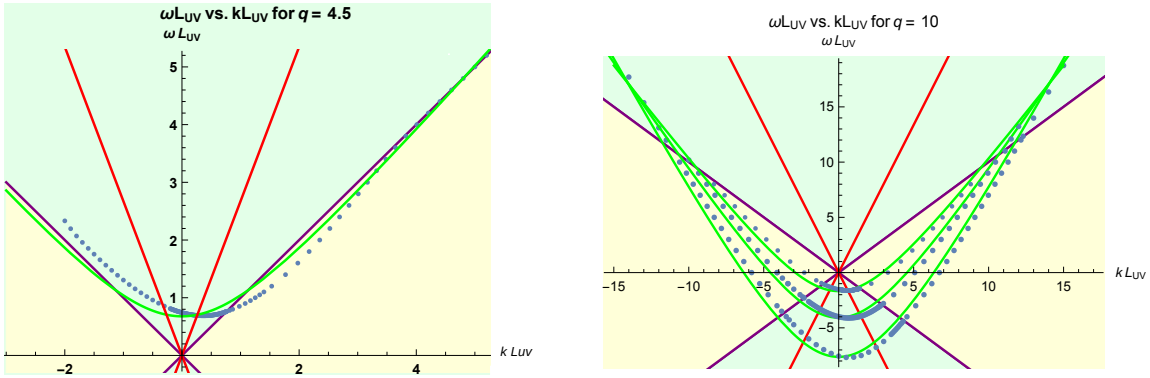

(a) Dispersion relation for $q = 4.5$

(b) Dispersion relation for $q = 10$

Figure 6.8: Spectral function for fermionic mode for $q = 4.5$ and $q = 10$. The solid purple lines and red lines represent boundaries of IR and UV lightcones respectively. Green lines show the fits. Light blue region shows a timelike region and light brown region is a spacelike region.

condense. For a black hole background, this critical temperature is a monotonically decreasing function of conformal dimension $\triangle$ [80]. Therefore, at zero temperature, if $\mathcal{O}_\eta$ is responsible for the condensation, it should have lowest conformal dimension and in order to check that we compare the dimension to those of other chiral primaries in the dual theory.

We begin with IIB on S^5 and as shown in [86] the chiral primary operators of dimension $\triangle = k$, represented by symmetrised traceless combinations $tr(\Phi^{i_1}...\Phi^{i_k})$ correspond to the first family of scalar fields, which admits modes with $m^2 = k(k-4), k \geq 2$. As one can observe, for $k = 2$ this operator has conformal dimension $\triangle = 2$ which is less than that of $\mathcal{O}_\eta$. Next, we consider IIB on $T^{1,1}$, for which the chiral

primaries are discussed in [85]. Here $tr(A_iB_j)$ represents a chiral primary with $\triangle = 3/2 < 3$. As we see IIB on an orbifold of 5-sphere is a suitable option. If we consider compactification on S^5/Γ, where $\Gamma \in SU(3)$, we obtain a supersymmetric quiver gauge theory as the dual field theory with supersymmetry $\mathcal{N} = 1$. The chiral primaries for orbifolds are discussed in [86] and as shown there, many of the modes arising in the compactification on S^5 disappear after orbifolding, as they are not invariant under the discrete symmetry. For $\Gamma = Z_3$ orbifold, we can analyze the supergravity mode corresponding to $k = 2$ mentioned above. They appear in the representation $20'$ of $SU(4)$. For $\Gamma = Z_3$, it decomposes under $SU(3)\times U(1)$ as $20' = 6(4/3) + \bar{6}(-4/3) + 8(0)$. Therefore, out of these modes, only the $8(0)$ survives the projection. But $8(0)$ does not couple to a chiral primary operator. Therefore, we will not have a chiral primary of dimension 2 in the dual theory. However, superpotential and $tr(W_\alpha W^\alpha)$ will survive the orbifolding making $\mathcal{O}_\eta$, chiral primary operator with the lowest dimension.

The fermions considered in [84] corresponds to the lowest rung of mass spectrum of fermions obtained by compactification of IIB on S^5 as given in fig.4 of [87]. In particular, the fermionic mode we are interested in corresponds to mass $\frac{7}{2}$, that occurs in $\mathbf{4}$ of $SU(4)$. In the notation of [88, 89] it occurs at the level 3 sets of modes in representation $D(p+5/2, 1/2, 0; 0, p-3, 1)+D(p+5/2, 0, 1/2; 1, p-3, 0)$ at $p = 3$. The surviving KK modes for IIB on $S^5/\mathbb{Z}_3$ has been discussed and classified in [89]. Under $SU(3) \times U(1)$ decomposition the Dynkin label splits into $(1, p-3, 0) = \oplus_{l=(p+1)/3}^{(2p-1)/3}(-1+2l-p, -1+2p-3l)_{2p-4l+1} \oplus_{l=(p/3+1}^{(2p/3}(-3+3l-p, 0+2p-3l)_{2p-4l+1}$. The mode we are interested in corresponds to $p = 3$ and in the second term in the splitting in this series and gives rise to a singlet of $SU(3)$. As explained in [89] it belongs to Gravitino multiplet II (λ^4 in their notation). The corresponding superfield in the dual theory is given by $L_{2\dot{\alpha}} = tr(e^V \bar{W}_{\dot{\alpha}} e^{-V} W^2)$, where V is the gauge superfield for the dual quiver gauge theory and W represents the field strength superfield.

6.5 Discussion

In the background of domain wall solution, we have studied the behaviour of the operator dual to a certain fermionic mode in the supergravity theory, which does not couple to gravitino or other fermionic modes. This domain wall solution appears as a bosonic solution of a five dimensional supergravity theory obtained through compactification on a Sasaki-Einstein manifold. The dual field theory is a quiver gauge theory in four dimension. In the dual field theory, the domain wall solution corresponds to condensation of a chiral primary operator, which is given by a linear combination of superpotential as $tr(W_\alpha W^\alpha)$. The fermionic operator dual to the supergravity mode belongs to a multiplet given by $tr(e^V \bar{W}_{\dot{\alpha}} e^{-V} W^2)$.

We have manually tuned the value of charges by hand and explored the existence of normal modes in the space-like region. For the charge $q = 1$ which follows from supergravity, we could not find any normal mode. By increasing the charge to higher value $q = 4.5$ we find normal modes but at $\omega > 0$ leading to gapped spectrum. If we increase charge further, there are normal modes at $\omega = 0$ as well, hence giving a gapless spectrum. We obtain a dispersion relation for the normal modes. Next, we analysed the time-like region, for $q = 4.5$ and $q = 10$ where we looked for peaks of the spectral function. The dispersion relation in the time-like region turns out to be quadratic in k, considering both timelike and spacelike regions a hyperbolic fit matches well. In the case of $q = 1$, the charge following from supergravity theory, however, we have not observed any peak. We have also explored the dependence of gap on Pauli coupling, where the gap shows local maxima at discrete values.

A similar gapped spectrum was observed in [39], where fermionic quasi-particles in the presence of condensate at zero temperature was studied. Gapped spectra have also been identified in four dimensional gauged supergravity dual to ABJM model with broken $U(1)$ symmetry [42, 43], where the gap has been attributed to the low charge or particle-hole interaction. In the present analysis, it seems that the small charge is responsible for the gapped spectrum. The condensed bosonic operator may play a significant role in the behaviour of the spectrum of fermionic operators

considered here. From the perspective of field theory, it would be interesting to understand the role of the condensed scalar operator in determining the fermionic spectrum.

The five dimensional supergravity obtained after suitable truncation results in various decoupled sectors of fermionic modes. We have limited ourselves to the case of the fermionic sector consisting of a single fermion in the present work. Extending this analysis to the fermionic modes in other sectors as well may be interesting. Those fermions, however, are coupled with each other and also coupled to gravitino, so it requires a more involved analysis.

Chapter 7

Conclusion

Various aspects of strongly correlated systems in condensed matter theories are not amenable to perturbative studies. Though Landau's Fermi liquid theory and other methods provide some understanding there are systems which elude such approaches. In particular, for various materials high T_c superconductors, heavy fermions, excitations are found to be in non-Fermi regime due to the absence of long-lived quasi-particles. Naturally, such systems call for new approaches. Gauge/gravity duality has been proved to be quite successful as it can translate the strongly coupled field theory problems in terms of weakly coupled gravity theories. In the present thesis, we have described the application of this duality in the understanding of behaviours of fermions in some strongly correlated systems.

Our approach is mostly top-down as this considers specific models in string theory/supergravity providing specific well defined field theories in the dual system. We begin with maximally gauged supergravity theory in seven dimension whose dual theory is conjectured to be (2,0) conformal field theory in six dimension. Being maximally symmetric it is interesting in its own right. We have considered a truncated version of it, which involves two $U(1)$ gauge fields and several scalar fields that follow from the compactification. The bosonic part of the theory admits a black hole solution charged under two $U(1)$ gauge fields. This is asymptotically anti-de Sitter. In the extremal limit, the near horizon geometry is AdS_2. According

to the duality should correspond to a specific state in the dual theory and it would be interesting to find whether this corresponds to the ground state.

We are interested to study the behaviour of fermions in this dual system. Therefore, we consider fermions of the supergravity theory and we have restricted our study to those which do not couple to gravitino. To begin with, we explore the possibility of Fermi surfaces from the poles of the Green's function in the extremal limit. In the non-extremal limit, on the other hand, we plotted the spectral density and look for peaks at $\omega = 0$. We have found the total charge of the fermion plays a critical role. For higher net charge $|q_1+q_2| = 2$ we find it admits two Fermi surfaces. However, the sign of the Fermi momentum is positive in both the cases and this has been confirmed from the study at the finite temperature. The occurrence of such multiple Fermi surfaces can be interpreted as having nested Fermi surface in analogy with results obtained for $N = 4$ SYM. A stark difference with their result is in the present case one branch completely lies in the Non-Fermi regime and the other branch is in the Fermi-regime. As we vary the electric charge associated with the black hole, in one extreme both the branches approach the limit of marginal Fermi liquid. in the other extreme, the non-Fermi branch enters the oscillatory region signalling the scaling dimension of the dual operator becomes complex. In the case of scalar operators, it can be considered as onset of instability [14]. From the study of the excitation width of the quasi-particles in the non-Fermi regime we find they are becoming more and more stable, as the branch approaches marginal Fermi liquid, as expected.

The other set of fermions, which has $|q_1 + q_2| = 1$ in the supergravity theory we get only a single Fermi surface both in the zero temperature and finite temperature. This branch, however, stays completely in the non-Fermi regime and approaches marginal Fermi liquid on both extremes as we vary the electric charge of the black hole. The width of the excitation increases on one extreme, while it becomes more stable on the other. we have also observed that for both the branches in the non-Fermi regime, Fermi momentum appears very close to the boundary of the oscilla-

tory region, which may be consistent with the fact that they are in the non-Fermi regime.

We have also considered a single charge limit of the black hole, which does not admit an extremal limit and therefore we studied it only at the finite temperature. In this case, the Fermion with higher charge $|q_1| = 3/2$ admits a Fermi surface as we find from the analysis of the spectral density, while the one with lower charge $|q_1| = 1/2$ does not admit any.

Considering the dual field theory, it has been established that the operators dual to the fermions in the supergravity consists of both scalars and gauginos and are of the form $tr(\Sigma^i \psi^a)$. Comparing our results it turns out that for two charge case the gauginos are playing a critical role in determining the nature of Fermi surface i.e. whether a system forms a single or multiple Fermi surfaces. With the change in charge of gaugino (ψ) in the operator nature of Fermi surface changes. This is in accordance with the argument given by [29] where the gaugino itself generates the Fermi surface. In case of a single charge case, however, we have observed that scalars also play a prominent role in determining the existence of Fermi surface. We found that the dual operators admit Fermi surface if the background corresponds to the non-zero expectation of the scalar. It may be in case of two charge parameter, all scalar might have a finite expectation value and thus it results in one or more Fermi surface/s.

Next, we have extended our analysis to the cases of background domain wall solution. This domain wall solution can be obtained as a truncation of the bosonic part of gauged supergravity theory. In this background $U(1)$ symmetry is broken spontaneously, so in a sense, it can be considered as the zero temperature limit of a superconductor. Another characteristic feature of such solutions is they do not suffer from zero-point entropy i.e. at zero temperature the entropy vanishes. This kind of zero-point entropy is usually encountered in black hole solution with near horizon structure being AdS_2.

In order to study the fermionic behaviour in such zero temperature limit of a

superconductor, we have considered those fermions which decouple from gravitino of this supergravity theory with this domain wall as our background. We have analysed the spectral function for the dual operators associated with each of these modes. Since the background corresponds to the superconductor, we expect a gapped spectrum.

We have obtained a domain wall solution in maximally gauged seven dimension supergravity theory which approaches AdS at both IR and UV. We have studied optical conductivity as a function of frequency, where we find the real part of conductivity obeys a power law. In the limit of high frequency, it obeys a cubic law while in case of small frequency it goes with certain exponent.

We have considered fermions that follow from supergravity theory and studied the spectral function. We find a gapped spectrum for the value of the parameters corresponding to the supergravity theory. As has been reported in the literature, the gapped spectrum may also result due to the inclusion of the Pauli term or due to an inadequate charge of fermions. In order to ensure that this gap cannot be attributed to either of these, we have artificially set the Pauli term zero and dialled the value of the charge to some higher value. We find that this gap still persists upto the value of the charge that we have checked. Similar kind of gapped spectrum was also observed in [39] and [42, 43]. We have analysed the role of the degrees of freedom in the dual theory in this respect. It turns out that the operators dual to the fermionic modes that give rise to the gapped spectrum involve the scalar operators Σ_3 and Σ_4 in the dual theory. By analysing the asymptotic behaviour of the scalar fields in the gravity theory, we find these dual operators acquire vacuum expectation value for the state that corresponds to the domain wall solution. So we conclude that the fermionic operators involving bosons with non zero expectation value give rise to the gapped spectrum.

We have further extended our study to a supergravity theory obtained through compactification on a Sasaki-Einstein manifold. Due to nature of the compactification manifold, the supergravity theory has less supersymmetry; It lives in 5 dimen-

sion and its dual field theory turns out to be a superconformal quiver gauge theory living in 4 dimension and therefore it can be related to physical systems that occur naturally. On the flip side, the field content and dynamics of this quiver gauge theory is technically quite involved.

In order to study the fermions in zero temperature limit of a superconductor, we have considered a domain wall solution, which already existed in the literature [81]. For this solution, the metric structure approaches AdS geometry both in the IR and UV limit. From the asymptotic behaviour of the scalar field, it turns out it corresponds to condensation of a dual operator, which is chiral primary. From the analysis of the dual field theory, it can be established that this chiral primary is given by a linear combination of the superpotential of the superconformal field theory and an operator $tr(W_\alpha W^\alpha)$ obtained from the gauge superfield W_α. In order to ensure that this chiral primary operator has the lowest conformal dimension among all the chiral primaries in the dual field theories, we find that the compactification manifold can be considered as an orbifold, namely, C^3/Z_3. Due to orbifolding, other chiral primaries with less conformal dimensions are projected out.

Even though the behaviour of generic fermion in this background has been discussed earlier, but here we have considered the fermions which directly follows from the compactification of supergravity theory. Because of the complex nature of the compactification manifold the fermionic fields in the supergravity theory are being partitioned in different sectors [84]. It turns out, there is a special sector which consists of only a single fermion, which does not couple to a gravitino and we have restricted our analysis to that sector only. Since the IR geometry is AdS_4 the near-horizon behaviour of the fermions can be split into two different classes corresponding to spacelike and timelike momenta and we have analysed the modes for both the classes separately. We have artificially dialled the charges of the fermion over a range and studied the behaviour. In particular, we have presented the result for two different charges $q = 4.5$ and $q = 10$. For $q = 4.5$ we find normal modes at $\omega > 0$ in the spacelike region giving rise to the formation of the gapped spectrum.

We increase the charge further which resulted in the appearance of normal modes at $\omega = 0$, hence higher value of charge leads to a gapless spectrum.

We have elaborately studied the dispersion relation resulted from the fermionic modes for both the spacelike and timelike regions. For smaller charge, such as $q = 4.5$ the dispersion relation shows a hyperbolic nature in the positive ω region, in conformity with the gapped spectrum. As we increase the charge, the entire dispersion curve comes down and for a critical value of the charge, it touches $\omega = 0$ axis giving rise to a gapless spectrum. However, for the charge that follows from supergravity theory, we could not find a normal mode, or peak of the spectral function, as the value of the charge is quite small. We have also explored the dependence of gap on Pauli coupling, where the gap shows local maxima at discrete values. As mentioned above the dual theory is quite involved and consists of a number of different multiplets. The fermionic operators dual to the supergravity mode belongs to a multiplet given by $tr(e^V \bar{W}_{\dot{\alpha}} e^{-V} W^2)$. However, due to the complex nature of the field theory, it is difficult to study the roles of the various dual operators in this theory.

Though these studies have provided a deeper and clearer understanding of fermionic behaviour, it can be extended further in a number of ways. To begin with we have restricted ourselves in the probe limit. The holographic background, that we considered in the gravity theory is the solution of the bosonic part. After including the fermions, it should get modified and we have not considered the back reaction. This is expected to correct the result we obtain here further. Though we have considered only supergravity theories, a natural way to obtain more relevant gravity backgrounds is to consider intersecting branes. Some works have already been done on that score. One addition complexity that is being introduced for intersecting brane, however, it involves DBI action which may lead to technically more involved computation.

Another reason that makes the intersecting branes interesting is as follows. This usually involves, Chern-Simons terms and as has been pointed out [90] a back-

ground electric field gives rise to instability. Often these instabilities cause the solution to decay into linearly inhomogeneous solutions in the gravity theory. As has been established, such inhomogeneous solutions correspond to states in the dual theory, which are spatially modulated. Such striped phases occur in various materials [91]. A natural extension of our study is to consider fermionic behaviour in such striped phases. Some work has already appeared in the literature [92]. It will also be to incorporate the effect of lattice structure in the boundary [93]. There are various ways in which such periodicity in space can be incorporated, for example through introducing a periodic chemical potential. Another important variation is to consider the effects of dopings. There are several works where the effect of doping has been considered in a holographic set up [75, 94].

One advantage of top-down approach in holography is the theory on the gravity side follows from full fledged effective action of string theory. Therefore one can go beyond the Einstein gravity and accommodate further $\frac{1}{N}$ corrections. It would be interesting to consider the effect of the higher order terms in $\frac{1}{N}$ corrections. In fact, it has been found in the context of holographic superconductor that large N limit suppresses massless fluctuation in the dual field theory, which can invalidate condensation of scalar in superconductors.

Another interesting arena to explore in this context is the transport properties of the dual field theories. Many of the material in the regime of non-Fermi liquid exhibit anomalous behaviour of its transport properties. One example is linear temperature dependence of resistivity instead of quadratic dependence as follows from Fermi liquid theory. the holographic machinery can easily be used to study these properties.

To summarise, we have explored some of the aspects of strongly correlated systems using AdS/CFT correspondence, which is otherwise not amenable to standard non-perturbative techniques. Our study has shed light on the behaviour of the fermions of different states of strongly correlated systems as well as the roles played by different kinds of degrees of freedom in the dual theory. Considering the vast ex-

panse of phenomena that have appeared in cases of various materials in condensed matter, it provides a huge scope to explore the theories and make connections to the realistic phenomena in Nature.

Bibliography

[1] G. 't Hooft, "A Planar Diagram Theory for Strong Interactions," Nucl. Phys. B **72**, 461 (1974). doi:10.1016/0550-3213(74)90154-0

[2] J. M. Maldacena, "The Large N limit of superconformal field theories and supergravity", Int. J. Theor. Phys. **38**, 1113 (1999) [Adv. Theor. Math. Phys. **2**, 231 (1998)] doi:10.1023/A:1026654312961, 10.4310/ATMP.1998.v2.n2.a1 [hep-th/9711200].

[3] S. S. Gubser, I. R. Klebanov and A. M. Polyakov, "Gauge theory correlators from noncritical string theory," Phys. Lett. B **428**, 105 (1998) doi:10.1016/S0370-2693(98)00377-3 [hep-th/9802109].

[4] E. Witten, "Anti-de Sitter space and holography," Adv. Theor. Math. Phys. **2**, 253 (1998) doi:10.4310/ATMP.1998.v2.n2.a2 [hep-th/9802150].

[5] J. Zaanen, Y. W. Sun, Y. Liu and K. Schalm, "Holographic Duality in Condensed Matter Physics,"

[6] M. Ammon and J. Erdmenger, "Gauge/gravity duality : Foundations and applications,"

[7] S. A. Hartnoll, "Lectures on holographic methods for condensed matter physics," Class. Quant. Grav. **26**, 224002 (2009) doi:10.1088/0264-9381/26/22/224002 [arXiv:0903.3246 [hep-th]].

[8] R. G. Cai, L. Li, L. F. Li and R. Q. Yang, "Introduction to Holographic Superconductor Models," Sci. China Phys. Mech. Astron. **58**, no. 6, 060401 (2015) doi:10.1007/s11433-015-5676-5 [arXiv:1502.00437 [hep-th]].

[9] V. Ziogas, "Transport at Strong Coupling and Black Hole Dynamics,"

[10] S. Sachdev, "Condensed Matter and AdS/CFT," Lect. Notes Phys. **828**, 273 (2011) doi:10.1007/978-3-642-04864-7_9 [arXiv:1002.2947 [hep-th]].

[11] A. Amoretti, "Condensed Matter Applications of AdS/CFT : Focusing on strange metals," doi:10.1007/978-3-319-61875-3

[12] S. S. Lee, "A Non-Fermi Liquid from a Charged Black Hole: A Critical Fermi Ball," Phys. Rev. D **79**, 086006 (2009) doi:10.1103/PhysRevD.79.086006 [arXiv:0809.3402 [hep-th]].

[13] M. Cubrovic, J. Zaanen and K. Schalm, "String Theory, Quantum Phase Transitions and the Emergent Fermi-Liquid," Science **325**, 439 (2009) doi:10.1126/science.1174962 [arXiv:0904.1993 [hep-th]].

[14] H. Liu, J. McGreevy and D. Vegh, "Non-Fermi liquids from holography," Phys. Rev. D **83**, 065029 (2011) doi:10.1103/PhysRevD.83.065029 [arXiv:0903.2477 [hep-th]].

[15] T. Faulkner, H. Liu, J. McGreevy and D. Vegh, "Emergent quantum criticality, Fermi surfaces, and AdS(2)," Phys. Rev. D **83**, 125002 (2011) doi:10.1103/PhysRevD.83.125002 [arXiv:0907.2694 [hep-th]].

[16] M. Edalati, R. G. Leigh, K. W. Lo and P. W. Phillips, "Dynamical Gap and Cuprate-like Physics from Holography," Phys. Rev. D **83**, 046012 (2011) doi:10.1103/PhysRevD.83.046012 [arXiv:1012.3751 [hep-th]].

[17] M. Edalati, R. G. Leigh and P. W. Phillips, "Dynamically Generated Mott Gap from Holography," Phys. Rev. Lett. **106**, 091602 (2011) doi:10.1103/PhysRevLett.106.091602 [arXiv:1010.3238 [hep-th]].

[18] G. Vanacore and P. W. Phillips, Phys. Rev. D **90**, no. 4, 044022 (2014) doi:10.1103/PhysRevD.90.044022 [arXiv:1405.1041 [cond-mat.str-el]].

[19] J. P. Wu, "Emergence of gap from holographic fermions on charged Lifshitz background," JHEP **1304**, 073 (2013). doi:10.1007/JHEP04(2013)073

[20] J. P. Wu, "The charged Lifshitz black brane geometry and the bulk dipole coupling," Phys. Lett. B **728**, 450 (2014). doi:10.1016/j.physletb.2013.11.040

[21] X. M. Kuang, E. Papantonopoulos, B. Wang and J. P. Wu, "Formation of Fermi surfaces and the appearance of liquid phases in holographic theories with hyperscaling violation," JHEP **1411**, 086 (2014) doi:10.1007/JHEP11(2014)086 [arXiv:1409.2945 [hep-th]].

[22] X. M. Kuang, E. Papantonopoulos, B. Wang and J. P. Wu, "Dynamically generated gap from holography in the charged black brane with hyperscaling violation," JHEP **1504**, 137 (2015) doi:10.1007/JHEP04(2015)137 [arXiv:1411.5627 [hep-th]].

[23] M. Ammon, J. Erdmenger, M. Kaminski and A. O'Bannon, "Fermionic Operator Mixing in Holographic p-wave Superfluids," JHEP **1005**, 053 (2010) doi:10.1007/JHEP05(2010)053 [arXiv:1003.1134 [hep-th]].

[24] K. Jensen, S. Kachru, A. Karch, J. Polchinski and E. Silverstein, "Towards a holographic marginal Fermi liquid," Phys. Rev. D **84**, 126002 (2011) doi:10.1103/PhysRevD.84.126002 [arXiv:1105.1772 [hep-th]].

[25] J. P. Gauntlett, J. Sonner and D. Waldram, "Universal fermionic spectral functions from string theory," Phys. Rev. Lett. **107**, 241601 (2011) doi:10.1103/PhysRevLett.107.241601 [arXiv:1106.4694 [hep-th]].

[26] R. Belliard, S. S. Gubser and A. Yarom, "Absence of a Fermi surface in classical minimal four-dimensional gauged supergravity," JHEP **1110**, 055 (2011) doi:10.1007/JHEP10(2011)055 [arXiv:1106.6030 [hep-th]].

[27] J. P. Gauntlett, J. Sonner and D. Waldram, "Spectral function of the supersymmetry current," JHEP **1111**, 153 (2011) doi:10.1007/JHEP11(2011)153 [arXiv:1108.1205 [hep-th]].

[28] J. P. Gauntlett, J. Sonner and T. Wiseman, "Holographic superconductivity in M-Theory," Phys. Rev. Lett. **103**, 151601 (2009) doi:10.1103/PhysRevLett.103.151601 [arXiv:0907.3796 [hep-th]].

[29] O. DeWolfe, S. S. Gubser and C. Rosen, "Fermi Surfaces in Maximal Gauged Supergravity," Phys. Rev. Lett. **108**, 251601 (2012) doi:10.1103/PhysRevLett.108.251601 [arXiv:1112.3036 [hep-th]].

[30] O. DeWolfe, S. S. Gubser and C. Rosen, "Fermi surfaces in N=4 Super-Yang-Mills theory," Phys. Rev. D **86**, 106002 (2012) doi:10.1103/PhysRevD.86.106002 [arXiv:1207.3352 [hep-th]].

[31] O. DeWolfe, O. Henriksson and C. Rosen, "Fermi surface behavior in the ABJM M2-brane theory," Phys. Rev. D **91**, no. 12, 126017 (2015) doi:10.1103/PhysRevD.91.126017 [arXiv:1410.6986 [hep-th]].

[32] C. Cosnier-Horeau and S. S. Gubser, "Holographic Fermi surfaces at finite temperature in top-down constructions," Phys. Rev. D **91**, no. 6, 066002 (2015) doi:10.1103/PhysRevD.91.066002 [arXiv:1411.5384 [hep-th]].

[33] M. Berkooz, A. Frishman and A. Zait, "Degenerate Rotating Black Holes, Chiral CFTs and Fermi Surfaces I - Analytic Results for Quasinormal Modes," JHEP **1208**, 109 (2012) doi:10.1007/JHEP08(2012)109 [arXiv:1206.3735 [hep-th]].

[34] M. Berkooz, D. Reichmann and J. Simon, "A Fermi Surface Model for Large Supersymmetric AdS(5) Black Holes," JHEP **0701**, 048 (2007) doi:10.1088/1126-6708/2007/01/048 [hep-th/0604023].

[35] M. Berkooz and D. Reichmann, "Weakly Renormalized Near 1/16 SUSY Fermi Liquid Operators in N=4 SYM," JHEP **0810**, 084 (2008) doi:10.1088/1126-6708/2008/10/084 [arXiv:0807.0559 [hep-th]].

[36] O. DeWolfe, S. S. Gubser and C. Rosen, "Fermionic response in a zero entropy state of $\mathcal{N} = 4$ super-Yang-Mills," Phys. Rev. D **91**, no. 4, 046011 (2015) doi:10.1103/PhysRevD.91.046011 [arXiv:1312.7347 [hep-th]].

[37] S. S. Gubser and A. Nellore, "Ground states of holographic superconductors," Phys. Rev. D **80**, 105007 (2009) doi:10.1103/PhysRevD.80.105007 [arXiv:0908.1972 [hep-th]].

[38] G. T. Horowitz and M. M. Roberts, "Zero Temperature Limit of Holographic Superconductors," JHEP **0911**, 015 (2009) doi:10.1088/1126-6708/2009/11/015 [arXiv:0908.3677 [hep-th]].

[39] J. W. Chen, Y. J. Kao and W. Y. Wen, "Peak-Dip-Hump from Holographic Superconductivity," Phys. Rev. D **82**, 026007 (2010) doi:10.1103/PhysRevD.82.026007 [arXiv:0911.2821 [hep-th]].

[40] T. Faulkner, G. T. Horowitz, J. McGreevy, M. M. Roberts and D. Vegh, "Photoemission 'experiments' on holographic superconductors," JHEP **1003**, 121 (2010) doi:10.1007/JHEP03(2010)121 [arXiv:0911.3402 [hep-th]].

[41] S. S. Gubser, F. D. Rocha and P. Talavera, "Normalizable fermion modes in a holographic superconductor," JHEP **1010**, 087 (2010) doi:10.1007/JHEP10(2010)087 [arXiv:0911.3632 [hep-th]].

[42] O. DeWolfe, S. S. Gubser, O. Henriksson and C. Rosen, "Fermionic Response in Finite-Density ABJM Theory with Broken Symmetry," Phys. Rev. D **93**, no. 2, 026001 (2016) doi:10.1103/PhysRevD.93.026001 [arXiv:1509.00518 [hep-th]].

[43] O. DeWolfe, S. S. Gubser, O. Henriksson and C. Rosen, "Gapped Fermions in Top-down Holographic Superconductors," Phys. Rev. D **95**, no. 8, 086005 (2017) doi:10.1103/PhysRevD.95.086005 [arXiv:1609.07186 [hep-th]].

[44] S. Mukhopadhyay and N. Rai, "Holographic Fermi surfaces in the six-dimensional (2, 0) theory," Phys. Rev. D **96**, no. 2, 026005 (2017). doi:10.1103/PhysRevD.96.026005

[45] S. Mukhopadhyay and N. Rai, "Holographic Fermi surface at finite temperature in six-dimensional (2, 0) theory," Phys. Rev. D **96**, no. 6, 066001 (2017). doi:10.1103/PhysRevD.96.066001

[46] S. Mukhopadhyay and N. Rai, "Gapped fermionic spectrum from a domain wall in seven dimension," Phys. Lett. B **780**, 608 (2018). doi:10.1016/j.physletb.2018.03.037

[47] S. Mukhopadhyay and N. Rai, "Fermionic spectrum from a domain wall in five dimensions," Phys. Rev. D **98**, no. 2, 026007 (2018) doi:10.1103/PhysRevD.98.026007 [arXiv:1904.06147 [hep-th]].

[48] A. V. Ramallo, "Introduction to the AdS/CFT correspondence", Springer Proc. Phys. **161**, 411 (2015) [arXiv:1310.4319 [hep-th]].

[49] B. Zwiebach, "A first course in string theory," Cambridge, UK: Univ. Pr. (2009) 673 p

[50] J. D. Lykken, "Introduction to supersymmetry", hep-th/9612114.

[51] E. D'Hoker and D. Z. Freedman, "Supersymmetric gauge theories and the AdS / CFT correspondence", hep-th/0201253.

[52] J. Polchinski, "Dirichlet Branes and Ramond-Ramond charges," Phys. Rev. Lett. **75**, 4724 (1995) doi:10.1103/PhysRevLett.75.4724 [hep-th/9510017].

[53] D. Serban, "Integrability and the AdS/CFT correspondence," J. Phys. A **44**, 124001 (2011) doi:10.1088/1751-8113/44/12/124001 [arXiv:1003.4214 [hep-th]].

[54] A. Hickling, "Bulk spacetime geometries in AdS/CFT". PhD thesis, Imperial College London, 2016.

[55] O. Aharony, S. S. Gubser, J. M. Maldacena, H. Ooguri and Y. Oz, "Large N field theories, string theory and gravity," Phys. Rept. **323**, 183 (2000) doi:10.1016/S0370-1573(99)00083-6 [hep-th/9905111].

[56] E. Papantonopoulos, "From gravity to thermal gauge theories: The AdS/CFT correspondence," Lect. Notes Phys. **828**, 1 (2011). doi:10.1007/978-3-642-04864-7

[57] J. Polchinski, "Introduction to Gauge/Gravity Duality," doi:10.1142/9789814350525_0001 arXiv:1010.6134 [hep-th].

[58] J. Penedones, "TASI lectures on AdS/CFT," doi:10.1142/9789813149441_0002 arXiv:1608.04948 [hep-th].

[59] D. Marolf, M. Rangamani and T. Wiseman, "Holographic thermal field theory on curved spacetimes," Class. Quant. Grav. **31**, 063001 (2014) doi:10.1088/0264-9381/31/6/063001 [arXiv:1312.0612 [hep-th]].

[60] K. Schalm and R. Davison "A simple introduction to AdS/CFT and its application to condensed matter physics", D-ITP Advanced Topics in Theoretical Physics Fall 2013.

[61] N. Iqbal, H. Liu and M. Mezei, "Lectures on holographic non-Fermi liquids and quantum phase transitions", arXiv:1110.3814 [hep-th].

[62] M. Natsuume, "AdS/CFT Duality User Guide," Lect. Notes Phys. **903**, pp.1 (2015) doi:10.1007/978-4-431-55441-7 [arXiv:1409.3575 [hep-th]].

[63] P. Coleman, "Landau Fermi-liquid theory. In Introduction to Many-Body Physics," Cambridge University Press, pp.127-175 (2015) doi:10.1017/CBO9781139020916.008

[64] M. Vojta, "Quantum phase transitions," Reports on Progress in Physics, Volume 66, Issue 12, pp. 2069-2110 (2003) doi:10.1088/0034-4885/66/12/r01 [arXiv:cond-mat/0309604].

[65] D. T. Son and A. O. Starinets, "Minkowski space correlators in AdS / CFT correspondence: Recipe and applications," JHEP **0209**, 042 (2002) doi:10.1088/1126-6708/2002/09/042 [hep-th/0205051].

[66] A. Chamblin, R. Emparan, C. V. Johnson and R. C. Myers, "Charged AdS black holes and catastrophic holography," Phys. Rev. D **60**, 064018 (1999) doi:10.1103/PhysRevD.60.064018 [hep-th/9902170].

[67] H. Nastase, D. Vaman and P. van Nieuwenhuizen, "Consistent nonlinear K K reduction of 11-d supergravity on AdS(7) x S(4) and selfduality in odd dimensions," Phys. Lett. B **469**, 96 (1999) doi:10.1016/S0370-2693(99)01266-6 [hep-th/9905075].

[68] H. Nastase, D. Vaman and P. van Nieuwenhuizen, "Consistency of the AdS(7) x S(4) reduction and the origin of selfduality in odd dimensions," Nucl. Phys. B **581**, 179 (2000) doi:10.1016/S0550-3213(00)00193-0 [hep-th/9911238].

[69] M. Pernici, K. Pilch and P. Van Nieuwenhuizen, "Gauged Maximally Extended Supergravity In Seven-dimensions," *Salam, A. (ed.), Sezgin, E. (ed.): Supergravities in diverse dimensions, vol. 1* 310-314. (Phys. Lett. B143 (1984) 103-107). (see Book Index)

[70] J. T. Liu and R. Minasian, "Black holes and membranes in AdS(7)," Phys. Lett. B **457**, 39 (1999) doi:10.1016/S0370-2693(99)00500-6 [hep-th/9903269].

[71] M. Cvetic *et al.*, "Embedding AdS black holes in ten-dimensions and eleven-dimensions," Nucl. Phys. B **558**, 96 (1999) doi:10.1016/S0550-3213(99)00419-8 [hep-th/9903214].

[72] R. G. Leigh and M. Rozali, "The Large N limit of the (2,0) superconformal field theory," Phys. Lett. B **431**, 311 (1998) doi:10.1016/S0370-2693(98)00495-X [hep-th/9803068].

[73] E. Bergshoeff, E. Sezgin and A. Van Proeyen, "(2,0) tensor multiplets and conformal supergravity in D = 6," Class. Quant. Grav. **16**, 3193 (1999) doi:10.1088/0264-9381/16/10/311 [hep-th/9904085].

[74] N. Iqbal and H. Liu, "Real-time response in AdS/CFT with application to spinors," Fortsch. Phys. **57**, 367 (2009) doi:10.1002/prop.200900057 [arXiv:0903.2596 [hep-th]].

[75] L. Q. Fang, X. M. Kuang, B. Wang and J. P. Wu, "Fermionic phase transition induced by the effective impurity in holography," JHEP **1511**, 134 (2015) doi:10.1007/JHEP11(2015)134 [arXiv:1507.03121 [hep-th]].

[76] C. M. Varma, P. B. Littlewood, S. Schmitt-Rink, E. Abrahams and A. E. Ruckenstein, "Phenomenology of the normal state of Cu-O high-temperature superconductors," Phys. Rev. Lett. **63**, 1996 (1989). doi:10.1103/PhysRevLett.63.1996

[77] A. J. Nurmagambetov and I. Y. Park, "On the M5 and the AdS(7) / CFT(6) correspondence," Phys. Lett. B **524**, 185 (2002) doi:10.1016/S0370-2693(01)01375-2 [hep-th/0110192].

[78] S. S. Gubser and F. D. Rocha, "Peculiar properties of a charged dilatonic black hole in AdS_5," Phys. Rev. D **81**, 046001 (2010) doi:10.1103/PhysRevD.81.046001 [arXiv:0911.2898 [hep-th]].

[79] J. P. Gauntlett, J. Sonner and T. Wiseman, "Quantum Criticality and Holographic Superconductors in M-theory," JHEP **1002**, 060 (2010) doi:10.1007/JHEP02(2010)060 [arXiv:0912.0512 [hep-th]].

[80] S. S. Gubser, C. P. Herzog, S. S. Pufu and T. Tesileanu, "Superconductors from Superstrings," Phys. Rev. Lett. **103**, 141601 (2009) doi:10.1103/PhysRevLett.103.141601 [arXiv:0907.3510 [hep-th]].

[81] S. S. Gubser, S. S. Pufu and F. D. Rocha, "Quantum critical superconductors in string theory and M-theory," Phys. Lett. B **683**, 201 (2010) doi:10.1016/j.physletb.2009.12.017 [arXiv:0908.0011 [hep-th]].

[82] S. S. Gubser and F. D. Rocha, "The gravity dual to a quantum critical point with spontaneous symmetry breaking," Phys. Rev. Lett. **102**, 061601 (2009) doi:10.1103/PhysRevLett.102.061601 [arXiv:0807.1737 [hep-th]].

[83] D. Tong, "Lectures on holographic conductivity", presented at Cracow School of Theoretical Physics, Cracow Poland (2013).

[84] I. Bah, A. Faraggi, J. I. Jottar and R. G. Leigh, "Fermions and Type IIB Supergravity On Squashed Sasaki-Einstein Manifolds," JHEP **1101**, 100 (2011) doi:10.1007/JHEP01(2011)100 [arXiv:1009.1615 [hep-th]].

[85] A. Ceresole, G. Dall'Agata, R. D'Auria and S. Ferrara, "Spectrum of type IIB supergravity on AdS$(5) \times T^{11}$: Predictions on N=1 SCFT's," Phys. Rev. D **61**, 066001 (2000) doi:10.1103/PhysRevD.61.066001 [hep-th/9905226].

[86] Y. Oz and J. Terning, "Orbifolds of AdS$(5) \times S^5$ and 4-d conformal field theories," Nucl. Phys. B **532**, 163 (1998) doi:10.1016/S0550-3213(98)00454-4 [hep-th/9803167].

[87] H. J. Kim, L. J. Romans and P. van Nieuwenhuizen, "The Mass Spectrum of Chiral N=2 D=10 Supergravity on S^5," Phys. Rev. D **32**, 389 (1985). doi:10.1103/PhysRevD.32.389

[88] M. Gunaydin and N. Marcus, "The Spectrum of the S^5 Compactification of the Chiral N=2, D=10 Supergravity and the Unitary Supermultiplets of U(2, 2/4)," Class. Quant. Grav. **2**, L11 (1985). doi:10.1088/0264-9381/2/2/001

[89] A. Arabi Ardehali, J. T. Liu and P. Szepietowski, "The spectrum of IIB supergravity on $AdS_5 \times S^5/Z_3$ and a $1/N^2$ test of AdS/CFT," JHEP **1306**, 024 (2013) doi:10.1007/JHEP06(2013)024 [arXiv:1304.1540 [hep-th]].

[90] S. Nakamura, H. Ooguri and C. S. Park, "Gravity Dual of Spatially Modulated Phase," Phys. Rev. D **81** (2010) 044018 doi:10.1103/PhysRevD.81.044018 [arXiv:0911.0679 [hep-th]].

[91] A. Donos, "Striped phases from holography," JHEP **1305**, 059 (2013) doi:10.1007/JHEP05(2013)059 [arXiv:1303.7211 [hep-th]].

[92] S. Cremonini, L. Li and J. Ren, "Holographic Fermions in Striped Phases," JHEP **1812**, 080 (2018) doi:10.1007/JHEP12(2018)080 [arXiv:1807.11730 [hep-th]].

[93] Y. Ling, P. Liu, C. Niu, J. P. Wu and Z. Y. Xian, "Holographic fermionic system with dipole coupling on Q-lattice," JHEP **1412**, 149 (2014) doi:10.1007/JHEP12(2014)149 [arXiv:1410.7323 [hep-th]].

[94] G. Giordano, N. Grandi, A. Lugo and R. Soto-Garrido, "Strange metal crossover in the doped holographic superconductor," JHEP **1810**, 068 (2018) doi:10.1007/JHEP10(2018)068 [arXiv:1808.02145 [hep-th]].